

**INVESTIGATIONS INTO CYCLOPROPANATION AND  
ETHYLENE POLYMERIZATION VIA SALICYLALDIMINATO  
COPPER(II) COMPLEXES.**

A Thesis Submitted to the College of

Graduate Studies and Research

in Partial Fulfillment of the Requirements

for the Degree of Masters of Science

in the Department of Chemistry

University of Saskatchewan

Saskatoon, SK

By

**Ramon Boyd**

© Ramon Boyd, January 2007. All rights reserved.

## **PERMISSION TO USE**

In presenting this thesis in partial fulfillment of the requirements for a Postgraduate degree from the University of Saskatchewan, I agree that the Libraries of this University may make it freely available for inspection. I further agree that permission for copying of this thesis in any manner, in whole or in part, for scholarly purposes may be granted by the professor or professors who supervised my thesis work or, in their absence, by the Head of the Department or the Dean of the College in which my thesis work was done. It is understood that any copying or publication or use of this thesis or parts thereof for financial gain shall not be allowed without my written permission. It is also understood that due recognition shall be given to me and to the University of Saskatchewan in any scholarly use which may be made of any material in my thesis.

Requests for permission to copy or to make other use of material in this thesis in whole or part should be addressed to:

Head of the Department of Chemistry  
University of Saskatchewan  
Saskatoon, Saskatchewan (S7N 5C9)

## ABSTRACT

Two distinct overall research objectives are in this Master's thesis. Very little relates the two chapters apart from the ligands. The first chapter addresses diastereoselective homogeneous copper catalyzed cyclopropanation reactions. Cyclopropanation of styrene and ethyl diazoacetate (EDA) is a standard test reaction for homogeneous catalysts. Sterically bulky salicylaldimine (SAL) ligands should select for the ethyl *trans*-2-phenylcyclopropanecarboxylate diastereomer. Steric bulk poorly influences *trans:cis* ratios. Salicylaldimine ligands do not possess the correct symmetry to affect diastereoselectivity. The SAL ligand belongs to the  $C_s$  point group in the solid state. Other ligand motifs are more effective at altering the *trans:cis* ratios. The second chapter addresses the general route toward successful copper(II) ethylene polymerization catalysts. Catalytic activity of the copper(II) complexes is very low. Polymer chain growth from a copper catalyst is very unlikely. Copper-carbon bonds decompose by homolytic cleavage or C-H activation. Copper-alkyls and -aryls readily decompose into brown colored oils and salts with different colors. Ligand transfer to trimethylaluminum (TMA) appears to explain low yield ethylene polymerization.

# TABLE OF CONTENTS

PERMISSION TO USE.....	i
ABSTRACT.....	ii
TABLE OF CONTENTS.....	iii
LIST OF TABLES.....	x
LIST OF FIGURES.....	xi
LIST OF SCHEMES.....	xiii
LIST OF ABBREVIATIONS.....	xii

## CHAPTER 1: INVESTIGATION OF DIASTEREOSELECTIVE CONTROL FOR BIS(SALICYLALDIMINATO) COPPER(II) CYCLOPROPANATION CATALYSTS

<b>1.1</b>	<b>INTRODUCTION.....</b>	<b>2</b>
1.1.1	Overall Research Objectives.....	2
1.1.2	Knowledge Gap to Bridge in this Masters Thesis.....	8
1.1.3	Research Objectives.....	9
1.1.4	Hypothesis.....	11
<b>1.2</b>	<b>RESULTS AND DISCUSSION.....</b>	<b>12</b>
1.2.1	Salicylaldimine Ligand Synthesis.....	13
1.2.1.1	2,6-Diisopropylphenyl-3,5-di- <i>tert</i> -butyl-salicylaldimine (Compound A).....	14
1.2.1.2	2-Hydroxy-biphenyl-3-carbaldehyde.....	15
1.2.1.3	2,6-Diisopropylphenyl-5-phenyl-salicylaldimine (Compound B).....	15
1.2.1.4	Phenyl-3-chloro-salicylaldimine (Compound C).....	16

1.2.1.5	2,4,6-Triphenylaniline.....	17
1.2.1.6	Attempted Synthesis of 2,4,6-Triphenyl-3,5-di- <i>tert</i> -butylsalicylaldimine (Compound <b>D</b> ).....	17
1.2.1.7	Attempted Synthesis of 2,4,6-Triphenyl-5-phenyl-salicylaldimine (Compound <b>E</b> ).....	18
1.2.2	Bis(salicylaldiminato)copper(II) Complex Synthesis.....	18
1.2.2.1	Bis(2,6-diisopropylphenyl-3,5-di- <i>tert</i> -butylsalicylaldiminato)copper(II) (Complex <b>1</b> ).....	18
1.2.2.2	Bis(2,6-diisopropylphenyl-5-phenyl-salicylaldiminato)copper(II) (Complex <b>2</b> ).....	23
1.2.2.3	{Bis(2,6-diisopropylphenyl-5-phenyl-salicylaldiminato)pyridine} copper(II) (Complex <b>2</b> • <i>py</i> ).....	23
1.2.2.4	Bis(phenyl-3-chloro-salicylaldiminato)copper(II) (Complex <b>3</b> ).....	28
1.2.3	Cyclopropanation Reactions.....	28
<b>1.3</b>	<b>CONCLUSION.....</b>	<b>33</b>
1.3.1	Recommendations for future investigation.....	33
<b>1.4</b>	<b>EXPERIMENTAL SECTION.....</b>	<b>34</b>
1.4.1	General considerations.....	34
1.4.2	X-ray Structural Analysis for Complexes <b>1</b> and <b>2</b> • <i>py</i> .....	35
1.4.3	Ligand synthesis.....	36
1.4.3.1	2,6-diisopropylphenyl-3,5-di- <i>tert</i> -butyl-salicylaldimine (Compound <b>A</b> ).....	36
1.4.3.2	2-hydroxy-biphenyl-3-carbaldehyde.....	37
1.4.3.3	2,6-diisopropylphenyl-5-phenyl-salicylaldimine (Compound <b>B</b> ).....	37

1.4.3.4	phenyl-3-chloro-salicylaldimine (Compound C).....	38
1.4.3.5	2,4,6-triphenylaniline.....	39
1.4.3.6	Attempted synthesis of 2,4,6-triphenyl-3,5-di- <i>tert</i> -butylsalicylaldimine (Compound D).....	39
1.4.3.7	Attempted synthesis of 2,4,6-triphenyl-5- phenyl-salicylaldimine (Compound E).....	40
1.4.4	Bis(salicylaldiminato)copper(II) complexes.....	41
1.4.4.1	bis(2,6-diisopropylphenyl-3,5-di- <i>tert</i> - butylsalicyldiminato)copper(II) (Complex 1).....	41
1.4.4.2	bis(2,6-diisopropylphenyl-5-phenyl- salicylaldiminato)copper(II) (Complex 2).....	42
1.4.4.3	{bis(2,6-diisopropylphenyl-5-phenyl- salicylaldiminato)pyridine}copper(II) (Complex 2 • <i>py</i> ).....	42
1.4.4.4	bis(phenyl-3-chloro-salicylaldiminato)copper(II) (Complex 3).....	43
1.4.5	General procedure for catalytic cyclopropanation reactions.....	43
<b>1.5</b>	<b>REFERENCES AND NOTES.....</b>	<b>45</b>
 <b>CHAPTER 2: SALICYLALDIMINATO COPPER(II) COMPLEXES</b>		
<b>AS INEFFECTIVE ETHYLENE</b>		
<b>POLYMERIZATION CATALYSTS</b>		
<b>2.1</b>	<b>INTRODUCTION.....</b>	<b>51</b>
2.1.1	Overall Research Objectives.....	51
2.1.2	Knowledge Gap to Bridge in this Masters Thesis.....	56
2.1.3	Research Objectives.....	57
2.1.4	Hypothesis.....	57

<b>2.2</b>	<b>RESULTS AND DISCUSSION.....</b>	<b>57</b>
2.2.1	Salicylaldimine Ligand Synthesis.....	59
2.2.2	Proposed Salicylaldiminato Copper(II) Precatalysts.....	60
2.2.2.1	(Tri- <i>n</i> -butylammonium) dichloro(2,6-diisopropylphenyl- 3,5-di- <i>tert</i> -butylsalicylaldiminato)copper(II) (Complex <b>4</b> ).....	60
2.2.2.2	(Tri- <i>n</i> -butylammonium) dichloro(2,6-diisopropylphenyl- 5-phenyl-salicylaldiminato)copper(II) (Complex <b>5</b> ).....	65
2.2.3	Chloride Bridged Salicylaldiminato Copper(II) Dimer Complex.....	66
2.2.3.1	( $\mu$ -Chloro)(2,6-diisopropylphenyl-3,5-di- <i>tert</i> - butylsalicylaldiminato)copper(II) (Complex <b>6</b> ).....	66
2.2.4	Ethylene Polymerization by Proposed Homogeneous Copper(II) Catalysts.....	71
<b>2.3</b>	<b>CONCLUSION.....</b>	<b>78</b>
<b>2.4</b>	<b>EXPERIMENTAL SECTION.....</b>	<b>79</b>
2.4.1	General Considerations.....	79
2.4.2	X-ray Structural Analysis for Complexes <b>4</b> and <b>6</b> .....	79
2.4.3	Ligand Synthesis.....	80
2.4.4	Salicylaldiminato Copper(II) Complex Synthesis.....	80
2.4.4.1	(Tri- <i>n</i> -butylammonium) dichloro(2,6-diisopropylphenyl- 3,5-di- <i>tert</i> -butylsalicylaldiminato)copper(II) (Complex <b>4</b> ).....	80
2.4.4.2	(Tri- <i>n</i> -butylammonium) dichloro(2,6-diisopropylphenyl- 5-phenyl-salicylaldiminato)copper(II) (Complex <b>5</b> ).....	82

2.4.5	Chloride Bridged Salicylaldiminato copper(II) Dimer Complex Synthesis.....	83
2.4.5.1	( $\mu$ -Chloro)(2,6-diisopropylphenyl-3,5-di- <i>tert</i> - butylsalicylaldiminato)copper(II) (Complex <b>6</b> ).....	83
2.4.5.1.1	Procedure 1: One-Pot Reaction.....	83
2.4.5.1.2	Procedure 2: Isolate Sodium Salt and Synthesize Chloride Bridged Dimer.....	84
2.4.6	General Procedure for Olefin Polymerization Reaction.....	85
2.4.6.1	Polyethylene Synthesis.....	85
<b>2.5</b>	<b>REFERENCES AND NOTES.....</b>	<b>87</b>



## APPENDICES..... 92

<b>A1.</b>	Proton NMR Spectra of 2,6-Diisopropylphenyl-3,5-di- <i>tert</i> -butylsalicylaldimine (Compound <b>A</b> ) in CDCl <sub>3</sub> .....	92
<b>A2.</b>	Proton NMR Spectra of 2,6-Diisopropylphenyl-3,5-di- <i>tert</i> -butylsalicylaldimine (Compound <b>A</b> ) in C <sub>6</sub> D <sub>6</sub> .....	93
<b>A3.</b>	FT-IR Spectra of 2,6-Diisopropylphenyl-3,5-di- <i>tert</i> - butylsalicylaldimine (Compound <b>A</b> ) .....	94
<b>A4.</b>	Proton NMR Spectra of 2-Hydroxy-biphenyl- 3-carbaldehyde in CDCl <sub>3</sub> .....	95
<b>A5.</b>	Proton NMR Spectra of 2,6-Diisopropylphenyl-5-phenyl- salicylaldimine (Compound <b>B</b> ) in CDCl <sub>3</sub> .....	96
<b>A6.</b>	FT-IR Spectra of 2,6-Diisopropylphenyl-5-phenyl- salicylaldimine (Compound <b>B</b> ).....	97
<b>A7.</b>	Proton NMR Spectra of Phenyl-3-chloro- salicylaldimine (Compound <b>C</b> ) in CDCl <sub>3</sub> .....	98
<b>A8.</b>	FT-IR Spectra of Phenyl-3-chloro- salicylaldimine (Compound <b>C</b> ).....	99
<b>A9.</b>	Proton NMR Spectra of 2,4,6-Triphenylaniline in CDCl <sub>3</sub> .....	100
<b>A10.</b>	Proton NMR Spectra of Incomplete Reaction to Synthesize 2,4,6-Triphenyl-3,5-di- <i>tert</i> - Butylsalicylaldimine (Compound <b>D</b> ) in CDCl <sub>3</sub> .....	101
<b>A11.</b>	Proton NMR Spectra of Incomplete Reaction to Synthesize Synthesis of 2,4,6-Triphenyl-5-phenyl- salicylaldimine (Compound <b>E</b> ) in CDCl <sub>3</sub> .....	102
<b>A12.</b>	FT-IR Spectra of Bis(2,6-diisopropylphenyl-3,5-di- <i>tert</i> - butylsalicylaldiminato)copper(II) (Complex <b>1</b> ).....	103
<b>A13.</b>	FT-IR Spectra of Bis(2,6-diisopropylphenyl-5-phenyl- salicylaldiminato)copper(II) (Complex <b>2</b> ).....	104
<b>A14.</b>	FT-IR Spectra of Bis(phenyl-3-chloro- salicylaldiminato)copper(II) (Complex <b>3</b> ).....	105

<b>A15.</b>	Proton NMR Spectra of Cyclopropanation by Bis(phenyl-3-chloro-salicylaldiminato)copper(II)(Complex <b>3</b> ) in CDCl <sub>3</sub> Corresponding to Entry 7 in Table 1.5.....	106
<b>A16.</b>	FT-IR Spectra of (Tri-n-butylammonium) dichloro(2,6-diisopropylphenyl-3,5-di- <i>tert</i> -butylsalicylaldiminato)copper(II) (Complex <b>4</b> ) [HNnBu <sub>3</sub> ][(SAL <sup>1</sup> )CuCl <sub>2</sub> ].....	107
<b>A17.</b>	FT-IR Spectra of (Tri-n-butylammonium) dichloro(2,6-diisopropylphenyl- 5-phenyl-salicylaldiminato)copper(II) (Complex <b>5</b> ) [HNnBu <sub>3</sub> ][(SAL <sup>2</sup> )CuCl <sub>2</sub> ].....	108
<b>A18.</b>	FT-IR Spectra of ( $\mu$ -Chloro)(2,6-diisopropylphenyl-3,5-di- <i>tert</i> -butylsalicylaldiminato)copper(II) (Complex <b>6</b> ) [(SAL <sup>1</sup> )Cu( $\mu$ -Cl)].....	109

# LIST OF TABLES

Table	Page
1.1. Crystallographic Data and details of Refinement for Complex <b>1</b> .....	21
1.2. Selected Bond Distances (Å) and Angles (°) for Complex <b>1</b> .....	22
1.3. Crystallographic Data and Details of Refinement for Complex <b>2 • py</b> .....	26
1.4. Selected Bond Distances (Å) and Angles (°) for Complex <b>2 • py</b> .....	27
1.5. Cyclopropanation Results.....	30
2.1. Crystallographic Data and Details of Refinement for Complex <b>4</b> .....	63
2.2. Selected Bond Distances (Å) and Angles (°) for Complex <b>4</b> .....	64
2.3. Crystallographic Data and Details of Refinement for Complex <b>5</b> .....	68
2.4. Selected Bond Distances (Å) and Angles (°) for Complex <b>5</b> .....	69
2.5. Results for Polymerization Catalyzed by Complexes <b>1, 4, and 5</b> .....	73

# LIST OF FIGURES

Figure		Page
1.1.	Early Copper Cyclopropanation Catalyst Developed by Nozaki and Colleagues.....	3
1.2.	C <sub>2</sub> Symmetric Copper Cyclopropanation Catalysts.....	4
1.3.	Bis(pyrazolyl)pyridinecopper Cyclopropanation Catalyst.....	4
1.4.	Tris(pyrazolyl <sup>X</sup> )boratecopper(I) Cyclopropanation Catalyst.....	5
1.5.	Salicylalimine Ligands.....	8
1.6.	Copper(II) Cyclopropanation Precatalysts.....	10
1.7.	Molecular Structure of <b>1</b> with Thermal Ellipsoids at the 50% Probability Level. H Atoms are Omitted for Clarity.....	20
1.8.	Molecular Structure of <b>2</b> • <i>py</i> with Thermal Ellipsoids at the 50% Probability Level. H Atoms are Omitted for Clarity.....	24
1.9.	Molecular Structure of <b>2</b> • <i>py</i> with Thermal Ellipsoids at the 50% Probability Level. H Atoms and <sup>i</sup> Pr Groups are Omitted for Clarity.....	25
2.1.	Nickel(II) and Palladium(II) Ethylene and α-Olefin Polymerization Catalysts.....	52
2.2.	A Low Activity Iron(II) Olefin Polymerization Catalyst.....	52

<b>2.3.</b>	2,6-Bis(imino)pyridyl Cobalt and Iron Ethylene Polymerization Catalysts Developed by Brookhart and Gibson.....	53
<b>2.4.</b>	Copper(II) Catalysts used for Ethylene Polymerization and Copolymerization.....	55
<b>2.5.</b>	Proposed Copper(II) Precatalysts for Ethylene Polymerization.....	58
<b>2.6.</b>	Chloride Bridged Dimer Complex.....	58
<b>2.7.</b>	Salicylaldimine Ligands.....	60
<b>2.8.</b>	Molecular Structure of <b>4</b> with Thermal Ellipsoids at the 50% Probability Level. H Atoms on the SAL Ligand Omitted for Clarity. A Single H Atom on Tributylammonium Was Not Removed.....	62
<b>2.9.</b>	ORTEP Plot for Complex <b>6</b> Hydrogen Atoms and Labels for Carbon Atoms Are Removed for Simplicity and Clarity. Percent Thermal Ellipsoids Shown is 50% Probability.....	67
<b>2.10.</b>	Complexes <b>1</b> , <b>4</b> , and <b>5</b> as Proposed Precatalysts, for Ethylene Polymerization.....	71

## LIST OF SCHEMES

Scheme	Page
1.1. Proposed Reaction Sequence and Catalytic Cycle.....	7
2.1. Catalytic Cycle for Grubb's Neutral Nickel(II) Catalyst.....	54
2.2. Synthesis and Activation of Aluminum Single Site Ethylene Polymerization Catalysts.....	75
2.3. Ligand Transfer from Copper(II) Precatalyst to Trimethylaluminum.....	76
2.4. Proposed Mechanism for Ethylene Polymerization.....	77
2.5. Proposed Mechanism for Copper(II) Precatalysts.....	85

# LIST OF ABBREVIATIONS

## 1. CHEMICAL AND LIGANDS

Ar	aryl substituent
Bu	butyl ( <sup>t</sup> Bu, tertiary-butyl)
E	element
EDA	ethyl diazoacetate
HDPE	high density polyethylene
L	ligand
M	central atom (usually a metal) in a compound
MAO	methylaluminoxane
Me	methyl
Mes	2,4,6-triphenylbenzene
PE	polyethylene
Ph	phenyl, C <sub>6</sub> H <sub>5</sub>
<sup>i</sup> Pr	iso-propyl
R	alkyl or aryl group
SAL	salicylaldimine ligand
THF or thf	tetrahydrofuran
TMA	trimethylaluminum
Tpb	tris(pyrazolylborate)
X	halogen

## 2. MISCELLANEOUS

Å	angstrom unit, 10 <sup>-10</sup> m
atm	atmosphere, 760 torr (mm Hg 0 °C)
BM	Bohr magneton
cm <sup>-1</sup>	wavenumber
eq	equivalents
EA	elemental analysis

ESD	estimated standard deviation
FT-IR	Fourier transform infrared
g	gram
Hz	hertz
IR	infrared
ml	milliliter
mmol	millimole
MHz	megahertz
Mp	melting point
NMR or nmr	nuclear magnetic resonance
ppm	parts per million
psi	pounds per square inch, 51.7 torr (mm Hg °C)
$\mu_{\text{eff}}$	effective magnetic moment in Bohr magnetons



## **CHAPTER 1:**

# **INVESTIGATION OF DIASTEREOSELECTIVE CONTROL FOR BIS(SALICYLALDIMINATO) COPPER(II) CYCLOPROPANATION CATALYSTS**

## 1.1 INTRODUCTION

### 1.1.1 Overall Research Objectives

Cyclopropanes are cyclic organic compounds. Bond angles between three  $\text{-CR}_2\text{-}$  groups are 60 degrees.<sup>1</sup> Small bond angles make cyclopropanes highly strained. These highly strained rings are susceptible to ring opening reactions with electrophiles or nucleophiles. Various alkyls- and aryls- incorporate into the  $\text{-CR}_2\text{-}$  groups. Cyclopropanes are versatile natural product intermediates.<sup>1-4</sup> Ethyl 2-phenylcyclopropanecarboxylate is an important di-substituted cyclopropane. This cyclopropane is useful for testing diastereoselectivity because it has two stereogenic centers. *Cis*- and *trans*- diastereomers are two non-mirror image isomers of ethyl 2-phenylcyclopropanecarboxylate. Transition metal (TM) catalysts make *cis*- and *trans*- diastereomers of ethyl 2-phenylcyclopropanecarboxylate. Diazo compounds ( $\text{N}_2=\text{CRR}'$ ) and substituted olefins are reagents for transition metal catalyzed cyclopropanation. Relatively few TM catalysts are selective for a single diastereomer. Copper(II) complexes are selective for C=C bonds. Selectivity for C=C bonds make copper catalysts attractive for cyclopropanation reactions. The overall research objective of this chapter is to test homogeneous copper(II) catalysts for cyclopropane diastereoselectivity. To date, there are no investigations on how bis(salicylaldiminato)copper(II) catalysts direct cyclopropane diastereoselectivity. Chiral salicylaldiminato copper(II) complexes induce asymmetric cyclopropanation of styrene with ethyl diazoacetate (EDA).<sup>5</sup> Salicylaldiminato ligands have been known for four decades for olefin cyclopropanation. The ligand frame work is relatively easy to synthesize. Steric bulk should influence diastereoselectivity.

Several noteworthy discoveries are worth mentioning at the beginning of the first chapter. First, a brief review of copper cyclopropanation catalysts. Following the review is an introduction to Salomon and Kochi's pioneering mechanistic study.<sup>6</sup> The mechanistic study is influential because it demonstrates that diazo compounds reduce copper(II) catalysts. The last part of Section 1.1.1 briefly introduces the proposed catalytic cycle.

Early bis(salicylaldiminato)copper(II) complexes were not diastereoselective (Figure 1.1).<sup>5,7</sup>

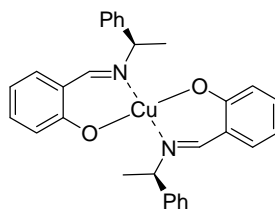


**Figure 1.1.** Early Copper Cyclopropanation Catalyst Developed by Nozaki and Colleagues.

Bisoxolazine and semicorrin copper(II) complexes are also poorly diastereoselective cyclopropanation catalysts (Figure 1.2).<sup>8,9,10</sup>

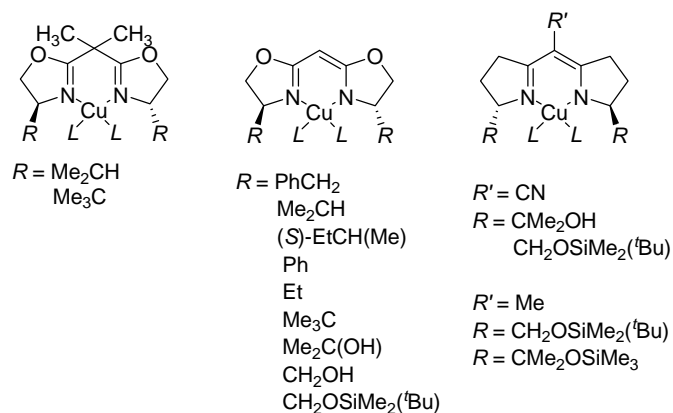


**Figure 1.2.**  $C_2$  Symmetric Copper Cyclopropanation Catalysts.

The rings of the  $C_2$  symmetric ligands constrain ligand flexibility.<sup>11,8</sup> Steric bulk at the R positions does not preferentially block olefin access to copper. Bis(pyrazolyl)pyridine ligands are also  $C_2$  symmetric ligands. However, the bis(pyrazolyl)pyridine copper cyclopropanation catalysts are poorly diastereoselective (Figure 1.3).<sup>11,12</sup>

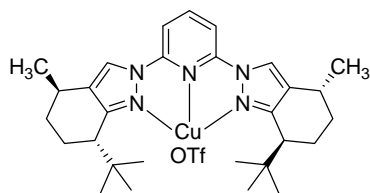
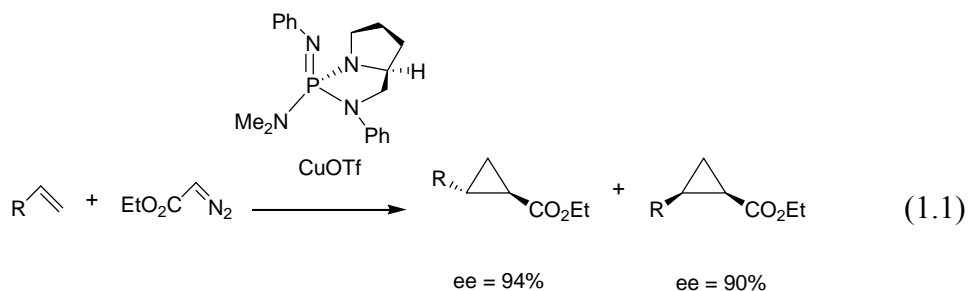


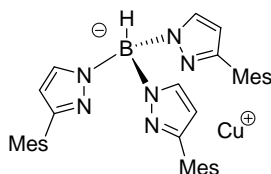
**Figure 1.3.** Bis(pyrazolyl)pyridine Copper Cyclopropanation Catalyst.

The Iminophosphorane copper(I) catalyst was the first highly *trans*- diastereoselective catalyst (Equation 1.1).<sup>13</sup>



High *trans:cis* ratios (98:2) for the EDA/styrene are noteworthy.<sup>13</sup>

*Cis*- diastereoselectivity remains a major synthetic challenge. A single copper catalyst favors high *cis*- diastereoselectivity. The tris(pyrazolylborate) (Tpb) ligands demonstrate 98:2 *cis:trans* ratios for the EDA/styrene reaction (Figure 1.4).<sup>14</sup>

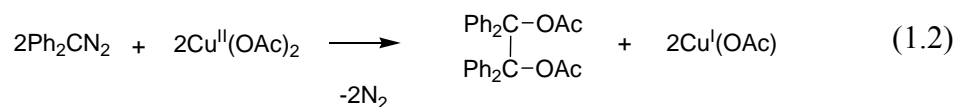


Mes = 2,4,6-triphenylbenzene

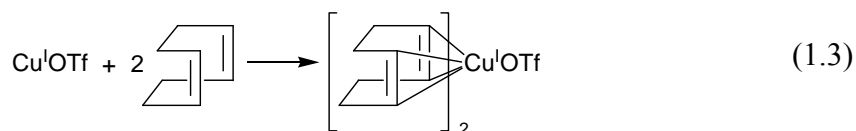
**Figure 1.4.** Tris(pyrazolyl<sup>X</sup>)borate-copper(I) Cyclopropanation Catalyst.

Tris(pyrazolylborate) ligands belong to the  $C_{3V}$  point group. Pendant groups on the pyrazolyl rings greatly influence diastereoselectivity. The mesityl groups arrange themselves orthogonal to the plane of the pyrazolyl ligand. Steric bulk forms a protective catalytic pocket. The combination of symmetry and steric bulk makes the tris(pyrazolyl<sup>X</sup>)borate-copper(I) cyclopropanation catalyst diastereoselective.

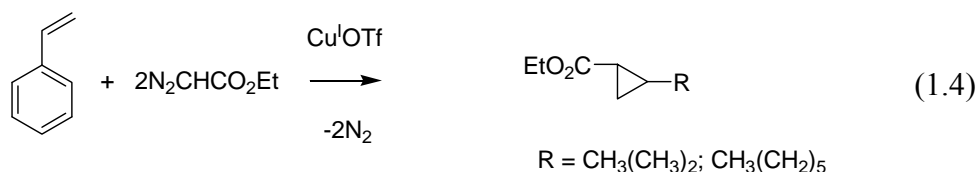
Copper acetate complexes are the first understood cyclopropanation catalysts.<sup>6</sup> Salomon and Kochi demonstrated the redox chemistry necessary to reduce copper(II) carboxylates with diphenyldiazomethane.<sup>6</sup> The reaction produces copper(I) triflates. The copper(I) intermediates are catalytically active for cyclopropanation (Equation 1.2).



Copper(I) carboxylates disproportionate to copper(0) and copper(II). Colloidal copper(0) is an insoluble black product. Copper(I) triflate compounds behave analogously to copper(I) carboxylates. Olefins stabilize copper(I) intermediates *in situ*. Copper(I) triflate compounds coordinate with olefin ligands (Equation 1.3).

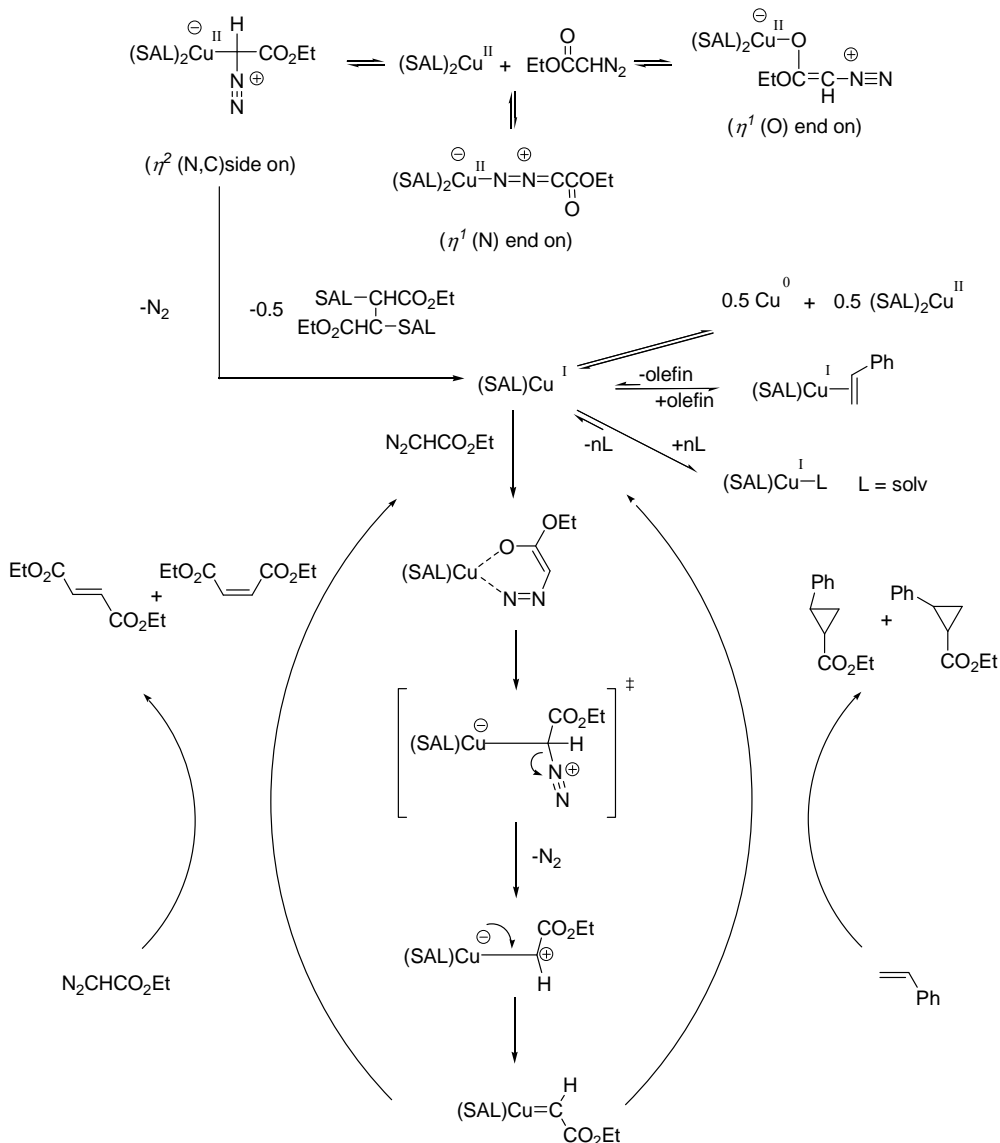


*In situ* the copper(I) intermediates become active catalysts for cyclopropanation (Equation 1.4).



Salomon and Kochi demonstrated that copper(I) intermediates cyclopropanate substituted olefins and diazo compounds.<sup>6</sup> The precatalyst is a copper(II) complex. Copper(II) precatalysts are reduced to copper(I) intermediates *in situ*. The copper(I) intermediates cyclopropanate styrene and EDA. Neutral copper(I) intermediates freely coordinate with styrene.

Characterizable intermediates are difficult to identify.<sup>5</sup> However, it is possible to infer a sequence of mechanisms (Scheme 1.1)



**Scheme 1.1.** Proposed Reaction Sequence and Catalytic Cycle.

An equivalent of ethyl diazoacetate (EDA) reduces bis(salicylaldiminato)copper(II). The C=N bond is reactive because it is polar. A stoichiometric amount of dinitrogen evolves and the copper-carbon bond decomposes by homolytic cleavage. The copper(I) intermediate becomes the active catalyst.<sup>15,6</sup> Free triplet carbenes and liberated SAL ligands probably form diesters. Salomon and Kochi observe similar diester compounds from oxidation of diazo compounds by copper(II) complexes.<sup>6</sup> The 14-electron copper(I) intermediate is safe from disproportionation.<sup>6</sup> Colloidal copper(0) may darken the reaction mixture. Copper(I) intermediates freely coordinates with styrene molecules present. However, the 14 electron intermediates preferentially coordinate with a second equivalent of EDA to form a metal-carbene/ylide. Electrophilic copper-carbene/ylide complexes are well known to be efficient cyclopropanation catalysts.<sup>16</sup> An equivalent of styrene yields one of the *cis:trans* cyclopropane diastereomers. Alternately, a third equivalent of EDA yields one of the *cis:trans* dimer compounds.

### 1.1.2 Knowledge Gap to Bridge in this Masters Thesis

There are two distinct research objectives in this Master's thesis. Compounds **A** and **B** are common to both chapters (Figure 1.5).

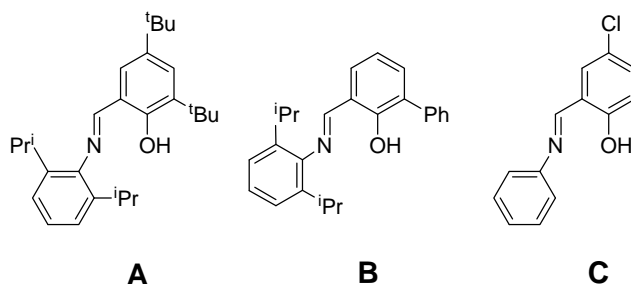


**Figure 1.5.** Salicylaldehyde Ligands.

Compound **C** is exclusive to the first chapter. The salicylaldehyde (SAL) ligand is relatively easy to synthesize. There is a simple reason why there are two separate



research objectives. Copper(II) complexes are not effective olefin polymerization catalysts. Bis(salicylaldiminato)copper(II) complexes do cyclopropanate diazo compounds and EDA. A single knowledge gap exists in the first chapter which is steric influence on di-substituted cyclopropane diastereoselectivity. SAL ligands may not have the right symmetry to influence the *cis:trans* ratio. Sterics is a moot point if the ligand has the incorrect symmetry. Tpb ligands seem to be the most effective for diastereoselective control. There is no way to predict the outcome of the experiments. Cyclopropanation is an accessible organic transformation. The reactions are also attractive because cyclopropanes are synthetically important compounds.<sup>1-4</sup>

### 1.1.3 Research Objectives

There are three short term objectives for this phase of the project. The first short term objective is to synthesize ligands. The second short term objective is to synthesize four coordinate copper(II) complexes. The third short term objective is to investigate cyclopropanation reactions. Bis(salicylaldiminato)copper(II) complexes catalyze cyclopropanation of EDA and styrene. Discussion of significant research contributions appear in the results and discussion section (see Section 1.2). A summary of significant research contributions for this chapter appears in the conclusion (see Section 1.3). Synthetic details appear in the experimental section (see Section 1.4). Three copper(II) precatalysts are under investigation (Figure 1.6).

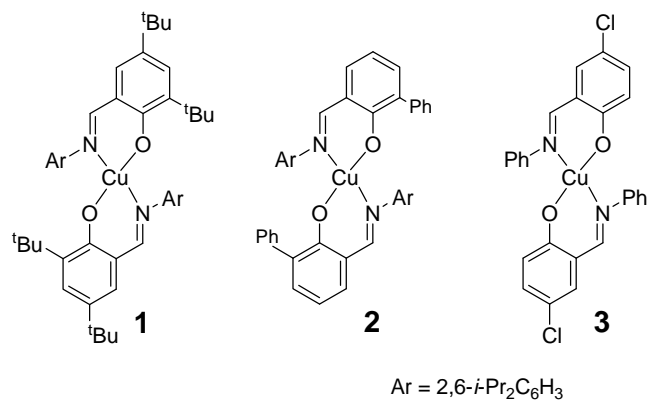
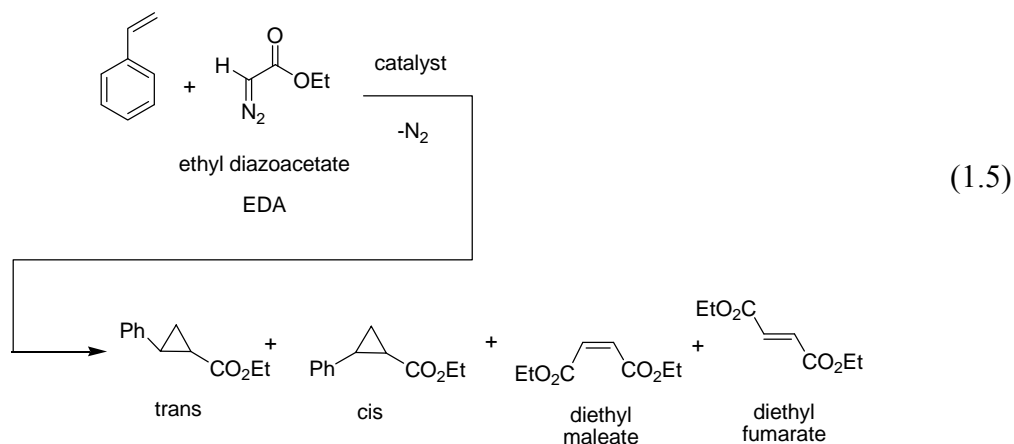
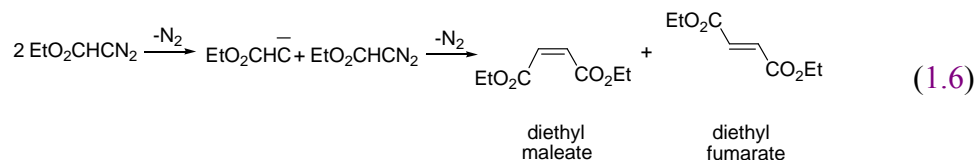


**Figure 1.6.** Copper(II) Cyclopropanation Precatalysts.

Complexes **1**, **2**, and **3** have varying degrees of steric bulk. The standard reaction to measure catalytic activity is cyclopropanation of styrene with EDA (Equation 1.5).



EDA addition rate is slow to maximize cyclopropane yield.<sup>17</sup> Copper(II) precatalysts are selective for the reactive C=N bond. EDA reduces the copper(II) precatalyst. Excess EDA in the reaction mixture produces unwanted side products. Diethyl maleate and diethyl fumarate result from thermal decomposition of EDA in the presence of styrene (Equation 1.6).<sup>18</sup>



Slow addition of EDA to the reaction mixture reduces side product formation. Ideally, the concentration of EDA is kept low.<sup>17</sup> The catalyst is able to tie up EDA in cyclopropanation reactions. The di-substituted cyclopropanes have unique <sup>1</sup>H NMR resonances.<sup>19</sup> Diethyl fumarate and diethyl maleate <sup>1</sup>H NMR resonances do not overlap with those of the target products. Gravimetric analysis determines product yields.

#### 1.1.4 Hypothesis

Sterically bulky salicylaldiminato copper(II) catalysts should influence cyclopropane diastereoselectivity. Increased steric bulk should correlate with increased *trans:cis* cyclopropane ratio.

## 1.2 RESULTS AND DISCUSSION

Three bis(salicylaldiminato)copper(II) complexes were synthesized (Figure 1.6).

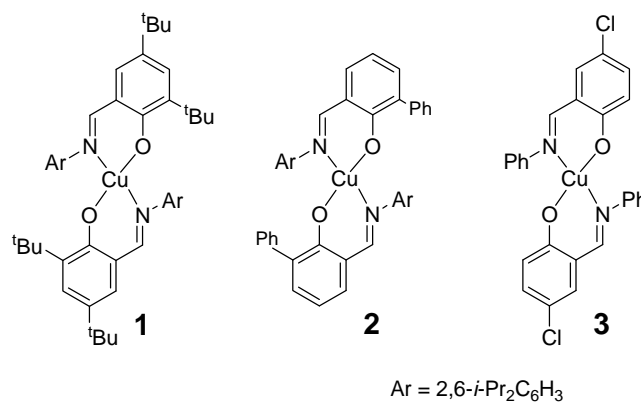


**Figure 1.6.** Copper(II) Cyclopropanation Precatalysts.

Complexes **1**, **2**, and **3** were used to investigate diastereoselective cyclopropanation of styrene with EDA. Complex **3** had significantly reduced steric bulk compared to complexes **1** and **2**. Bulky ligands were to influence the *cis:trans* diastereoselective ratio. Complexes **1**, **2**, and **3** were synthesized by the same procedure. The nature of the electronic characteristics of the aromatic, aliphatic, and halide substituents upon the complexes was not completely known.

### 1.2.1 Salicylaldimine Ligand Synthesis

Three salicylaldimine ligands were synthesized. Compound **A** was 2,6-diisopropylphenyl-3,5-di-*tert*-butylsalicylaldimine. Compound **B** was 2,6-diisopropylphenyl-5-phenyl-salicylaldimine. Compound **C** was phenyl-3-chloro-salicylaldimine (Figure 1.5).

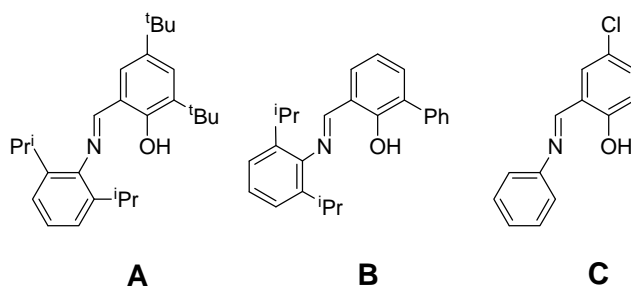


**Figure 1.5.** Salicylaldimine Ligands.

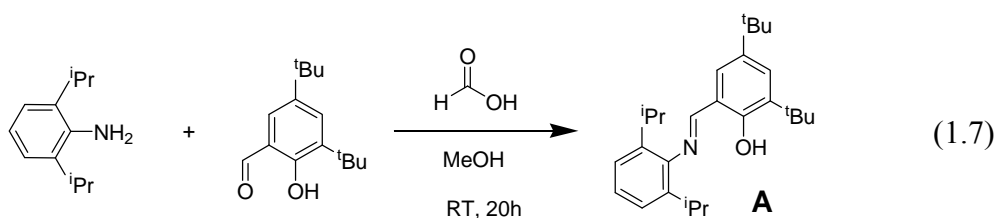
Compounds **A**, **B**, and **C** were the bulkiest salicylaldimine ligands synthesized from the literature.<sup>20,21,22</sup> Compound **C** was made by the same modified literature procedure that was used for compounds **A** and **B**.<sup>21,22</sup> Literature preparations were often modified to optimize the mass of product. Some organic preparations were designed to produce an undesirable quantity of product. Refer to Section 1.4.3 for the synthetic details.

Copper(II) catalyzed cyclopropanation was a new application for ligands **A**, **B**, and **C**. Compounds **A** and **B** were available from the literature.<sup>22,21</sup> Ligand **A** had an electron donating and sterically bulky *tert*-butyl group *ortho* to the hydroxy substituent. Ligand **B** had a phenyl group *ortho* to the hydroxy substituent. Phenyl donated electron density inductively through the C-C bond to the phenolic ring. Grubbs attempted to modify the *ortho*- position of the phenolic ring.<sup>22</sup> The *ortho*- position was difficult to modify. Grubbs achieved 26% yield using 9-phenthrenyl and 24% yield using 9-anthrecenyl.<sup>22</sup> The ketimine nitrogen position of SAL was not easier to modify. The decision was

made to reduce steric bulk at the *ortho*- position and at the ketimine nitrogen position. Ligand **C** had less steric bulk proximal to the N- and O- donor atoms.

#### 1.2.1.1 2,6-Diisopropylphenyl-3,5-di-*tert*-butylsalicylaldimine (Compound **A**).

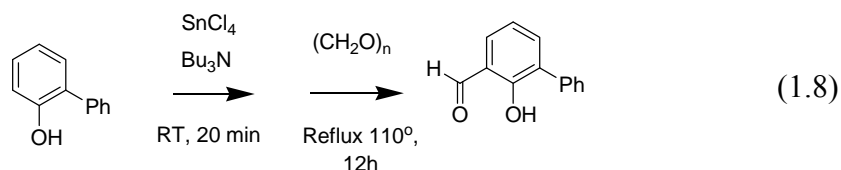
2,6-Diisopropylphenyl-3,5-di-*tert*-butylsalicylaldimine (**A**) was synthesized by slight modification of literature procedure (Equation 1.7).<sup>21</sup>



Compound **A** was synthesized by reacting 2,5-di-*tert*-hydroxybenzaldehyde and 2,6-diisopropylaniline. The reaction took place in the presence of formic acid. Yellow crystals were obtained upon crystallization from methanol in 76.3% yield. <sup>1</sup>H NMR in CDCl<sub>3</sub> resonances for the following proton environments were diagnostic (Appendix A1): (a) an alcoholic proton appeared as a singlet at 13.46 ppm and integrated for a single proton, (b) an imine proton appeared as a singlet at 8.29 ppm and integrated for a single proton. <sup>1</sup>H NMR in C<sub>6</sub>D<sub>6</sub> resonances for the following proton environments were diagnostic (Appendix A2): (a) an alcoholic proton appeared as a singlet at 13.98 ppm and integrated for a single proton, (b) an imine proton appeared as a singlet at 7.97 ppm and integrated for a single proton. Compound **A** was characterized by FT-IR spectroscopy. The imine C=N stretch appeared at 1622 cm<sup>-1</sup> (Appendix A3).

#### 1.2.1.2 2-Hydroxy-biphenyl-3-carbaldehyde

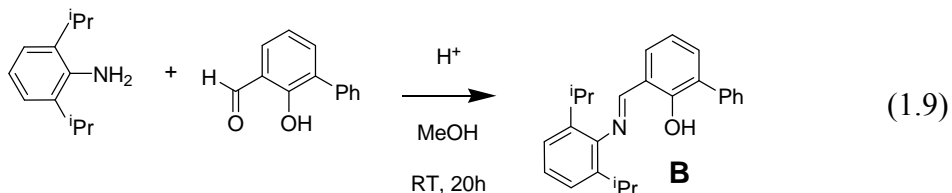
Synthesis of 2-hydroxy-biphenyl-3-carbaldehyde was conducted by slight modification of literature (Equation 1.8).<sup>23</sup>



The compound 2-hydroxy-biphenyl-3-carbaldehyde was made by reacting 2-hydroxybiphenyl,  $\text{SnCl}_4$ , and tributylamine in dry toluene. The reaction took place under nitrogen gas. 2-Hydroxy-biphenyl-3-carbaldehyde was produced in 50% yield. Proton NMR revealed the crude to be a 50/50 mixture of 2-hydroxy-biphenyl-3-carbaldehyde and 2-hydroxybiphenyl. The product was used without further purification. The OH for 2-hydroxy-biphenyl-3-carbaldehyde appeared as a singlet at 11.56 ppm (Appendix A4). An aldehyde proton was clearly visible at 9.97 ppm. The singlet assigned to OH for 2-hydroxybiphenyl appeared at 5.39 ppm. Eight aromatic protons appeared between 7.77 and 7.00 ppm which were assigned to 2-hydroxy-biphenyl-3-carbaldehyde. Nine aromatic protons in the same region were assigned to 2-hydroxybiphenyl.

#### 1.2.1.3 2,6-Diisopropylphenyl-5-phenyl-salicylaldimine (Compound **B**).

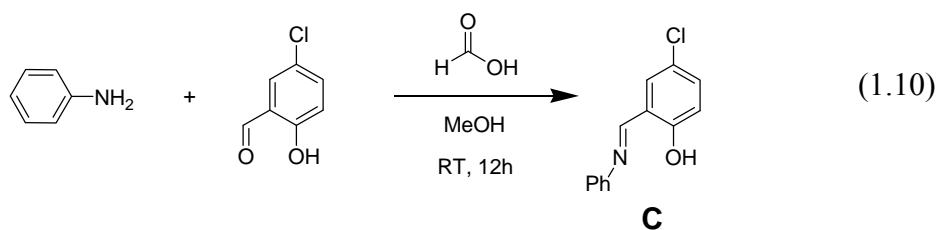
Synthesis of 2,6-diisopropylphenyl-5-phenyl-salicylaldimine (**B**) was conducted by slight modification of literature procedure (Equation 1.9).<sup>21</sup>



Compound **B** was synthesized by reacting 2-hydroxy-biphenyl-3-carbaldehyde and 2,6-diisopropylaniline. The reaction took place in the presence of formic acid. Yellow crystals were obtained upon crystallization from methanol in 49.8% yield. Several diagnostic proton NMR resonances were observed (Appendix A5). The hydroxy proton for compound **B** appeared as a singlet at 13.68 ppm. An imine proton appeared at 8.43 ppm. A septet for the isopropyl groups appeared at 3.08 ppm. The septet integrated for two protons. Compound **B** was characterized by FT-IR spectroscopy. The imine C=N stretch appeared at 1616  $\text{cm}^{-1}$  (Appendix A6).

#### 1.2.1.4 Phenyl-3-chloro-salicylaldimine (Compound C).

Synthesis of phenyl-3-chloro-salicylaldimine (**C**) was conducted by slight modification of literature procedure to lower product mass (Equation 1.10).<sup>20</sup>



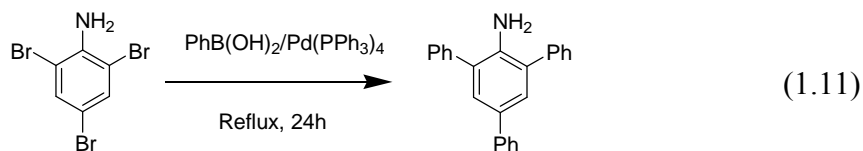
Compound **C** was synthesized by reacting 5-chlorosalicylaldehyde and aniline. The reaction took place in the presence of formic acid. Orange crystals were obtained upon crystallization from methanol in 94.6% yield.  $^1\text{H}$  NMR resonances for diagnostic proton environments are clearly visible (Appendix A7). The OH singlet appeared at 13.25 ppm and integrated for a single proton. An imine singlet appeared at 8.56 ppm and integrated



for a single proton. Compound **C** was characterized by FT-IR spectroscopy. The imine C=N stretch appeared at  $1615\text{ cm}^{-1}$  (Appendix A8).

#### 1.2.1.5 2,4,6-Triphenylaniline

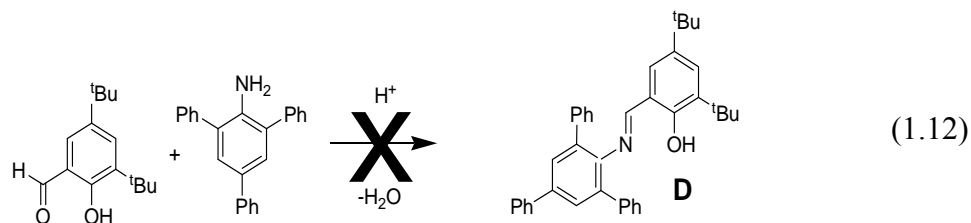
Efforts were made to increase steric bulk at the ketimine nitrogen position of the SAL ligand. Aromatic substituents were joined by Suzuki coupling reactions. The super bulky aniline derivative 2,4,6-triphenylaniline was synthesized by slight modification of literature procedure to lower product mass (Equation 1.11).<sup>24,25</sup>



2,4,6-Triphenylaniline was synthesized by making an ethanolic slurry of phenylboronic acid, 2.0M  $\text{Na}_2\text{CO}_3$ , and  $\text{Pd}(\text{PPh}_3)_4$ . The slurry was added to 2,4,6-tribromoaniline dissolved in benzene. White powder was obtained after purification by chromatography (95:5 hexane:acetate) in 78.2%. Several diagnostic  $^1\text{H}$  NMR resonances were clearly visible (Appendix A9). A multiplet between 7.67 and 7.44 ppm integrated for 17 protons. A broad singlet appeared at 3.97 ppm for the two aniline protons.

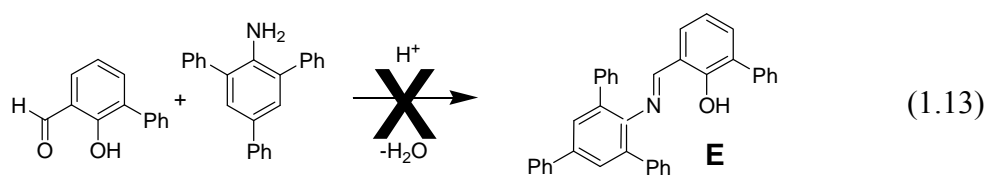
#### 1.2.1.6 Attempted Synthesis of 2,4,6-Triphenyl-3,5-di-*tert*-butylsalicylaldimine (Compound **D**).

Synthesis of 2,4,6-triphenyl-3,5-di-*tert*-butylsalicylaldimine (**D**) was attempted under rigorous reaction conditions. No reaction was observed in methanol. Refluxing in cumene for 24 hours did not complete the reaction (Equation 1.12) (Appendix A12).



#### 1.2.1.7 Attempted Synthesis of 2,4,6-Triphenyl-5-phenyl-salicylaldimine (Compound **E**).

Likewise, 2,4,6-triphenyl-5-phenyl-salicylaldimine was attempted with little success. No reaction was observed for proposed compound **E** in methanol. Refluxing in cumene 24 hours did not complete the reaction (Equation 1.13) (Appendix A11).



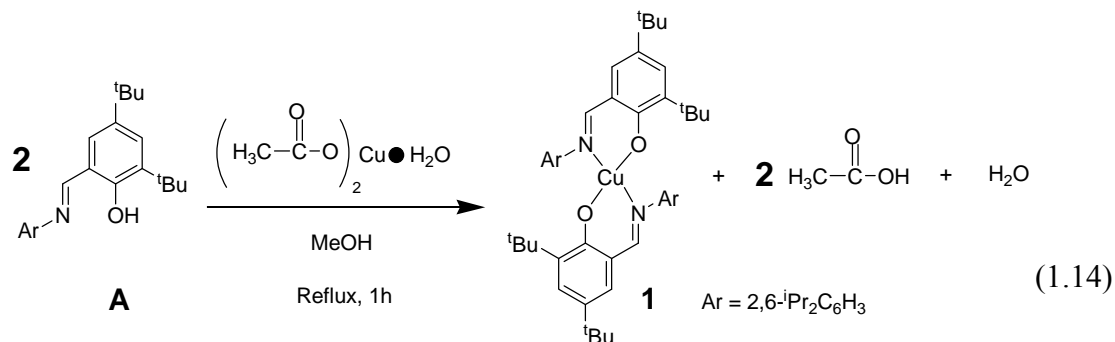
Starting materials were recovered from the reactions. Further reactions with 2,4,6-triphenylaniline were abandoned.

### 1.2.2 Bis(salicylaldiminato)copper(II) Complex Synthesis

Two bis(salicylaldiminato) copper(II) complexes have been characterized by X-ray crystallography. Refer to Section 1.4.4 for the synthetic details.

#### 1.2.2.1 Bis(2,6-diisopropylphenyl-3,5-di-*tert*-butylsalicylaldiminato)copper(II) (Complex **1**).

Bis(2,6-diisopropylphenyl-3,5-di-*tert*-butylsalicylaldiminato)copper(II) was the first cyclopropanation catalyst synthesized (Equation 1.14).



Complex **1**, or bis(2,6-diisopropylphenyl-3,5-di-*tert*-butylsalicylaldiminato)copper(II), was synthesized by reacting two equivalents of compound **A** with a single equivalent of copper(II)acetate monohydrate. Methanol was added to the reagents. The mixture was refluxed under nitrogen for one hour. A brown product was crystallized from methanol. Needle like crystals were X-ray quality. Yield: 0.66 g (78.3 %). Elemental analysis confirmed the presence of complex **1**. The product decomposed between 243.0-250.0 °C. Complex **1** was characterized by FT-IR spectroscopy. The imine C=N stretch appeared at 1611 cm<sup>-1</sup> (Appendix A12). Compound **A** imine C=N stretch appeared at 1622 cm<sup>-1</sup> (Appendix A3). The imine C=N stretch shift was consistent with coordination of the imine nitrogen atom to electrophilic copper(II). The number of wavenumbers was expected to decrease by 10-20 cm<sup>-1</sup>. The bond strength increased as electron density increased in the C=N bond. The effective magnetic moment was 1.78 BM. Complex **1** had a single unpaired electron.

As X-ray quality crystals were obtained. The structure of complex **1** was determined (Figure 1.7, plus Tables 1.1 and 1.2).

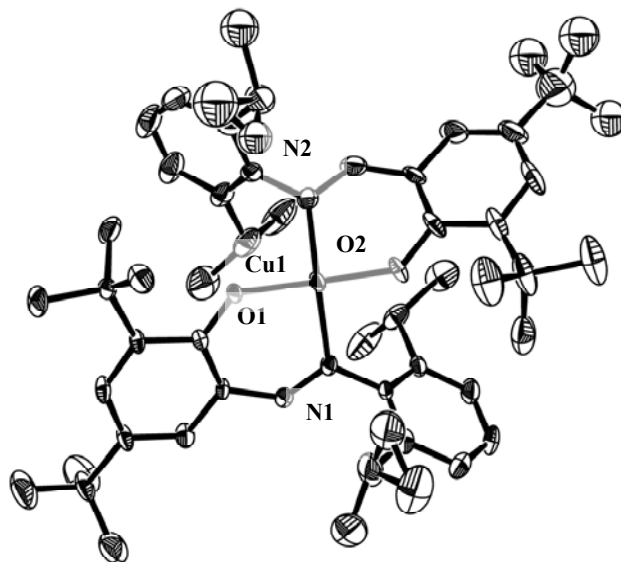


**Figure 1.7.** Molecular Structure of **1** with Thermal Ellipsoids at the 50% Probability Level. H Atoms are Omitted for Clarity.

The crystal system was monoclinic and belonged to the C 2/c space group (Table 1.1).

**Table 1.1.** Crystallographic Data and Details of Refinement for Complex 1.

---

Empirical formula	C <sub>54.50</sub> H <sub>76.50</sub> Cl <sub>11.50</sub> Cu N <sub>2</sub> O <sub>2</sub>
Formula weight	908.39 ( <i>calc.</i> 848.74)
Crystal system	Monoclinic
Space group	C 2/c
<i>a</i> , <i>b</i> , <i>c</i> , (Å)	38.2167(19), 13.6552(16), 27.1678(13)
$\alpha$ (°)	90
$\beta$ (°)	133.362(2)
$\gamma$ (°)	90
<i>V</i> (Å <sup>3</sup> )	10307.7(14)
<i>Z</i>	8
<i>D</i> <sub>calcd</sub> (Mg/m <sup>3</sup> )	1.171
Absorption coefficient (mm <sup>-1</sup> )	0.541
<i>T</i> (K)	173(2)
Total reflections	34676
Independent reflections	6238 [R(int) = 0.1109]
R indices (all data)	R1 = 0.0966, wR2 = 0.1839
Final R indices [I>2sigma(I)]	R1 = 0.0768, wR2 = 0.1710
Goodness-of-fit on F <sup>2</sup>	1.062

---

Final R indices were reasonably good R1 = 0.0768. The crystal structure was publication quality. Nitrogen and oxygen donor atoms occupied a four coordinate environment about the copper atom (Table 1.2).

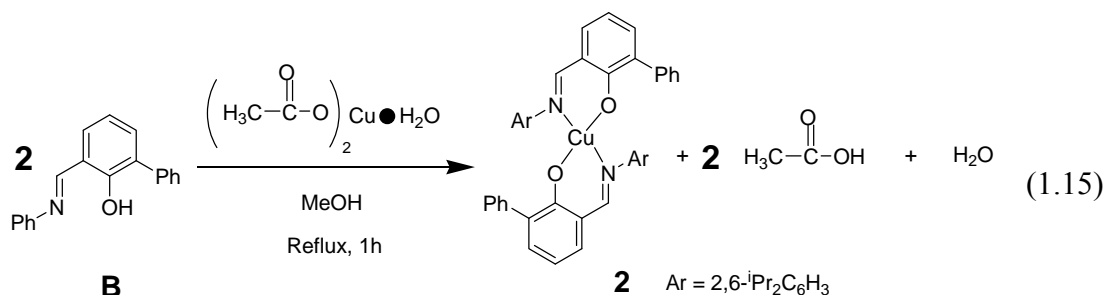
**Table 1.2.** Selected Bond Distances (Å) and Angles (°) for Complex 1.

	<u>Bond Distances (Å)</u>
Cu(1)-N(1)	1.993(5)
Cu(1)-O(1)	1.895(3)
Cu(1)-N(2)	1.989(5)
Cu(1)-O(2)	1.890(4)
O(2)-Cu(1)-O(1)	150.40(16)
O(2)-Cu(1)-N(2)	93.63(19)
O(1)-Cu(1)-N(2)	95.12(18)
O(2)-Cu(1)-N(1)	96.01(18)
O(1)-Cu(1)-N(1)	94.15(17)
N(2)-Cu(1)-N(1)	142.34(19)
	<u>Angle (°)</u>
Dihedral angle	46.99(0.16)

The four coordinate copper complex had two chelating salicylaldiminato ligands. The dihedral angle of 47° indicated a distorted geometry. Geometry of the nitrogen and oxygen donor atoms coordinated to copper were between distorted tetrahedral and a square planar geometry. Bond length between Cu(1)-N(1) was 1.993 Å. The estimated standard deviation for the bond between Cu(1)-N(1) was +/- 0.005 Å. Bond length between Cu(1)-N(2) was 1.989 Å. The estimated standard deviation for the bond between Cu(1)-N(2) was +/- 0.005 Å. Bond lengths between Cu(1)-N(1) and Cu(1)-N(2) were within estimated standard deviation (1.99Å). Bond length between Cu(1)-O(1) was 1.895 Å. The estimated standard deviation for the bond between Cu(1)-O(1) was +/- 0.003 Å. Bond length between Cu(1)-O(2) was 1.890 Å. Copper-oxygen bond distances were within ESD, at 1.89Å.

### 1.2.2.2 Bis(2,6-diisopropylphenyl-5-phenyl-salicylaldiminato)copper(II) (Complex **2**).

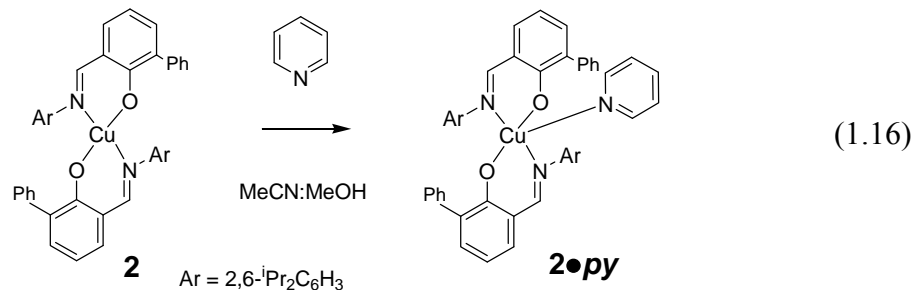
Bis(2,6-diisopropylphenyl-5-phenyl-salicylaldiminato)copper(II) was the second complex synthesized. Complex **2** was similar to complex **1**. The phenyl substituent on ligand **B** was slightly less bulky than the tert-butyl substituent of ligand **A**. Complexes **1**, **2**, and **3** were synthesized by the same procedure (Equation 1.15).



Complex **2** was characterized by FT-IR spectroscopy. The imine C=N stretch appeared at  $1604\text{ cm}^{-1}$  (Appendix A13). Compound **B** imine C=N stretch appeared at  $1616\text{ cm}^{-1}$  (Appendix A6). The imine C=N stretch shift was consistent with coordination of the imine nitrogen atom to electrophilic copper(II). The number of wavenumbers was expected to decrease by approximately  $10\text{-}20\text{ cm}^{-1}$ . The bond strength increased as electron density increased in the C=N bond.

### 1.2.2.3 Bis(2,6-diisopropylphenyl-5-phenyl-salicylaldiminato)pyridine copper(II) (Complex **2** • *py*).

X-ray quality crystals were not grown for complex **2**. An air stable pyridine adduct was synthesized (Equation 1.16).



Green-brown product was crystallized from acetonitrile and methanol. Crystallization took place in the presence of pyridine. Block-like crystals were X-ray quality. The crystals of **2 • py** were grown by slow evaporation (Figure 1.8).

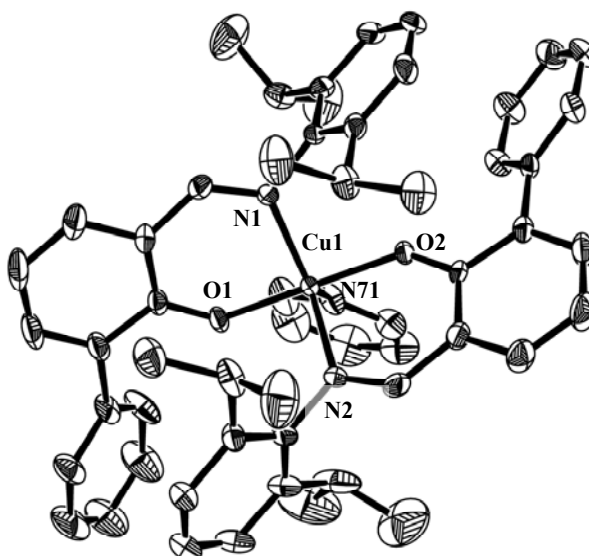


**Figure 1.8.** Molecular Structure of **2 • py** with Thermal Ellipsoids at the 50% Probability Level. H Atoms are Omitted for Clarity.



The copper complex had distorted trigonal bipyramidal geometry (Figure 1.9).

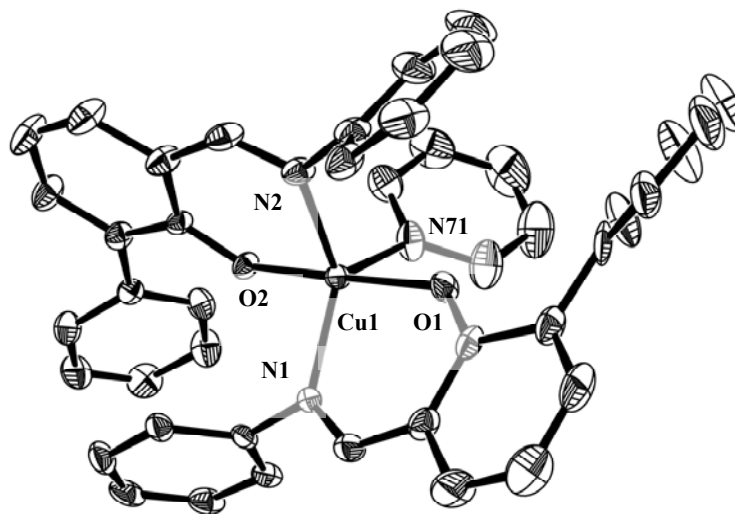


**Figure 1.9.** Molecular Structure of **2 • py** with Thermal Ellipsoids at the 50% Probability Level. H Atoms and <sup>i</sup>Pr Groups are Omitted for Clarity.

The crystal system was monoclinic and belonged to the  $P2_1/c$  space group (Table 1.3).

**Table 1.3.** Crystallographic Data and Details of Refinement for Complex **2** • *py*.

Empirical formula	C55 H57 Cu N3 O2
Formula weight	855.58
Crystal system	Monoclinic
Space group	$P2_1/c$
$a, b, c$ , (Å)	14.3190(7), 20.2260(9), 18.7410(17)
$\alpha$ (°)	90
$\beta$ (°)	122.149(3)
$\gamma$ (°)	90
$V$ (Å <sup>3</sup> )	4595.4(5) (calc. 4595.5(5))
$Z$	4
$D_{\text{calcd}}$ (Mg/m <sup>3</sup> )	1.237
Absorption coefficient (mm <sup>-1</sup> )	0.520
$T(K)$	173(2)
Total reflections	34676
Independent reflections	9347 [R(int) = 0.0000]
R indices (all data)	R1 = 0.0966, wR2 = 0.1839
Final R indices [I > 2sigma(I)]	R1 = 0.0520, wR2 = 0.1126
Goodness-of-fit on $F^2$	1.040

Final R indices were reasonably good, R1 = 0.0520. The crystal was publication quality. Nitrogen and oxygen donor atoms coordinated to copper(II) were arranged in trigonal bipyramidal geometry (Table 1.4).

**Table 1.4.** Selected Bond Distances (Å) and Angles (°) for Complex **2 • py**.

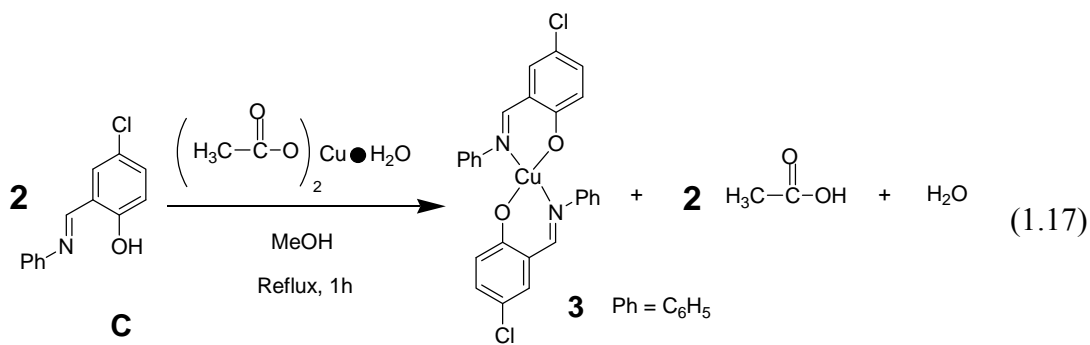
	<u>Bond Distances (Å)</u>
Cu(1)-N(1)	2.0398(19)
Cu(1)-N(2)	2.070(2)
Cu(1)-N(71)	2.198(2)
Cu(1)-O(1)	1.9146(16)
Cu(1)-O(2)	1.9177(16)
	<u>Angle (°)</u>
O(1)-Cu(1)-O(2)	172.32(7)
N(1)-Cu(1)-N(2)	125.89(8)
N(1)-Cu(1)-N(71)	122.57(8)
N(2)-Cu(1)-N(71)	111.54(9)
O(1)-Cu(1)-N(1)	90.73(7)
O(2)-Cu(1)-N(1)	92.42(7)
O(1)-Cu(1)-N(2)	93.03(8)
O(2)-Cu(1)-N(2)	90.79(7)
O(1)-Cu(1)-N(71)	86.00(8)
O(2)-Cu(1)-N(71)	86.41(8)

Oxygen donor atoms occupied the axial position. Nitrogen donor atoms from the ligands occupied the equatorial positions. Axial oxygen atoms were nearly 180° apart, O(1)-Cu(1)-O(2) is 172.32(7)°. The sum of three angles between equatorial nitrogen atoms was exactly 360°: (a) N(1)-Cu(1)-N(2) = 125.89(8)°, (b) N(1)-Cu(1)-N(71) 122.57(8)°, and (c) N(2)-Cu(1)-N(71) 111.54(9)°. Bond length between Cu(1)-N(1) was 2.0398 Å. The estimated standard deviation between Cu(1)-N(1) was +/- 0.0019 Å. Bond length between Cu(1)-N(2) was 2.07 Å. The estimated standard deviation between Cu(1)-N(2) was +/- 0.002 Å. The bond lengths between Cu(1)-N(1) and Cu(1)-N(2) were not within a standard deviation. The bond length between Cu(1)-N(71) was 2.198 Å. The estimated standard deviation between Cu(1)-N(71) was +/- 0.002 Å. Bond length between copper and the pyridine nitrogen atom were not within a standard of the other copper-nitrogen bond lengths. The Cu(1)-N(71) bond length was shorter than the

only other reported (SAL)<sub>2</sub>copper(II)py complex, 2.308(6) Å.<sup>26</sup> Bond length between Cu(1)-O(1) was 1.9146 Å. The estimated standard deviation between Cu(1)-O(1) was +/- 0.0016 Å. Bond length between Cu(1)-O(2) was 1.9177 Å. The estimated standard deviation between Cu(1)-O(2) was +/- 0.0016 Å. Bond lengths between Cu(1)-O(1) and Cu(1)-O(2) were identical within estimated standard deviation (1.92 Å).

#### 1.2.2.4 Bis(phenyl-3-chloro-salicylaldiminato)copper(II) (Complex 3).

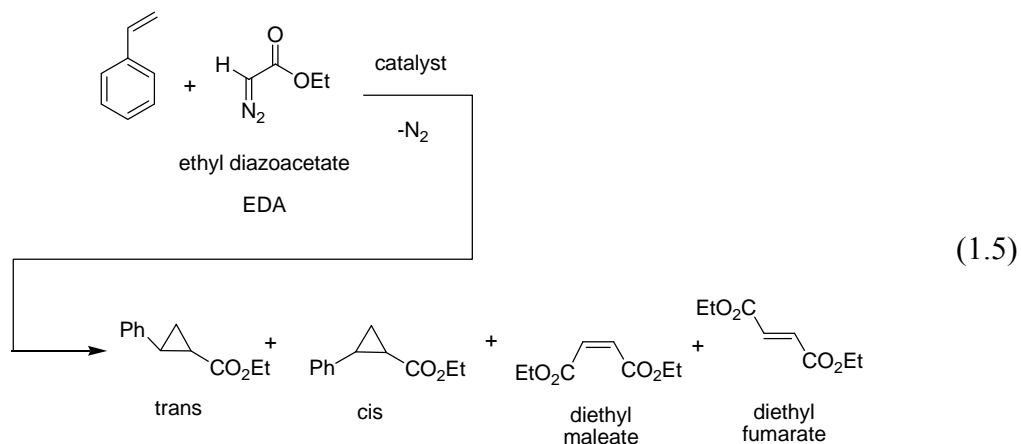
Complexes **1**, **2**, and **3** were synthesized by the same procedure.(Equation 1.17).<sup>20</sup>



Complex **3** was characterized by FT-IR spectroscopy. The imine C=N stretch appeared at 1608 cm<sup>-1</sup> (Appendix A14). Compound **C** imine C=N stretch appeared at 1615 cm<sup>-1</sup> (Appendix A8). The imine C=N stretch shift was consistent with coordination of the imine nitrogen atom to electrophilic copper(II). The bond strength should increase as electron density increased in the C=N bond. The number of wavenumbers was expected to decrease by 10-20 cm<sup>-1</sup>.

#### 1.2.3 Cyclopropanation Reactions

Reaction temperature and EDA addition rates were carefully controlled. Homogeneous copper(II) catalyzed cyclopropanation of styrene and EDA were tested (Equation 1.5).



Refer to Section 1.4.5 for the synthetic details. Catalytic activity was determined by product yield. Cyclopropanation yields were determined by gravimetric analysis and  $^1\text{H}$  NMR spectroscopy. The last proton NMR spectra in the appendix show the chemical shift frequency in Hz. The chemical shift scale is best displayed in parts per million (ppm). Chemical shift may be converted from Hz to ppm by dividing chemical shift in Hz by the operating frequency of the instrument.<sup>27</sup> The Bruker instrument operates at 500.2331 Mhz. A diagnostic  $\text{CH}_2$ -quadruplet appears at 4.16 ppm (or, averaged to 2082.68 Hz) for ethyl *trans*-2-phenylcyclopropanecarboxylate. Ethyl *cis*-2-phenylcyclopropanecarboxylate has a diagnostic  $\text{CH}_2$ -quadruplet 3.86 ppm(or, averaged to 1933.1 Hz) (Appendix A15). The *cis*- diastereomer  $\text{CH}_2$ -quadruplets are shielded by 0.3 ppm. The  $\text{CH}_2$ -quadruplets are shielded because the phenyl rings are located *cis*- to the ethyl  $\text{CH}_2$  protons.<sup>19</sup> Yields were calculated based on the moles of ethyl diazoacetate used for each the experiment. Side products were also monitored by  $^1\text{H}$  NMR spectroscopy. Results were tabulated in Table 1.5.

**Table 1.5.** Cyclopropanation Results

Entry	Catalyst	Temp. (°C)	Addition Time (hrs)	Cyclopropanation Averages			Dimerization Averages		
				%yield	cis	trans	%yield	cis	trans
1 <sup>a</sup>	1	50.0	4	41.8	29.0	71.0	5.4	36.2	63.8
2 <sup>a</sup>	1	80.0	4	63.8	25.2	74.8	0.8	63.1	36.9
3 <sup>b</sup>	1	rt	4	9.3	30.7	69.3	0.0	0.0	0.0
4 <sup>b</sup>	2	50.0	4	62.6	28.2	71.8	0.5	55.7	44.3
5 <sup>a</sup>	2	80.0	4	61.9	23.2	76.8	0.8	57.9	42.1
6 <sup>b</sup>	2	rt	4	0.0	0.0	0.0	0.0	0.0	0.0
7 <sup>*,c</sup>	3	60.0	6	81.7	25.3	74.7	0.0	0.0	0.0
8 <sup>*,c</sup>	1	60.0	6	70.6	25.5	74.5	0.0	0.0	0.0
9 <sup>*,c,†</sup>		60.0	6	16.2	29.3	70.7	0.6	58.9	41.1
10 <sup>*,c,†</sup>		60.0	6	10.7	27.7	72.3	0.6	55.6	44.4

\*Run in 1,2-dichloroethane, (all other runs in CH<sub>2</sub>Cl<sub>2</sub>).

<sup>a</sup>Three samples were run per entry.

<sup>b</sup>Two samples were run per entry.

<sup>c</sup>A single sample was run per entry.

<sup>†</sup>No catalyst was employed.

The cyclopropane *cis:trans* ratios are similar because the SAL ligand mildly influenced diastereoselectivity. Steric bulk had no significant effect because SAL did not possess the correct symmetry. The ligand belonged to the C<sub>1</sub> point group in the solid state.

There was no way to predict how steric bulk and symmetry affect *cis:trans* ratios.

However, it is possible to qualitatively infer how the ligand's electronic properties influenced the experimental results. Entries 1 and 2 for complex **1** demonstrated increased percent yield of *cis*- and *trans*- diastereomers. Increasing reaction temperature from 50 to 80 °C appears to have increased yield. The relative ratio of *cis:trans* diastereomers remains approximately constant. Side product yields decrease with increased reaction temperature. The reversal in *cis:trans* diastereomers for side products does not have an explanation. Entry 3 at room temperature demonstrated significant decrease in cyclopropane yield. Diastereomeric ratios were consistent with trials 1 and 2. Perhaps the activation energy barrier was just low enough at room temperature to initiate low catalytic activity. Side products were not formed. The EDA was tied up in cyclopropanation. Higher temperatures were required to increase cyclopropane yield. The room temperature reaction in entry 3 produced a 9.3% yield of *cis:trans* cyclopropanated products for two sample runs. Yield increased to 42% at 50° C . At 80° C the yield increased to 63.8%. Side product yield increased marginally when temperature increased from room temperature to 80° C. Generally, at a higher temperature more of the EDA and styrene was converted to cyclopropanes. Some EDA thermally decomposed. Dimerization resulted from interaction of free triplet carbenes with EDA. Few side products are produced at room temperature because complex **1** is very effective. Side products are observed in entries 9 and 10 of Table 1.5. In the absence of a copper catalyst EDA thermally decomposed. Free triplet carbenes are produce *in situ*. Dimers are produced when carbenes react with EDA.

A similar trend is noted for catalyst **2**. Catalyst **2** was not active at room temperature. The steric and electronic characteristics of compound **B** were likely responsible for inactivity. Magnetic susceptibility measurements may have revealed that catalyst **2** did not have a single unpaired electron. Elemental analysis revealed that the catalyst was not impure. Catalyst **2** may have decomposed before elemental analysis was complete. Perhaps catalyst **2** had a higher activation energy barrier to form the

copper-carbene/ylide intermediate. There appears to be a mild effect of the ligand environment upon catalytic activity. Increasing reaction temperature from 50 to 80° C produced no significant change in *cis:trans* diastereoselectivity. The percent yield of dimerization products displayed little sensitivity to reaction temperature changes. Room temperature reactions for catalyst **2**, as seen in entry 6 of Table 1.5, appeared to be completely inactive. The precatalyst does not have the ability to surmount the energy barrier to form an intermediate copper-carbene and/or copper-ylide species. There was not sufficient thermal energy to decompose the ethyl diazoacetate. No products or side products were formed. Copper(I)-carbene/ylide transition state species may have become unstable and less active at low temperature.

Catalyst **3** (see entry 7 of Table 1.5) produced higher yield than catalyst **1** (see entry 8 of Table 5). Higher reaction temperature over trials 1 and 4 may have contributed to improved results. Diazo compounds have very reactive C=N bonds. Slow addition of EDA to the copper catalyst maximized cyclopropane yield. Physicochemical data for dichloromethane and 1,2-dichloroethane in cyclopropanation reactions had not been worked out. No correlation between solvent and yield could have been determined. Longer reaction time and changing solvent appears to increase cyclopropane yields. Side products are reduced by combining slow EDA addition rate and 1,2-DCE solvent. Catalyst **3** produced moderately higher yields than catalyst **1**. Electronic and steric characteristics appear partly to be responsible for mildly improved performance.



## 1.3 CONCLUSION

There were a number of important scientific contributions made during this project. Three catalysts were synthesized and two new crystal structures were solved. Two of the SAL ligands employed were only previously seen in group 6 and group 10 catalysts. A pilot investigation was undertaken to study the diastereoselective copper(II) catalyzed cyclopropanation. All three complexes were active for the cyclopropanation. Steric bulk has not been found to significantly influence diastereoselectivity. Mild differences were observed between the catalysts. However, many of the findings need to be reproduced before a confidence level is attached to the observations. The ligand environment does not have the correct symmetry. SAL has  $C_1$  symmetry in the solid state. No amount of steric bulk can significantly influence the *cis:trans* ratio for the SAL ligand. The results indicated that non-catalyzed and catalyzed cyclopropanation reactions had similar diastereoselectivity ratios. Ligand environment, solvent choice, and reaction temperature affect catalytic activity. Some general trends were observed from this investigation. Our results indicated that 1,2-dichloroethane may contribute to higher cyclopropane yields. Dichloromethane was a poorer solvent choice. The relative amount of dimerization products significantly decreased with 1,2-dichloroethane. Reactions run at six hours in 1,2-dichloroethane cannot be compared directly. It is likely that optimal reaction conditions are reached when 1,2-DCE was used with slow addition of EDA. Slow addition of diazo compound decreased side product formation.<sup>17</sup> Publication quality X-ray crystal structures are significant research contributions. The research contribution is significant because the complexes have never been used to study diastereoselective cyclopropanation reactions.

### 1.3.1 Recommendations for future investigation

Improved methodology would permit comparison between reaction conditions. Again, many of the findings need to be reproduced. Control variables needed to be held fixed. A single independent variable was needed to compare results. Firm conclusions about catalytic activity will require a more rigorous scientific investigation.

## 1.4 EXPERIMENTAL SECTION

### 1.4.1 General Considerations

All reactions were carried out using standard Schlenk techniques or in a glovebox. Glassware was flame and oven dried prior to use. THF, diethyl ether, acetonitrile, and toluene were dried using a Braun solvent purification system. Methanol was HPLC grade and was not dried prior to use. Xylene, cumene, and super dry ethanol were ACS grade and not dried prior to use. 1,2-DCE was ACS grade and was dried over 4 Angstrom molecular sieves. Formic acid and hydrochloric acid 95% purity was ACS grade. Aniline 99.5% purity was purchased from Sigma Aldrich. Sodium chloride and magnesium sulfate were ACS grade reagents purchased from EMD Chemicals Inc.. Copper(II) acetate monohydrate 98+% purity was ACS grade and purchased from Sigma Aldrich. Sodium sulfate and sodium carbonate were GR ACS grade reagents and purchased from EMD Chemicals Inc.. 2,4,6-Tribromoaniline 98% purity and 2-hydroxybiphenyl 99% purity were high purity research grade reagents purchased from Alfa Aesar. Tributylamine 99% purity was puriss grade and purchased from Sigma Aldrich. 2,6-Diisopropylaniline 90% was a technical grade reagent purchased from Sigma Aldrich. Ethyl diazoacetate  $\leq 10\%$  DCM was purum grade and purchased from Sigma Aldrich. Pyridine  $\geq 99\%$  purity and styrene  $\geq 99\%$  purity were reagent plus grade and purchased from Sigma Aldrich. 3,5-Di-*tert*-butyl-hydroxybenzaldehyde 99% purity, paraformaldehyde 95% purity, 5-chlorosalicylaldehyde 98% purity, phenylboronic acid

95% purity, and tetrakis(triphenylphosphine) palladium(0) 99% purity were reagent grade and purchased from Sigma Aldrich. Tin(IV) chloride anhydrous 99% purity was a “metals basis” reagent purchased from Lancaster Synthesis, Inc.. Reagents were not purified or dried prior to use. Modified literature procedures were also used for making 2-hydroxy-biphenyl-3-carbaldehyde.<sup>23</sup> Literature preparations were often modified to optimize the mass of product. Some organic preparations were designed to produce an undesirable quantity of product. Compounds **A**, **B** and **C** were synthesized by slight modifications of the literature procedures.<sup>21</sup> Phenoxyimines incorporating greater steric bulk were attempted by condensation reactions with bulky triphenylanilines and substituted benzaldehydes by modification of published procedures.<sup>24, 25</sup> 2,4,6-Triphenylaniline was columned on silica gel 60. The silica gel was purchased from EMD Chemicals Inc.. Complex **3** is a literature compound.<sup>20</sup> Complexes **1**, **2**, and **3** were synthesized by the same procedure. Typical cyclopropanation reactions were run according to literature procedure.<sup>28</sup> Proton NMR spectra were recorded on a 500 MHz Bruker DRK NMR spectrometer with a 5 mm BBI probe. <sup>1</sup>H chemical shifts were referenced to the residual protons of the deuterated solvents (CDCl<sub>3</sub> at  $\delta$  7.26 and C<sub>6</sub>D<sub>6</sub> at  $\delta$  7.16). Elemental analyses were performed on a Perkin-Elmer 2400 CHN elemental analyzer. Potassium bromide FT-IR was performed on a Bruker Tensor 27 DTGS CsI. Magnetic susceptibility measurements were performed on a Johnson Matthey MSB Mark 1.

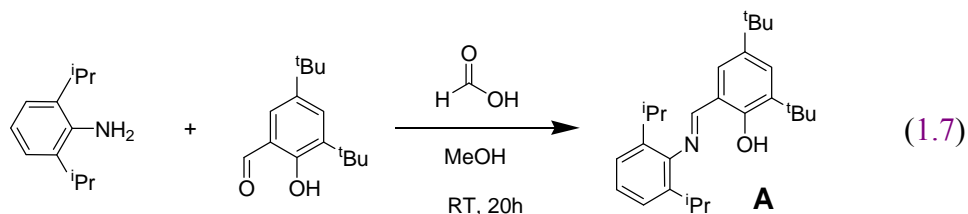
#### 1.4.2 X-ray Structural Analysis for Complexes **1** and **2** • *py*

Crystallographic data for structures **1** and **2** • *py* were collected at -100°C on a Nonius Kappa CCD diffractometer, using the COLLECT program.<sup>29</sup> Cell refinement plus data reductions used the programs DENZO and SCALEPACK.<sup>30</sup> SHELXS97<sup>31</sup> was used to solve the structure and SHELXL97<sup>31</sup> was used to refine the structure. ORTEP-3

for Windows<sup>32</sup> was used for molecular graphics, and PLATON<sup>33</sup> was used to prepare material for publication.

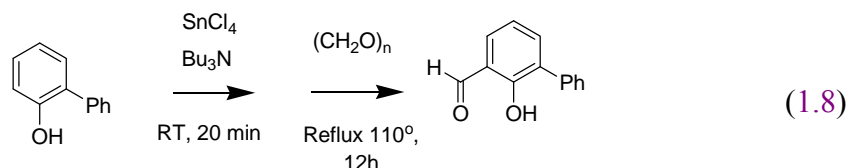
### 1.4.3 Ligand Synthesis

#### 1.4.3.1 2,6-Diisopropylphenyl-3,5-di-*tert*-butyl-salicylaldimine (Compound A).



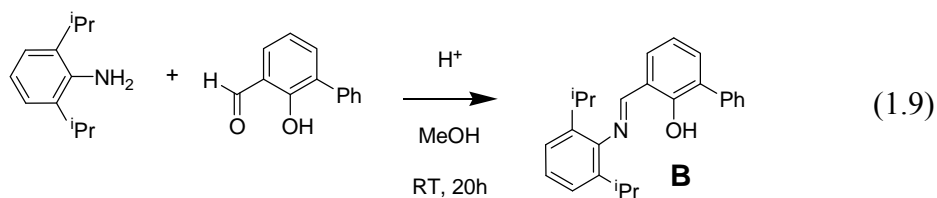
3,5-Di-*tert*-butyl-hydroxybenzaldehyde (2.81 g, 12.0 mmol) was dissolved in methanol (15 ml). The solution was stirred under nitrogen. Formic acid (0.50 ml, 13.2 mmol) was added to the solution. 2,6-Diisopropylaniline (2.84 g, 16.0 mmol) was added to the reaction mixture. The solution was stirred at room temperature for 20h. A yellow oil was isolated and dried under vacuum. Yellow crystals were obtained from methanol at -27 °C. Yield: 4.74 g (76.3%). Mp 87.5-90.0 °C; <sup>1</sup>H NMR (500 MHz, CDCl<sub>3</sub>): δ 13.46 (s, 1H, Ar-OH), 8.29 (s, 1H, Ar-N=CH-Ar), 7.51 (d, *J* = 2.3 Hz, 1H, Ar-*H*), 7.04-7.20 (m, 4H, Ar-*H*), 3.02 (sept., *J* = 6.8 Hz, 2H, CH(CH<sub>3</sub>)<sub>3</sub>), 1.50 (s, 9H, *t*-Bu), 1.34 (s, 9H, *t*-Bu), 1.18 (d, *J* = 6.8 Hz, 12 H, CH(CH<sub>3</sub>)<sub>3</sub>) (Appendix A1). <sup>1</sup>H NMR (500 MHz, C<sub>6</sub>D<sub>6</sub>): δ 13.98 (s, 1H, Ar-OH), 7.97 (s, 1H, Ar-N=CH-Ar), 7.65 (d, *J* = 2.3 Hz, 1H, Ar-*H*), 7.16-7.08 (m, 4H, Ar-*H*), 3.02 (sept., *J* = 6.8 Hz, 2H, CH(CH<sub>3</sub>)<sub>3</sub>), 1.67 (s, 9H, *t*-Bu), 1.30 (s, 9H, *t*-Bu), 1.06 (d, *J* = 6.8 Hz, 12 H, CH(CH<sub>3</sub>)<sub>3</sub>) (Appendix A2). IR (KBr, cm<sup>-1</sup>): at 1622 (s) (C=N) (Appendix A3). UV-Vis (hexane): ε<sub>max</sub> = 1.96 x 10<sup>7</sup> m<sup>2</sup> mol<sup>-1</sup>, λ<sub>max</sub> = 368 nm.

#### 1.4.3.2 2-Hydroxy-biphenyl-3-carbaldehyde



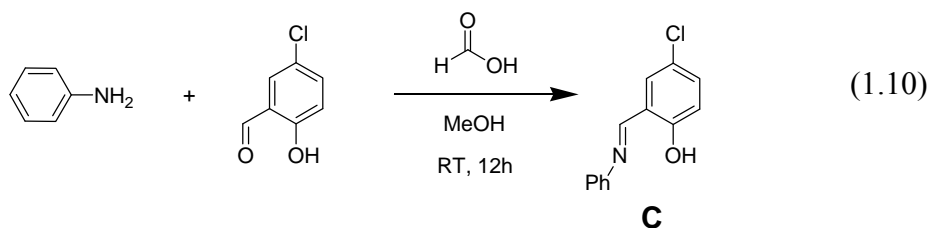
2-Hydroxybiphenyl (85.1 g, 0.50 mmol) was dissolved in dry toluene (100 ml). The solution was stirred under nitrogen. Tributylamine (47.6 ml, 0.20 mmol) was added via syringe.  $\text{SnCl}_4$  (5.84 ml,  $5.0 \times 10^{-1}$  mmol) was added by syringe to the reaction flask. The solution was stirred for 20 minutes. Paraformaldehyde (33.0 g) was added to the reaction flask under a high flow of nitrogen gas. The solution was refluxed at 110 °C for 12h. The crude was cooled and poured into water acidified to pH 2 with 2N-hydrochloric acid. The organic phase was extracted with ether. The crude was washed with saturated NaCl. The remaining water from the dilute acid was removed from the organic phase with  $\text{Na}_2\text{SO}_4$ . Organic solvent was removed *in vacuo*. The light yellow oily crude used without further purification. The product consisted of a 50/50 mixture of 2-hydroxy-biphenyl-3-carbaldehyde and 2-hydroxybiphenyl. Yield: 85.1 g (50.0%).  $^1\text{H}$  NMR (500 MHz,  $\text{CDCl}_3$ )  $\delta$  11.56 (s, 1H), 9.97 (s, 1H), 7.00-7.77 (m, 8H) (Appendix A4).

#### 1.4.3.3 2,6-Diisopropylphenyl-5-phenyl-salicylalimine (Complex **B**).



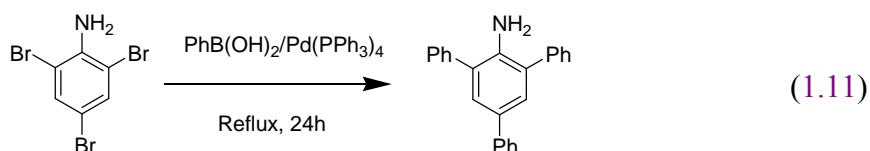
2-Hydroxy-biphenyl-3-carbaldehyde (9.00 g, 24.4 mmol) was dissolved in methanol (30 ml). The solution was stirred under nitrogen. Formic acid (1.02 ml, 27.0 mmol) was added to the solution. 2,6-Diisopropylaniline (5.76 g, 32.5 mmol) was added and the reaction mixture. The reaction mixture was stirred at room temperature for 20h. Yellow crystals were obtained from methanol at -27 °C. Yield: 4.35 g (49.8%). Mp 72.5-76.0 °C; <sup>1</sup>H NMR (500 MHz, CDCl<sub>3</sub>) δ 13.68 (s, 1H, Ar-OH), 8.43 (s, 1H, Ar-N=CH-Ar), 7.60-7.07 (m, 11H, Ar-H), 3.08 (sept., *J* = 6.8 Hz, 2H, CH(CH<sub>3</sub>)<sub>3</sub>), 1.25 (d, *J* = 6.8 Hz, 12 H, CH(CH<sub>3</sub>)<sub>3</sub>) (Appendix A5). IR (KBr, cm<sup>-1</sup>): 1616 (s) (C=N) (Appendix A6). UV-Vis (hexane): ε<sub>max</sub> = 5.10 x 10<sup>7</sup> m<sup>2</sup> mol<sup>-1</sup>, λ<sub>max</sub> = 361 nm.

#### 1.4.3.4 Phenyl-3-chloro-salicylaldimine (Compound C).



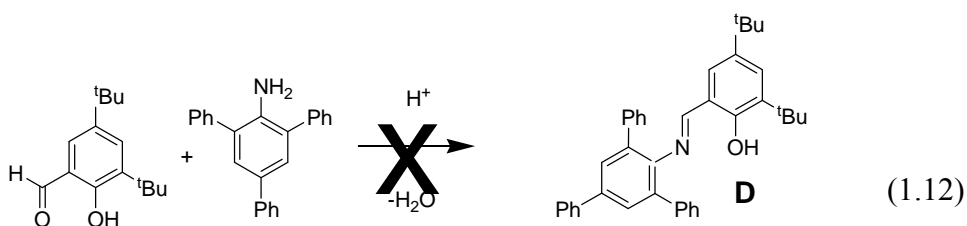
5-Chlorosalicylaldehyde (3.01 g, 19.2 mmol) was dissolved in methanol (20 ml). The solution was stirred under nitrogen. Formic acid (0.80 ml, 21.1 mmol) was added to the solution. Aniline (2.38 g, 25.6 mmol) was added to the reaction mixture. The solution was stirred at room temperature for 12h. Orange crystals were obtained from methanol at room temperature. Additional crystals were obtained by crystallizing from methanol at -27 °C. Yield: 3.84 g (94.6 %). Mp 100.0-111.0 °C; <sup>1</sup>H NMR (500 MHz, CDCl<sub>3</sub>): δ 13.25 (br s, 1H, Ar-OH), 8.56 (s, 1H, Ar-N=CH-Ar), 7.46-7.26 (m, 7H, Ar-H), 6.98 (d, *J* = 8.80 Hz, 1 H) (Appendix A7). IR (KBr, cm<sup>-1</sup>): 1615 (s) (C=N) (Appendix A8). UV-Vis (hexane): ε<sub>max</sub> = 2.16 x 10<sup>7</sup> m<sup>2</sup> mol<sup>-1</sup>, λ<sub>max</sub> = 368 nm.

#### 1.4.3.5 2,4,6-Triphenylaniline



2,4,6-Tribromoaniline (1.28 g, 3.89 mmol) was dissolved in benzene (38.9 ml). The solution was stirred under nitrogen. A second solution was prepared. Phenylboronic acid (1.89 g, 15.6 mmol) was dissolved in ethanol (7.78 ml). The second solution was stirred under nitrogen. 2.0M Na<sub>2</sub>CO<sub>3</sub> (15.6 ml) and Pd(PPh<sub>3</sub>)<sub>4</sub> (0.583 g, 0.466 mmol) were added to the second solution. The second solution was added to the 2,4,6-tribromoaniline solution under a high flow of nitrogen gas. The reactants were refluxed for 24h. The organic phase was extracted with ether (2 x 62 ml). The remaining water from the aqueous Na<sub>2</sub>CO<sub>3</sub> was removed from the organic phase with MgSO<sub>4</sub>. Organic solvents were removed *in vacuo*. The crude was purified by literature procedure.<sup>25</sup> 2,4,6-Triphenylaniline was chromatographed with benzene on silica gel, yield 78.2%. <sup>1</sup>H NMR (500 MHz, CDCl<sub>3</sub>):  $\delta$  7.67-7.44 (m, 17H, Ar-H), 3.97 (br s, 2H, Ar-NH<sub>2</sub>) (Appendix A9). Triphenylaniline was used to synthesize ligands **D** and **E**.

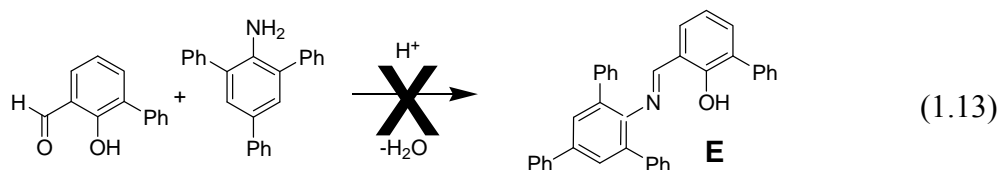
#### 1.4.3.6 Attempted Synthesis of 2,4,6-Triphenylbenzene-3,5-di-*tert*-butylsalicylaldimine (Compound **D**).



3,5-Di-*tert*-hydroxybenzaldehyde (165 mg, 0.7 mmol) was dissolved in methanol (10 ml). The solution was stirred under nitrogen. Formic acid (0.03 ml, 0.8 mmol) was

added to the solution. 2,4,6-Triphenylaniline (300 mg, 0.9 mmol) was added to the reaction mixture. The solution was stirred at room temperature for 10h. The solvent was removed *in vacuo*. Starting materials were recovered. The recovered starting materials were refluxed in xylene for over 12 h. Additional formic acid (0.03 ml, 0.772 mmol) was added to the reaction flask. Xylene was removed *in vacuo* after the reaction was terminated. Compound **D** was not observed by  $^1\text{H}$  NMR analysis. Starting materials were recovered. The recovered starting materials were refluxed in cumene for over 12h. Formic acid was not added to the cumene solution. Compound **D** was not observed in any detectable amount by  $^1\text{H}$  NMR analysis (Appendix A10).

#### 1.4.3.7 Attempted synthesis of 2,4,6-Triphenyl-5-phenyl-salicylaldimine (Compound **E**).



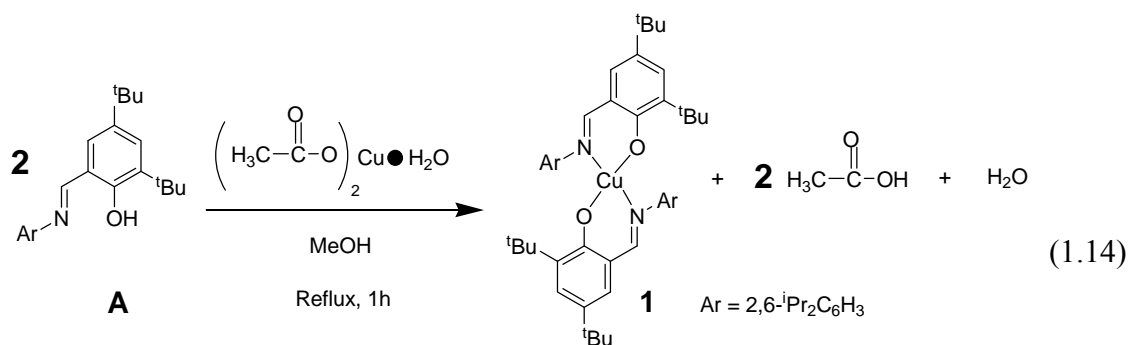
2-Hydroxy-biphenyl-3-carbaldehyde (257 mg, 0.7 mmol) was dissolved in methanol (10 ml). The solution was stirred under nitrogen. Formic acid (0.03 ml, 0.7 mmol) was added to the solution. 2,4,6-Triphenylaniline (277 mg, 0.9 mmol) was added to the reaction mixture. The solution was stirred at room temperature for 10h. The solvent was removed *in vacuo*. Starting materials were recovered. The recovered starting materials were refluxed in xylene for over 12h. Additional formic acid (0.03 ml, 0.8 mmol) was added to the reaction flask. Xylene was removed *in vacuo* after the reaction was terminated. Starting materials were recovered. Trace amounts of compound **E** were detectable by  $^1\text{H}$  NMR. Less than 5% of compound **E** was observed by  $^1\text{H}$  NMR analysis (Appendix A11). The recovered starting materials were refluxed in



cumene for over 12h. Formic acid was not added to the cumene solution. Compound **D** was not observed in any detectable amount by  $^1\text{H}$  NMR analysis.

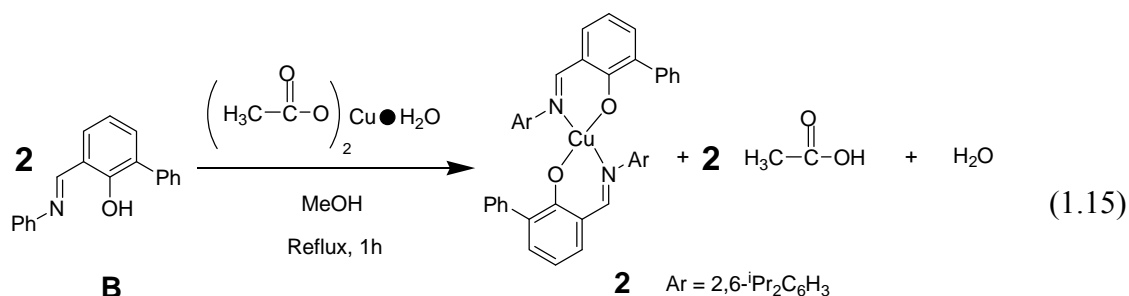
#### 1.4.4 Bis(salicylaldiminato) Copper(II) Complexes

##### 1.4.4.1 Bis(2,6-diisopropylphenyl-3,5-di-*tert*-butylsalicylaldiminato)copper(II) (Complex **1**).



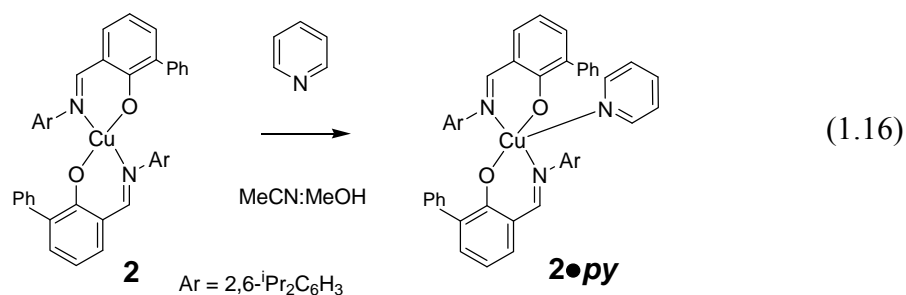
Compound **A** (0.79 g, 1.98 mmol) was dissolved in methanol (40 ml). Copper acetate monohydrate (0.20 g, 0.99 mmol) was quantitatively transferred to the solution with methanol (3 ml). The mixture was refluxed for 1 hour. Toluene boils at 110-111 °C. Afterward, the mixture was allowed to cool to room temperature. Solvent was removed *in vacuo*. The product was not purified. The solvent was removed *in vacuo*. Yield: 0.66 g, (78.3 %). Anal. Calcd for C<sub>54</sub>H<sub>76</sub>N<sub>2</sub>O<sub>2</sub>Cu: C, 76.42; H, 9.03; N, 3.30. Found: C, 75.01; H, 8.84; N, 2.76. Decomp. 243.0-250.0 °C; IR (KBr, cm<sup>-1</sup>): 1611 (s) (C=N) (Appendix A12). UV-Vis (hexane):  $\epsilon_{\text{max}} = 5.24 \times 10^7 \text{ m}^2 \text{ mol}^{-1}$ ,  $\lambda_{\text{max}} = 399 \text{ nm}$ .  $\mu_{\text{eff}} = 1.78 \text{ BM}$ . Brown needle-like crystals were obtained by slow evaporation of methanol. The X-ray quality crystals were grown in the fume hood.

1.4.4.2 Bis(2,6-diisopropylphenyl-5-phenyl-salicylaldiminato)copper(II) (Complex **2**).



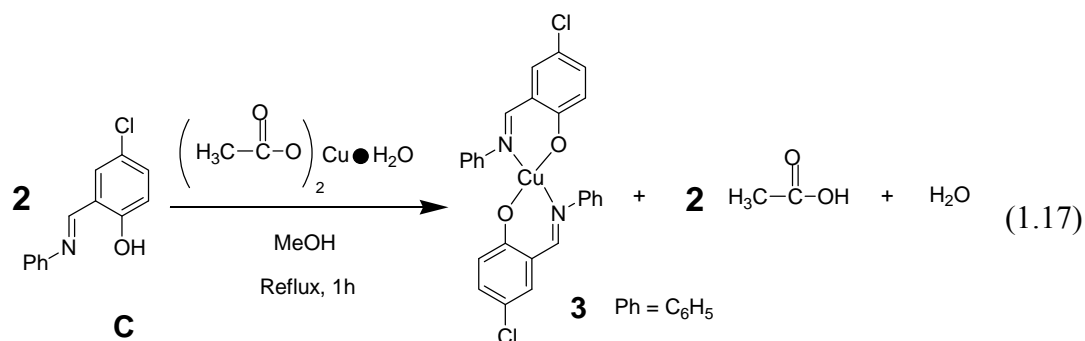
Compound **B** (0.51 g, 1.41 mmol) was dissolved in methanol (40 ml). Copper acetate monohydrate (0.14 g, 0.71 mmol) was quantitatively transferred to the above solution with methanol (3 ml). The mixture was refluxed for 1 hour. Afterward, the mixture was allowed to cool to room temperature. The solvent was removed *in vacuo*. The product was a brown powder. Yield: 0.46g (83.6 %). Anal. Calcd for  $\text{C}_{50}\text{H}_{52}\text{N}_2\text{O}_2\text{Cu}$ : C, 77.34; H, 6.75; N, 3.60. Found: C, 77.17; H, 6.21; N, 2.59. Mp 215.0-220.0 °C; IR (KBr,  $\text{cm}^{-1}$ ): 1604 (s) (C=N) (Appendix A13). UV-Vis (hexane):  $\epsilon_{\text{max}} = 1.63 \times 10^7 \text{ m}^2 \text{ mol}^{-1}$ ,  $\lambda_{\text{max}} = 393 \text{ nm}$ .  $\mu_{\text{eff}} = 1.00 \text{ BM}$ .

1.4.4.3 Bis(2,6-diisopropylphenyl-5-phenyl-salicylaldiminato)pyridine Copper(II) (Complex **2 • py**).



Complex **2** was dissolved in a solvent mixture of 1:1 acetonitrile and methanol. Green-brown block-like crystals were grown by slow evaporation. Pyridine was added to the crystallization solvent. Block-like crystals were obtained by slow evaporation. The X-ray quality crystals were grown in the fume hood.

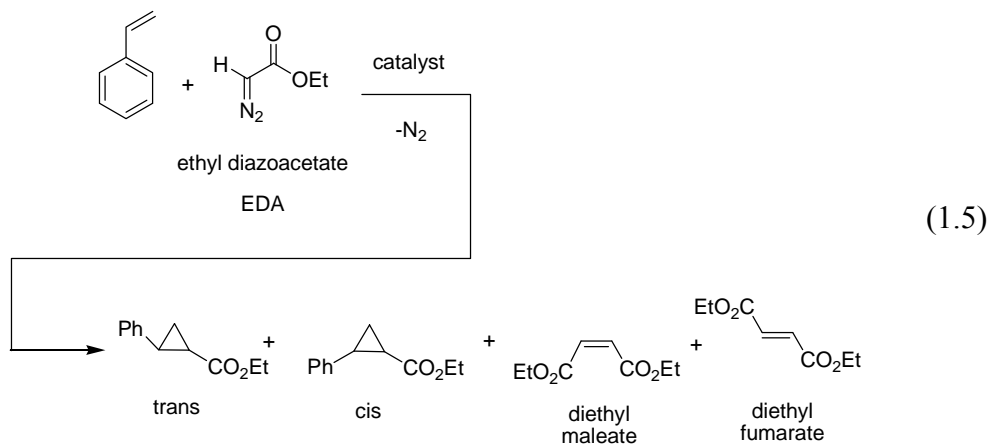
#### 1.4.4.4 Bis(phenyl-3-chloro-salicylaldiminato)copper(II) (Complex **3**)



Compound **C** (1.00 g, 4.32 mmol) was dissolved in methanol (40 ml). Copper acetate monohydrate (0.43 g, 2.16 mmol) was quantitatively transferred to the above solution with methanol (3 ml). The mixture was refluxed for 1 hour. Afterward, the mixture was allowed to cool to room temperature. The solvent was removed *in vacuo*. The product was a brown powder. Yield 1.07g (94.6 %). Decomp. 179.0-218.0 °C; IR (KBr, cm<sup>-1</sup>): 1608 (s) (C=N) (Appendix A14). UV-Vis (hexane):  $\epsilon_{\text{max}} = 5.90 \times 10^4 \text{ m}^2 \text{ mol}^{-1}$ ,  $\lambda_{\text{max}} = 399 \text{ nm}$ .  $\mu_{\text{eff}} = 2.03 \text{ BM}$ .

#### 1.4.5 General Procedure for Catalytic Cyclopropanation Reactions

Cyclopropanated yields were determined by gravimetric analysis and <sup>1</sup>H NMR spectroscopy, based on the moles of ethyl diazoacetate used during each the experiment. A typical reaction is described in the following way.



Catalyst **1**, **2**, or **3** (0.010 mmol) and styrene (8.73 mmol) were added to the reaction flask with 1,2-dichloroethane (2 ml). The reactants were stirred under nitrogen. Ethyl diazoacetate (1.00 mmol) in 1,2-dichloroethane (2 ml) by means of a syringe pump at 60 °C. EDA was added dropwise for 6 h. The reaction mixture was stirred for another 16 h at room temperature. Solvent was removed *in vacuo*. Products were characterized by NMR. The chemical shift scale is best displayed in parts per million (ppm). Chemical shift may be converted from Hz to ppm. Divide chemical shift in Hz by the operating frequency of the instrument.<sup>27</sup> The Bruker instrument operates at 500.2331 Mhz. A diagnostic CH<sub>2</sub>-quadruplet appears at 4.16 ppm (or, averaged to 2082.68 Hz) for ethyl *trans*-2-phenylcyclopropanecarboxylate. Ethyl *cis*-2-phenylcyclopropanecarboxylate has a diagnostic CH<sub>2</sub>-quadruplet 3.86 ppm(or, averaged to 1933.1 Hz) (Appendix A15). Yields were determined based on the moles of ethyl diazoacetate added to the reaction mixture (see Table 1.5).

## 5. REFERENCES AND NOTES

1. Wong, H. N. C.; Hon, M.-Y.; Tse, C.-W.; Yip, Y.-C.; Tanko, J.; Hudlicky, T. Use of cyclopropanes and their derivatives in organic synthesis. *Chem. Rev.* **1989**, *89* (1), 165-198.
2. Battiste, M. A.; Coxon, J. M. Acidity and basicity of cyclopropanes. In *The chemistry of the cyclopropyl group*; Part 1; John Wiley & Sons: New York, 1987; pp 255-305.
3. Li, A.-H.; Dai, L.-X. Asymmetric ylide reactions: Epoxidation, cyclopropanation, aziridination, olefination, and rearrangement. *Chem. Rev.* **1997**, *97* (6), 2341-2372.
4. Tidwell, T. T. Conjugative and substituent properties of the cyclopropyl group. In *The chemistry of the cyclopropyl group*; Part 1; John Wiley & Sons: New York, 1987; pp 565-632.
5. Nozaki, H.; Moriuti, S.; Takaya, H.; Noyori, R. Asymmetric induction in carbenoid reaction by means of a dissymmetric copper chelate. *Tetrahedron Lett.* **1966**, *7* (43), 5239-5244.
6. Salomon, R. G.; Kochi, J. K. Copper(I) catalysis in cyclopropanations with diazo compounds. The role of olefin coordination. *J. Am. Chem. Soc.* **1973**, *95* (10), 3300-3310.

7. Nozaki, H.; Takaya, H.; Moriuti, S.; Noyori, R. Homogeneous catalysis in the decomposition of diazo compounds by copper chelates: Asymmetric carbenoid reactions. *Tetrahedron* **1968**, *24* (9), 3655-3669.
8. Evans, D. A.; Woerpel, K. A.; Hinman, M. M.; Faul, M. M. Bis(oxazolines) as chiral ligands in metal-catalyzed asymmetric reactions. Catalytic, asymmetric cyclopropanation of olefins. *J. Am. Chem. Soc.* **1991**, *113* (2), 726-728.
9. Lowenthal, R. E.; Abiko, A.; Masamune, S. Asymmetric catalytic cyclopropanation of olefins: Bis-oxazoline copper complexes. *Tetrahedron Lett.* **1990**, *31* (42), 6005-6008.
10. Fritschi, H.; Leutenegger, U.; Pfaltz, A. Semicorrin metal complexes as enantioselective catalysts. Part 2. Enantioselective cyclopropane formation from olefins with diazo compounds catalyzed by chiral (semicorrinato)copper complexes. *Helv. Chim. Acta* **1988**, *71* (4), 1553-1565.
11. Doyle, M. J.; McKervey, M. A.; Ye, T. Intermolecular cyclopropanation and related addition reactions. In *Modern catalytic methods for organic synthesis with diazo compounds: From cyclopropanes to ylides*; John Wiley & Sons: New York, 1998; pp 163-237.
12. Christenson, D. L.; Tokar, C. J.; Tolman, W. B. New copper and rhodium cyclopropanation catalysts supported by chiral bis(pyrazolyl)pyridines. A metal-dependent enantioselectivity switch. *Organometallics* **1995**, *14* (5), 2148-2150.
13. Brunel, J. M.; Legrand, O.; Reymond, S.; Buono, G. First iminodiazaphospholidines with a stereogenic phosphorus center. Application to

asymmetric copper-catalyzed cyclopropanation. *J. Am. Chem. Soc.* **1999**, *121* (24), 5807-5808.

14. Diaz-Requejo, M. M.; Belderrain, T. R.; Trofimenko, S.; Pedro, J. P. Unprecedented highly *cis*-diastereoselective olefin cyclopropanation using copper homoscorpionate catalysts. *J. Am. Chem. Soc.* **2001**, *123* (13), 3167-3168.

15. Kirmse, W. Copper carbene complexes: Advanced catalysts, new insights. *Angew. Chem. Int. Ed.* **2003**, *42* (10), 1088-1093.

16. Li, Z.; Zheng, Z.; Chen, H. Highly efficient and enantioselective cyclopropanation of styrene with diazoacetates using a new copper-(Schiff-base) catalyst. *Tetrahedron: Asymmetry* **2000**, *11* (5), 1157-1163.

17. Maas, G. Transition-metal catalyzed decomposition of aliphatic diazo compounds-new results and applications in organic synthesis. In *Organic synthesis, reactions and mechanisms*; Springer-Verlag: Berlin, 1987; pp 75-253.

18. Smith, M. B.; March, J. Carbocations, carbanions, free radicals, carbenes, and nitrenes. In *March's advanced organic chemistry: Reactions, mechanisms, and structure*; 5 ed.; John Wiley & Sons: New York, 2001; pp 218-273.

19. Solladié-Cavallo, A.; Isarno, T. Unambiguous and rapid *cis/trans* assignment of aryl-carboxy disubstituted cyclopropanes using NMR. *Tetrahedron Lett.* **1999**, *40* (8), 1579-1582.

20. Harries, H. J.; Orford, B. F. 2-Phenyliminomethylphenols, 2-phenylaminomethylphenols and their copper(II) complexes. *Inorg. Chim. Acta* **1983**, *68*, 41-43.
21. Wang, C.; Friedrich, S.; Younkin, T. R.; Li, R. T.; Grubbs, R. H.; Bansleben, D. A.; Day, M. W. Neutral nickel(II)-based catalysts for ethylene polymerization. *Organometallics* **1998**, *17* (15), 3149-3151.
22. Younkin, T. R.; Connor, E. F.; Henderson, J. I.; Friedrich, S. K.; Grubbs, R. H.; Bansleben, D. A. Neutral, single-component nickel (II) polyolefin catalysts that tolerate heteroatoms. *Science* **2000**, *287* (5452), 460-462.
23. Casiraghi, G.; Casnati, G.; Puglia, G.; Sartori, G.; Terenghi, G. Selective reactions between phenols and formaldehyde. A novel route to salicylaldehydes. *J. Chem. Soc., Perkin Trans. I* **1980**, 1862-1865.
24. Dimroth, K.; Berndt, A.; Perst, H.; Reichardt, C.; Wat, E. K. W.; Benson, R. E. 2,4,6-Triphenylphenoxyl. *Org. Synth., Coll. Vol.* **1969**, *5*, 1130-1134.
25. Miura, Y.; Oka, H.; Momoki, M. A convenient and efficient synthesis of polyphenylmono-, -di-, and -triaminobenzenes. *Synthesis* **1995**, *No. 11*, 1419-1422.
26. Hall, D.; Sheat-Rumball, S. V.; Waters, T. N. The colour isomerism and structure of copper co-ordination compounds. Part XVII. The crystal structure of the pyridine solvate of bis-(*N*-phenylsalicylaldiminato)copper(II). *J. Chem. Soc. A* **1968**, 2721-2724.



27. Loudon, G. M. Nuclear magnetic resonance spectroscopy. In *Organic Chemistry*; Scanlan-Rohrer, A., Ed.; The Benjamin/Cummings Publishing Company, Inc.: Redwood City, CA, 1995; pp 579-644.
28. Iglesias, A. L.; Aguirre, G.; Somanathan, R.; Parra-Hake, M. New chiral Schiff base–Cu(II) complexes as cyclopropanation catalysts. *Polyhedron* **2004**, 23 (18), 3051-3062.
29. Nonius *COLLECT*; Nonius BV: Delft, The Netherlands, 1998.
30. Otwinowski, Z.; Minor, W. Methods in enzymology. In *Macromolecular crystallography*; Carter, C. W.; Sweet, R. M., Eds.; Academic Press: London, 1997; Vol. 276 Part A, pp 307-326.
31. Sheldrick, G. M. *SHELXL97*; University of Göttingen: Göttingen, Germany, 1997.
32. Farrugia, L. J. ORTEP-3 for Windows - a version of ORTEP-III with a graphical user interface (GUI). *J. Appl. Cryst.* **1997**, 30 (Part 5, No. 1), 565.
33. Spek, A. L. *PLATON*; University of Utrecht: Utrecht, The Netherlands, 2001.

## **CHAPTER 2:**

### **SALICYLALDIMINATO COPPER(II) COMPLEXES AS INEFFECTIVE ETHYLENE POLYMERIZATION CATALYSTS**

## 2.1 INTRODUCTION

### 2.1.1 Overall Research Objectives

Early transition metal (TM) complexes have long dominated the field of homogeneous ethylene polymerization.<sup>1,2,3</sup> Homogeneous catalysts from groups 3, 4, and 5 of the periodic table are important because the early TM catalysts are very active. This is because they have unfilled valence orbitals. In addition, early TM complexes are useful because they have coordination numbers of six or higher. One or more multidentate ligand can coordinate to early TM metals. However, there is much interest in transition metal catalysts from the right side of the periodic table. These late transition metals belong to groups 9, 10, and 11 of the periodic table. Late TM complexes have coordination geometries of five or lower. Low coordination numbers present some interesting challenges to ligand design. For instance, there are fewer ways for bulky ligands to coordinate with late transition metals. Late d-block metals have unique chemical properties because they have filled valence shells. Some late transition metal catalysts are active as early transition metal catalysts. Two nickel catalysts are prominent examples of active late transition metal catalysts. Brookhart was the first to discover  $\alpha$ -diimine nickel catalysts that produce high molecular weight polyethylene (PE).<sup>4,5,6</sup> Other nickel olefin polymerization catalysts are robust. For example, Grubb's neutral nickel catalysts are tolerant to functional groups like ketones and ethers.<sup>7,8</sup> These neutral nickel catalysts oligomerize ethylene in the presence of water and alcohol. Many research teams continue to investigate other late transition metal PE catalysts.<sup>1,3,9</sup> The overall research objective for many investigators is to find an alternative to group 4 and group 10 PE catalysts. A general trend has emerged to explore the reactivity of late transition metals not previously known to polymerize ethylene, via a migratory insertion mechanism (or coordination/insertion methodology).

Nickel(II) and palladium(II)  $\alpha$ -diimine complexes have created linear and highly branched ethylene homopolymers, respectively (Figure 2.1).<sup>10,11</sup>

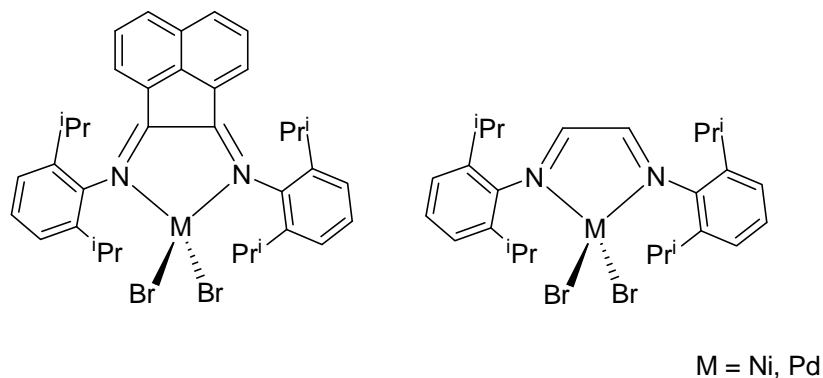


**Figure 2.1.** Nickel(II) and Palladium(II) Ethylene and  $\alpha$ -Olefin Polymerization Catalysts.

The nickel and palladium catalysts in Figure 2.1 are unique. Nickel(II) and palladium(II) catalysts can vary polymer microstructure with changes in olefin gas pressure and reaction temperature. Several variations of the ligand framework exist. The catalysts in Figure 2.1 produce high molecular weight copolymers. Nickel(II) and palladium(II) catalysts copolymerize vinyl monomers and ethylene. The catalysts in Figure 2.1 also copolymerize vinyl monomers and propylene. Iron(II)  $\alpha$ -diimine complexes exhibit poor olefin polymerization activity (Figure 2.2).<sup>12</sup>

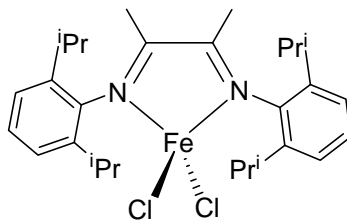


**Figure 2.2.** A Low Activity Iron(II) Olefin Polymerization Catalyst.

In contrast, 2,6-bis(imido)pyridyl Iron(II) and 2,6-bis(imido)pyridyl cobalt(II) catalysts are highly active polyethylene catalysts (Figure 2.3).<sup>13,14,15</sup>

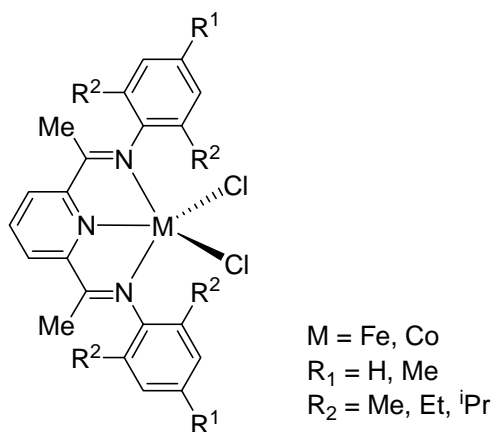
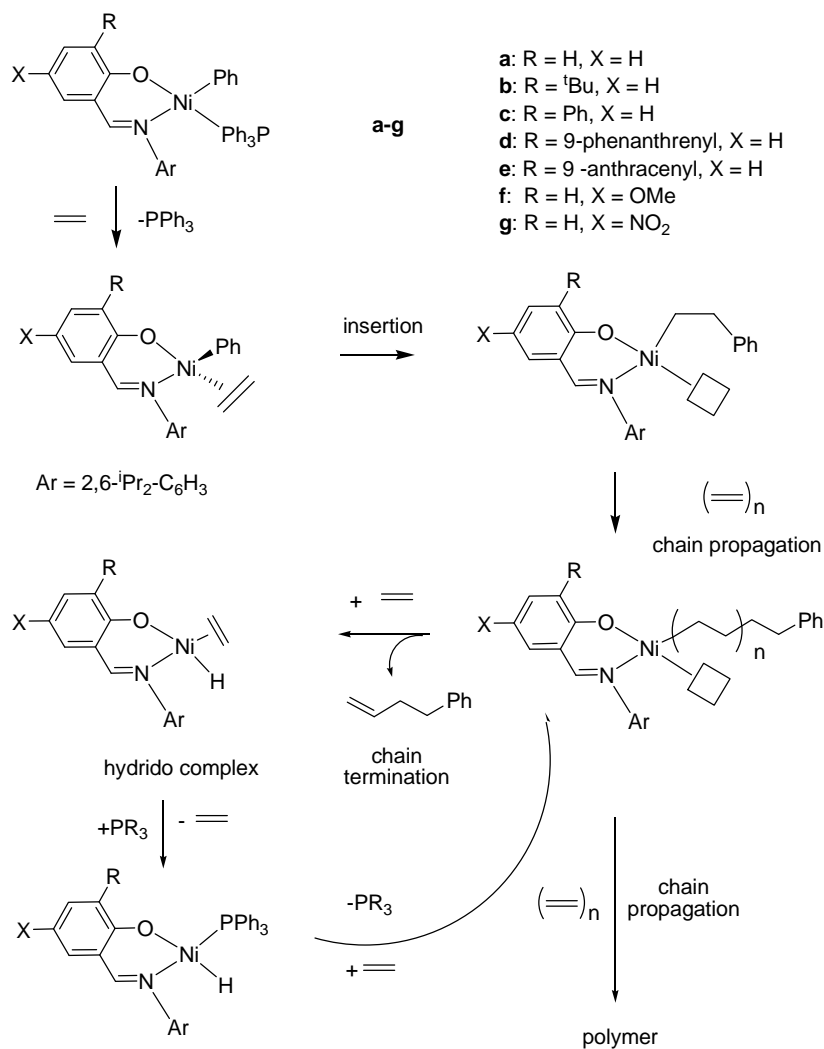


**Figure 2.3.** 2,6-Bis(imino)pyridyl Cobalt and Iron Ethylene Polymerization Catalysts Developed by Brookhart and Gibson.

Iron and cobalt catalysts are interesting. The catalysts in Figure 2.3 produce high density linear polyethylene (HDPE). 2,6-Bis(imido)pyridyl Iron(II) is the first iron catalyst known to polymerize ethylene. Molecular weight has been shown to be directly influenced by the steric bulk incorporated into the tridentate pyridine bis-imine ligand.

Neutral nickel catalysts are the first ethylene polymerization catalysts which operate without activating agents (Scheme 2.1).<sup>8,7</sup>

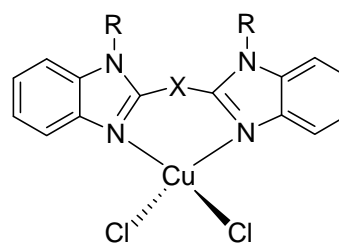
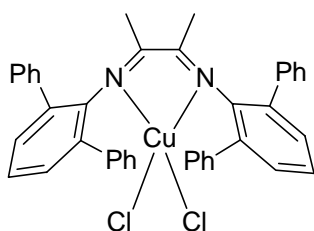


**Scheme 2.1.** Catalytic Cycle for Grubb's Neutral Nickel(II) Catalyst.

Steric bulk on the salicylaldimine (SAL) ligand controls branching and modifies catalytic activity. Steric bulk integrates into two positions on the SAL ligand. The first position is *ortho*- to the hydroxyl substituent on the phenolic ring. The second position is on the ketimine nitrogen position. Bulky SAL ligands also promote triphenylphosphine dissociation. Triphenylphosphine ties up an open coordination site

for the coordination/insertion mechanism. Grubb's neutral nickel catalysts are tolerant to functional groups like ketones and ethers.<sup>7,8</sup> Neutral nickel catalysts oligomerize ethylene in the presence of water and alcohol. Perhaps another first row late transition metal is also tolerant to functional groups.

Discovery of active iron, nickel, cobalt, and palladium PE catalysts further our interest in copper PE catalysts. Copper is a first row transition metal which belongs to group 11 in the periodic table. Copper(II) catalysts are hard to study. Investigations are usually superficial because intermediates are difficult to isolate. Copper(II)-carbon bonds decompose by homolytic cleavage or C-H activation. Paramagnetic copper(II) complexes are difficult to observe by NMR. Studies that observe catalytic activity are more common. The two copper(II) catalysts that Gibson and Stibrany synthesized produce high molecular weight polyethylene (PE).<sup>16,17</sup> These catalysts are  $\alpha$ -diimine and bisbenzimidazole copper(II) complexes (Figure 2.4).



- a: X = CHOH, R = CH<sub>3</sub>
- b: X = CH<sub>2</sub>, R = CH<sub>2</sub>CH<sub>3</sub>
- c: X = CH<sub>2</sub>, R = (CH<sub>2</sub>)<sub>3</sub>CH<sub>3</sub>
- d: 2,2-biphenyl, R = CH<sub>2</sub>CH<sub>3</sub>
- e: 2,2-biphenyl, R = (CH<sub>2</sub>)<sub>3</sub>CH<sub>3</sub>

**Figure 2.4.** Copper(II) Catalysts used for Ethylene Polymerization and Copolymerization.

Gibson and Stibrany did not propose reaction mechanisms for the copper catalysts.<sup>16,17</sup>

The complex on the left hand side of Figure 2.6 is Gibson's  $\alpha$ -diimine copper(II) complex. Earlier nickel and palladium  $\alpha$ -diimine olefin polymerization catalysts appear to inspire Gibson's copper(II) catalyst.<sup>16</sup> The complexes on the right hand side of Figure 2.4 are Stibrany's bis(benzimidazole)copper(II) catalysts.<sup>17</sup> Bis(benzimidazole)copper(II) complexes are active for olefin polymerization and copolymerization. Gibson and Stibrany's catalysts use methylaluminoxane (MAO) as the activating agent. Activation is the first step in the coordination/insertion mechanism. MAO abstracts anionic ligands and alkylates transition metal catalysts. The reader of Gibson's and Stibrany's papers must infer the coordination/insertion mechanism is working. Both catalysts showed good activity. Stibrany and colleagues postulate that high molecular weight linear PE is the product of a single site copper(II) catalyst. Stibrany indicates that steric protection is responsible for high catalytic activity.<sup>16</sup>

Herein, we report investigations towards the generality of copper(II) complexes for ethylene polymerization, and the roles of the copper center.

### 2.1.2 Knowledge Gap to Bridge in this Chapter

The first knowledge gap to bridge in this chapter is that published accounts of copper(II)-alkyl or -aryl intermediates do not exist. Copper(II)-carbon bonds decompose by homolysis or C-H activation. Bulky alkyls like  $\text{CH}(\text{SiMe}_3)_2$  may stabilize intermediates. Bulky salicylaldimine ligands may help to stabilize copper(II)-carbon intermediates. Aromatic ligands do not possess  $\beta$ -hydrogens. Phenyl ligands should be immune to  $\beta$ -hydrogen elimination. The second knowledge gap to bridge in this chapter is that PE chain growth from copper(II) catalysts is unlikely.  $\beta$ -Hydrogen elimination may compete with bond homolysis or C-H activation.



### 2.1.3 Research Objectives

The first short term objective is to synthesize low coordinate  $\text{SALCu}^{\text{II}}\text{-X}$  (X = halide) complexes. The second objective is to investigate route into synthesis of stable  $\text{SALCu}^{\text{II}}\text{-R}$  (R = alkyl, aryl) intermediates. Alkylating reagents include  $\text{Li}(\text{CH}_2)_3\text{CH}_3$  and  $\text{LiCH}(\text{SiMe}_3)_2$ . Arylation experiments use  $\text{PhMgBr}$  reagent. Results from the second objective should reveal how copper(II)-alkyls and -aryls decompose. The third objective is to study copper(II) PE catalytic activity. Methylaluminoxane (MAO) activates the copper(II) complexes.

### 2.1.4 Hypothesis

Copper(II) salicylaldiminato complexes are single-site PE catalysts. The copper(II) catalysts should polymerize ethylene by the coordination/insertion mechanism. Stable copper(II)-alkyls and -aryls should provide insight into polymer chain growth. Intermediates with stable metal-carbon bonds are hard to isolate. Copper(II)-carbon homolytic cleavage and C-H activation are difficult to avoid.

## 2.2 RESULTS AND DISCUSSION

Compounds **A** and **B** were used to synthesize three salicylaldiminato copper(II) complexes. Complexes **4** and **5** were low-coordinate  $\text{SALCu}^{\text{II}}\text{-X}$  (X = halide) complexes. Complex **4** was (Tri-*n*-butylammonium) dichloro(2,6-diisopropylphenyl-3,5-di-*tert*-butylsalicylaldiminato)copper(II). Complex **5** was (Tri-*n*-butylammonium) dichloro(2,6-diisopropylphenyl-5-phenyl-salicylaldiminato)copper(II) (Figure 2.5).

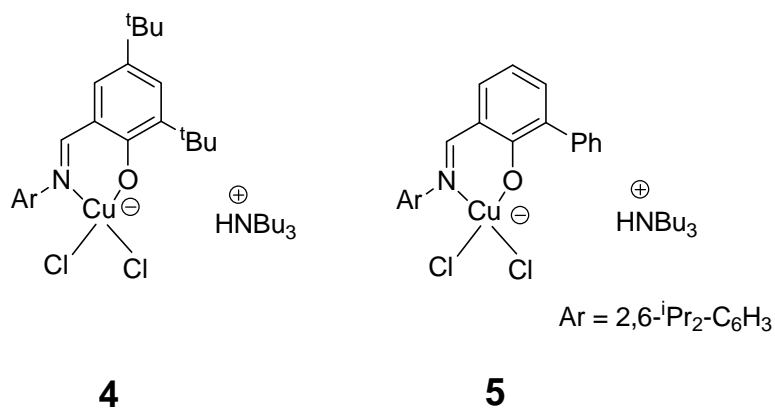


**Figure 2.5.** Proposed Copper(II) Precatalysts for Ethylene Polymerization.

Complex **6** was ( $\mu$ -Chloro)(2,6-diisopropylphenyl-3,5-di-*tert*-butylsalicylaldiminato)copper(II) (Figure 2.6).

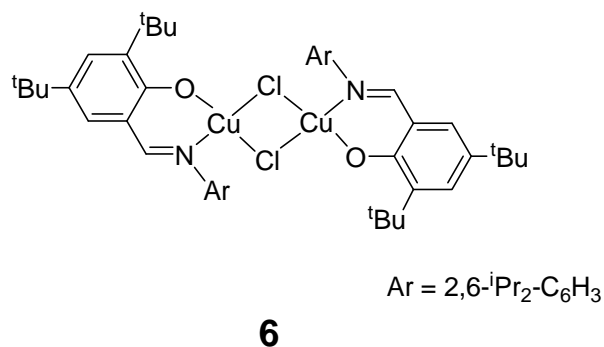
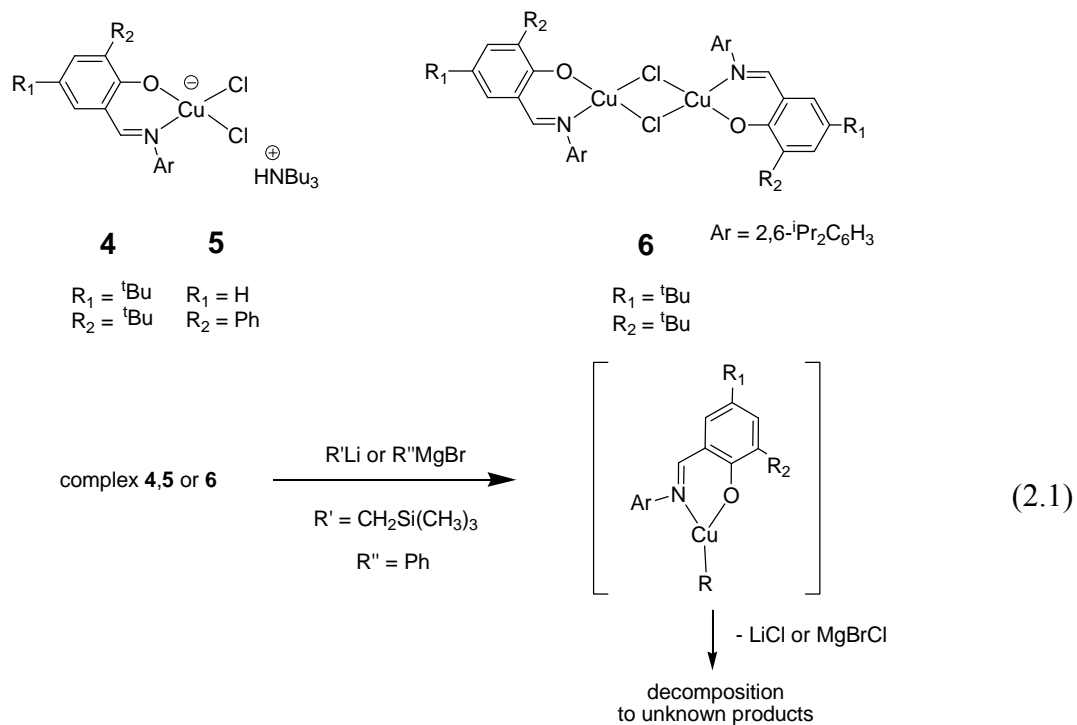


**Figure 2.6.** Chloride bridged dimer complex.

Complex **6** is a chloride bridged dimer complex. The dimer complex was reserved for arylation and alkylation experiments. The chloride bridged dimer and low-coordinate  $\text{SALCu}^{\text{II}}\text{-X}$  ( $\text{X} = \text{halide}$ ) were made by different routes. Alkylation and arylation experiments were unsuccessful. Pure copper(II)-alkyls and -aryls were not isolated. The alkylation and arylation experiments formed amorphous masses. Amorphous

masses decomposed into brown colored oils and a variety of salts with different colors (Equation 2.1).



### 2.2.1 Salicylaldimine Ligand Synthesis

Compounds **A** and **B** were used to make complexes **4**, **5**, and **6**. 2,6-Diisopropylphenyl-3,5-di-*tert*-butylsalicylaldimine and 2,6-diisopropylphenyl-5-phenylsalicylaldimine were discussed in chapter one (Figure 2.7).

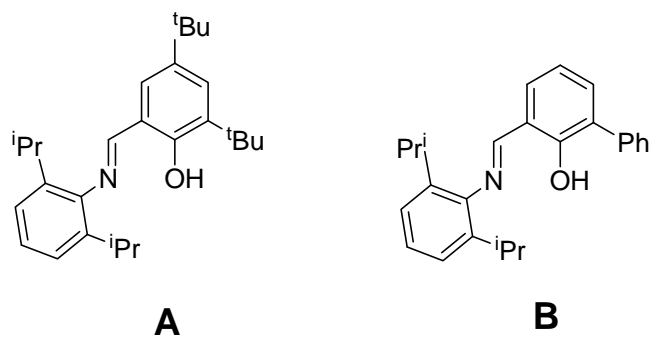


**Figure 2.7.** Salicylaldehyde Ligands.

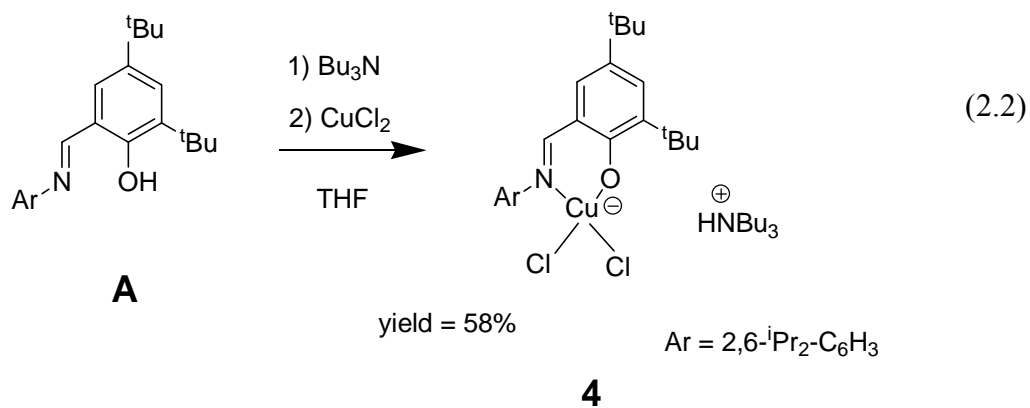
Synthetic details for compounds **A** and **B** are located in the first chapter (see Section 1.4.3, page 36).

### 2.2.2 Proposed Salicylaldehyde Copper(II) Precatalysts

X-ray crystal structures were solved for complexes **4** and **6**.

#### 2.2.2.1 (Tri-*n*-butylammonium) dichloro(2,6-diisopropylphenyl-3,5-di-*tert*-butylsalicylaldehyde)copper(II) (Complex **4**).

(Tri-*n*-butylammonium) dichloro(2,6-diisopropylphenyl-3,5-di-*tert*-butylsalicylaldehyde)copper(II) was complex **4** (Equation 2.2).



Complex **4** was synthesized by reacting ligand **A** with copper(II) chloride. The reaction took place in the presence of tributylamine. A deep green product was crystallized from toluene. The block shaped crystals were X-ray quality. Yield: 1.05 g (58.1%). Elemental analysis confirmed the presence of complex **4**. The product decomposed at 185.0 °C. Complex **4** was characterized by FT-IR spectroscopy. The imine C=N stretch appeared at 1612  $\text{cm}^{-1}$  (Appendix A16). Compound A imine C=N stretch appeared at 1622  $\text{cm}^{-1}$  (Appendix A3). The imine C=N stretch shift was consistent with coordination of an imine nitrogen atom to electrophilic copper(II). The effective magnetic moment was 1.87 BM. Complex **4** had a single unpaired electron.

X-ray quality crystals were obtained. The structure of complex **4** was solved (Figure 2.8, plus Tables 2.1 and 2.2).

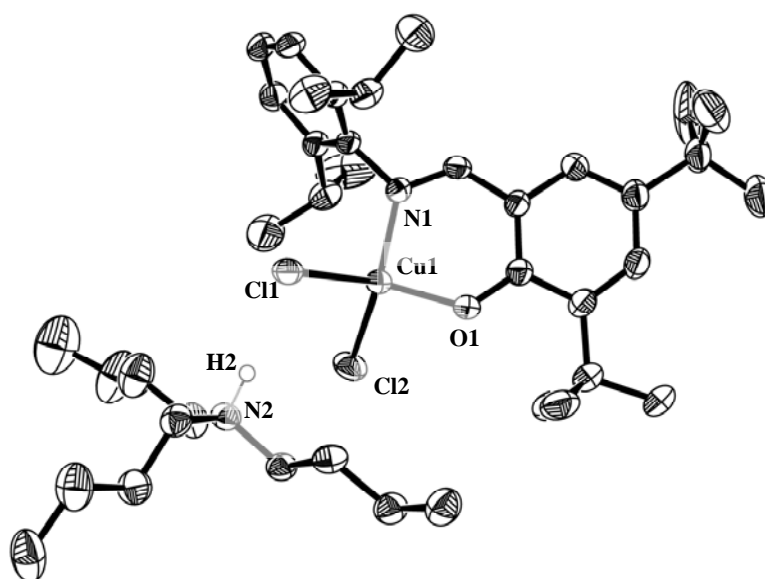


**Figure 2.8.** Molecular Structure of **4** with Thermal Ellipsoids at the 50% Probability Level. H Atoms on the SAL Ligand Omitted for Clarity. A Single H Atom on Tributylammonium Was Not Removed.

The crystal system was triclinic and belonged to the P-1 space group (Table 2.1).

**Table 2.1.** Crystallographic Data and Details of Refinement for Complex **4**.

Empirical formula	C40.75 H68.00 C12.00 Cu N2.00 O1.00
Formula weight	736.41
Crystal system	Triclinic
Space group	P -1
<i>a</i> , <i>b</i> , <i>c</i> , (Å)	10.2340(2), 14.1030(3), 15.7410(4)
$\alpha$ (°)	95.5600(10)
$\beta$ (°)	95.3750(11)
$\gamma$ (°)	93.8520(11)
<i>V</i> (Å <sup>3</sup> )	2244.59(9)
<i>Z</i>	2
<i>D</i> <sub>calcd</sub> (Mg/m <sup>3</sup> )	1.090
Absorption coefficient (mm <sup>-1</sup> )	0.634
<i>T</i> (K)	173(2)
Total reflections	16044
Independent reflections	8202 [R(int) = 0.0362]
R indices (all data)	R1 = 0.0702, wR2 = 0.1478
Final R indices [I>2sigma(I)]	R1 = 0.0502, wR2 = 0.1358
Goodness-of-fit on F <sup>2</sup>	1.030

The final R index was 5.02%. The crystal structure was publication quality. As expected, the crystal structure showed a four coordinate copper complex. Complex **4** had a single salicylaldiminato ligand and two chloride ligands. A tributylamonium counterion was also observed. The dihedral angle was 53 °. Complex **4** had a distorted tetrahedral geometry (Table 2.2).

**Table 2.2.** Selected Bond Distances (Å) and Angles (°) for Complex **4**.

	<u>Bond Distances (Å)</u>
Cu(1)-N(1)	1.952(2)
Cu(1)-O(1)	1.877(2)
Cu(1)-Cl(1)	2.278(1)
Cu(1)-Cl(2)	2.240(1)
Cl(1)-H(2)*	2.193
Cl(2)-H(2)*	3.309
Cl(1)-Cu(1)-Cl(2)	100.47(3)
O(1)-Cu(1)-Cl(1)	138.61(8)
O(1)-Cu(1)-Cl(2)	94.31(7)
N(1)-Cu(1)-Cl(1)	97.09(7)
N(1)-Cu(1)-Cl(2)	142.23(8)
N(1)-Cu(1)-O(1)	94.18(9)
	<u>Angle (°)</u>
Dihedral angle	53.47(8)

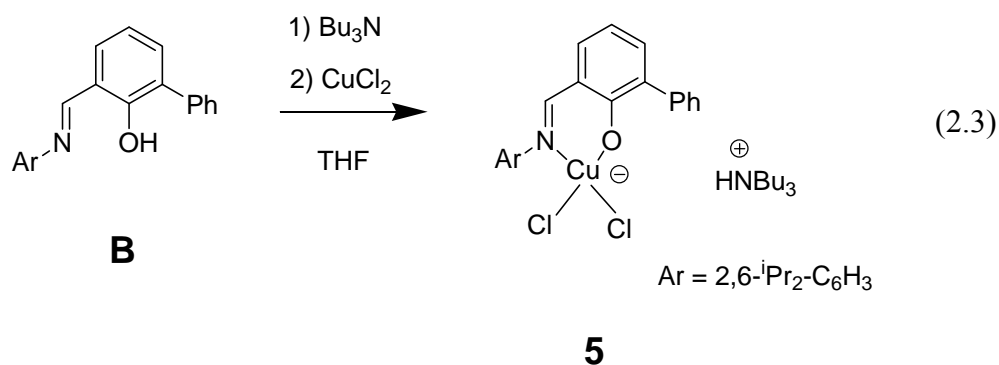
\*ESD (estimated standard deviation) not calculated by the ORTEP3 program.

Bond length between Cu(1)-Cl(1) was 2.278 Å. The estimated standard deviation for the bond between Cu(1)-Cl(1) is +/- 0.001 Å. Bond length between Cu(1)-Cl(2) was 2.240 Å. The estimated standard deviation for the bond between Cu(1)-Cl(1) was +/- 0.001 Å. Bond lengths between Cu(1)-Cl(1) and Cu(1)-Cl(2) were not within a standard deviation. The shorter Cu(1)-Cl(2) bond resulted from the Cu-Cl<sup>...</sup>HNnBu<sub>3</sub> interaction (see Figure 2.10). Tributylammonium donated electron density to the Cu(1)-Cl(2) bond. Therefore, the Cu(1)-Cl(2) bond became relatively stronger than the Cu(1)-Cl(1) bond. Bond distance between the chloride and copper increased.



2.2.2.2 (Tri-n-butylammonium) dichloro(2,6-diisopropylphenyl-5-phenyl-salicylaldiminato)copper(II) (Complex **5**).

(Tri-n-butylammonium) dichloro(2,6-diisopropylphenyl-5-phenyl-salicylaldiminato)copper(II) was complex **5**. Ligand **B** was less bulky than ligand **A**. The synthetic details for complex **5** were similar to those of complex **4** (Equation 2.3).



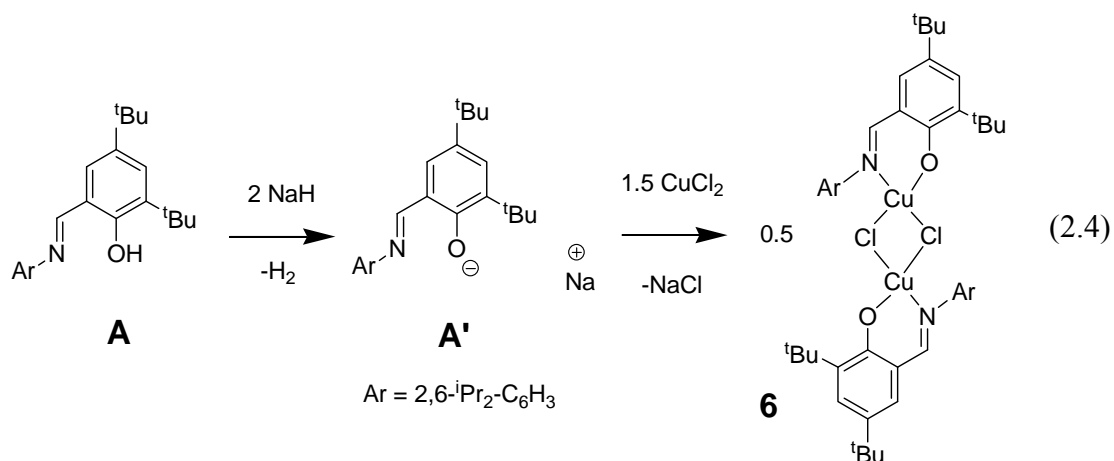
Complex **5** was synthesized by reacting ligand **B** with copper(II) chloride. The reaction took place in the presence of tributylamine. Yield: 0.41 g (43.6%). Elemental analysis confirmed the presence of complex **5**. The product decomposed at 162.0 °C. Complex **5** was characterized by FT-IR spectroscopy. The imine C=N stretch appeared at 1605 cm<sup>-1</sup> (Appendix A17). Compound **B** imine C=N stretch appeared at 1616 cm<sup>-1</sup> (Appendix A6). The imine C=N stretch shift was consistent with coordination of an imine nitrogen atom to electrophilic copper(II). The effective magnetic moment was 1.84 BM. Complex **5** had a single unpaired electron.

### 2.2.3 Chloride Bridged Salicylaldiminato Copper(II) Dimer Complex

( $\mu$ -Chloro)( 2,6-diisopropylphenyl-3,5-di-*tert*-butylsalicylaldiminato)copper(II) was complex **6**.

#### 2.2.3.1 ( $\mu$ -Chloro)(2,6-diisopropylphenyl-3,5-di-*tert*-butylsalicylaldiminato)copper(II) (Complex **6**).

Complex **6** were made in a one-pot reaction under N<sub>2</sub> (Equation 2.4).



The sodium salt of ligand **A** was produced *in situ*. Ligand **A** was reacted with two equivalents of sodium hydride. Excess sodium hydride remained *in situ*. Afterward, two equivalent of CuCl<sub>2</sub> was added to the one-pot mixture. Complex **6** was crystallized from a 1:1 solution of hexane and toluene. The X-ray quality crystal was grown under nitrogen. Subsequent reactions were performed under more controlled reaction conditions. Reaction steps depicted in Equation 2.4 were separated. The sodium salt of the salicylaldiminato ligand was first dried. Copper(II)chloride was added in a separate

reaction step. Yield 0.14g (34.8%). The product decomposed at 170.0 °C. Complex **6** was characterized by FT-IR spectroscopy. The imine C=N stretch appeared at 1612  $\text{cm}^{-1}$  (Appendix A18). Compound A imine C=N stretch appeared at 1622  $\text{cm}^{-1}$  (Appendix A3). The imine C=N stretch shift was consistent with coordination of an imine nitrogen atom to electrophilic copper(II). The effective magnetic moment was 2.23 BM. The copper atoms in complex **6** may have single unpaired electrons.

X-ray quality crystals were obtained. The structure of complex **6** was solved (Figure 2.11, plus Tables 2.3 and 2.4).

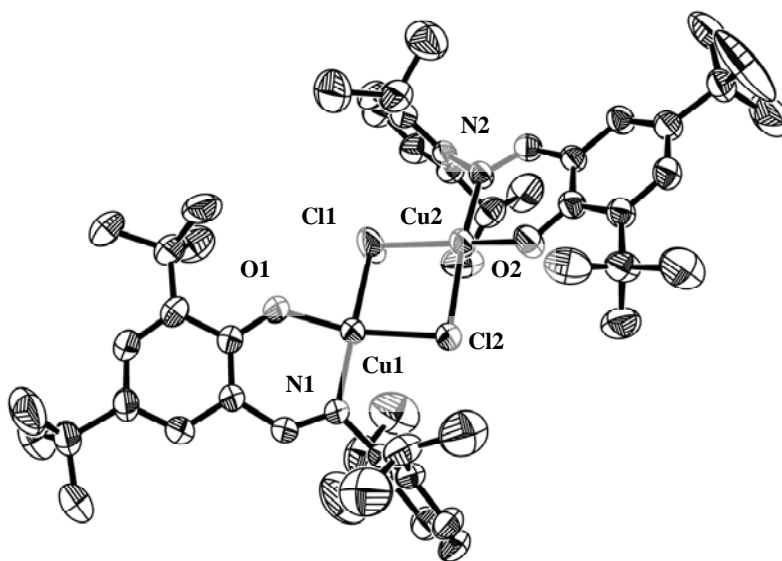


**Figure 2.9.** Molecular Structure of **6** with Thermal Ellipsoids at the 50% Probability Level. H Atoms are Omitted for Clarity.

The crystal system was triclinic and belonged to the P-1 space group (Table 2.3).

**Table 2.3.** Crystallographic Data and Details of Refinement for Complex **6**.

Empirical formula	C54.00 H76.00 Cl2.00 Cu2.00 N2.00 O2.00
Formula weight	983.15
Crystal system	Triclinic
Space group	P -1
<i>a</i> , <i>b</i> , <i>c</i> , (Å)	12.7591(6), 14.5248(9), 17.2981()
$\alpha$ (°)	111.594(2)
$\beta$ (°)	100.070(3)
$\gamma$ (°)	104.797(3)
<i>V</i> (Å <sup>3</sup> )	2750.00(3)
<i>Z</i>	2
<i>D</i> <sub>calcd</sub> (Mg/m <sup>3</sup> )	1.187
Absorption coefficient (mm <sup>-1</sup> )	0.908
<i>T</i> (K)	295(2)
Total reflections	14021
Independent reflections	8701 [R(int) = 0.0390]
R indices (all data)	R1 = 0.0832, wR2 = 0.1242
Final R indices [I>2sigma(I)]	R1 = 0.0512, wR2 = 0.1095
Goodness-of-fit on F <sup>2</sup>	1.053

The final R index was 5.12%. The crystal structure was publication quality. The copper, nitrogen, oxygen, and bridging chloride atoms were arranged in a nearly square planar environment (Table 2.4).

**Table 2.4.** Selected Bond Distances (Å) and Angles (°) for Complex **6**.

	<u>Bond Distances (Å)</u>
Cu(1)-Cl(1)	2.302(11)
Cu(1)-Cl(2)	2.263(10)
Cu(2)-Cl(1)	2.259(11)
Cu(2)-Cl(2)	2.304(11)
Cu(1)-N(1)	1.954(3)
Cu(1)-O(1)	1.861(2)
Cu(2)-N(2)	1.950(2)
Cu(2)-O(2)	1.853(3)
O(1)-Cu(1)-Cl(1)	86.99(8)
O(1)-Cu(1)-Cl(2)	164.79(9)
N(1)-Cu(1)-Cl(1)	167.45(10)
N(1)-Cu(1)-Cl(2)	96.07(9)
N(1)-Cu(1)-O(1)	94.37(11)
Cl(1)-Cu(1)-Cl(2)	85.22(4)
Cu(1)-Cl(1)-Cu(2)	93.77(4)
O(2)-Cu(2)-Cl(1)	162.38(10)
O(2)-Cu(2)-Cl(2)	88.70(9)
N(2)-Cu(2)-Cl(1)	96.36(9)
N(2)-Cu(2)-Cl(2)	165.37(10)
N(2)-Cu(2)-O(2)	93.66(12)
Cl(1)-Cu(2)-Cl(2)	85.26(4)
Cu(1)-Cl(2)-Cu(2)	93.62(4)
Central plane = Cu(1), Cl(1), Cl(2), and Cu(2)	
	<u>Angle (°)</u>
Dihedral angles	18.70(2)
	22.90(2)

Two dihedral angles were observed at 19° and 23° from the central plane defined by the Cu(1), Cl(1), Cl(2), and Cu(2) atoms. Distorted square planar geometries were observed about the copper atoms. Bond length between Cu(1)-Cl(1) was 2.302 Å. The estimated standard deviation for the bond between Cu(1)-Cl(1) was +/- 0.011 Å. The bond length between Cu(1)-Cl(2) was 2.263 Å. The estimated standard deviation between Cu(1)-

Cl(2) was  $\pm 0.010$  Å. The bond length between Cu(2)-Cl(1) was 2.259 Å. The estimated standard deviation between Cu(2)-Cl(1) was  $\pm 0.011$  Å. The bond length between Cu(2)-Cl(2) was 2.304 Å. The estimated standard deviation between Cu(2)-Cl(2) was  $\pm 0.011$  Å. Bond lengths between Cu(1)-Cl(1) and Cu(2)-Cl(2) were identical within estimated standard deviation (2.30 Å). Bond lengths between Cu(1)-Cl(2) and Cu(2)-Cl(1) were identical within estimated standard deviation (2.27 Å). Bond length between Cu(1)-N(1) was 1.954 Å. The estimated standard deviation between Cu(1)-N(1) was  $\pm 0.003$  Å. Bond length between Cu(1)-N(1) was 1.950 Å. The estimated standard deviation between Cu(2)-N(2) was  $\pm 0.002$  Å. Bond lengths between Cu(1)-N(1) and Cu(2)-N(2) were within estimated standard deviation (1.95 Å). Bond length between Cu(1)-O(1) was 1.861 Å. The estimated standard deviation between Cu(1)-O(1) was  $\pm 0.002$  Å. Bond length between Cu(2)-O(2) was 1.853 Å. The estimated standard deviation between Cu(2)-O(2) was  $\pm 0.003$  Å. Bond lengths between Cu(1)-O(1) and Cu(2)-O(2) were within estimated standard deviation (1.86 Å).

#### 2.2.4 Ethylene Polymerization by Proposed Homogeneous Copper(II) Catalysts

Three copper(II) catalysts were tested for ethylene polymerization (Figure 2.10).

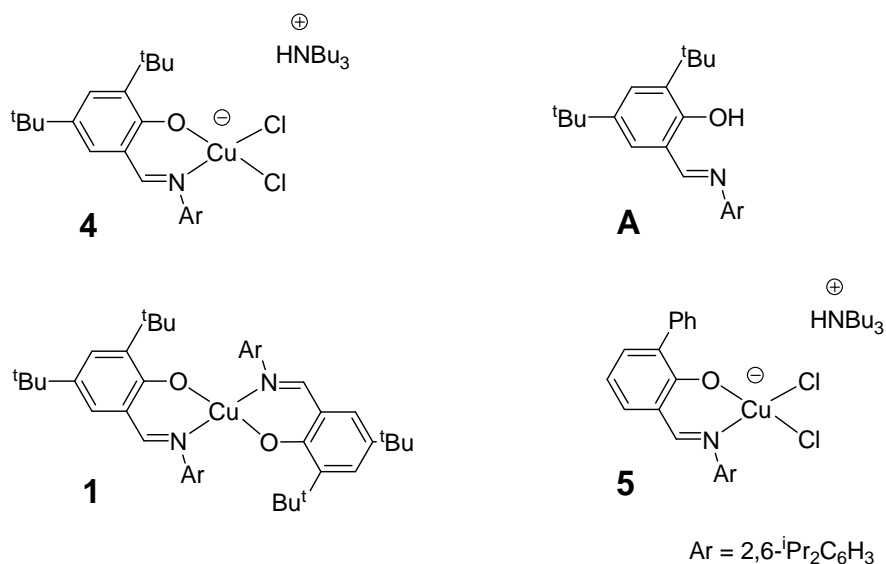
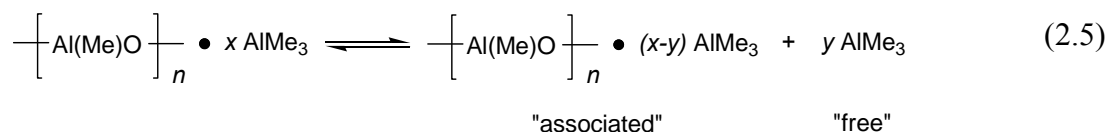


**Figure 2.10.** Complexes **1**, **4**, and **5** as Proposed Precatalysts for Ethylene Polymerization.

Ligand **A** was used to verify that copper(II) catalysts were not active PE catalysts. Ligand transfer to trimethylaluminum (TMA) was possible. TMA originated from methylaluminoxane (MAO). MAO was used to activate the copper(II) catalysts. The activating agent was formed by hydrolysis of trimethylaluminum (TMA) with water. The general formula of MAO is (MeAlO)<sub>n</sub>. MAO is commonly represented as a cyclic ring or linear chain structure.<sup>18</sup> Free and associated TMA is present in MAO (Equation 2.5).



MAO is a cocatalyst with early transition metal homogeneous metallocene catalysts.<sup>19</sup> Moreover, MAO also activates nickel, cobalt, iron, ruthenium, and rhodium catalysts. This activating agent is known to alkylate and abstract anionic ligands.<sup>20</sup> Halogens like the chloride ligand are anionic ligands. Vacant coordination site are opened to ligate  $\text{H}_2\text{C}=\text{CH}_2$  (Scheme 2.2).<sup>8</sup> Ligand transfer was possible because TMA is a very strong Lewis acid. Aluminum(III) should form stable complexes with good donor ligands. Copper(II) is a soft base. Copper(II) should be displaced by aluminum(III).

A Fisher-Porter pressure vessel was used to polymerize ethylene. MAO activator was added at 200 equivalents. Ethylene was added at 80 psi. Polymer samples were characterized by elemental analysis (EA) (Equation 2.6 and Table 2.5).

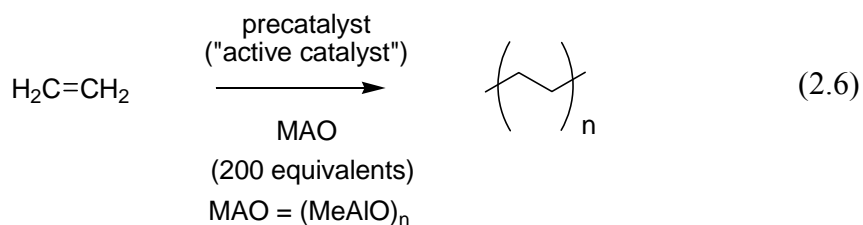




**Table 2.5.** Results for Polymerization Catalyzed by Complexes 1, 4, 5, and Ligand A.

Entry	Catalyst	Temp. (°C)	Polyethylene Yield (grams)
1	4	70.0	0.052
2	4	rt	trace amount
3	1	70.0	0.090
4	LigandA*	70.0	1.410
5	5	70.0	trace amount
6	blank**	80.0	0.000

Reaction conditions: toluene (20 mL), 80 psi ethylene, 200 eq. methylaluminoxane (MAO), reaction time 12h.

\*Reaction performed only with ligand A in absence of any copper species.

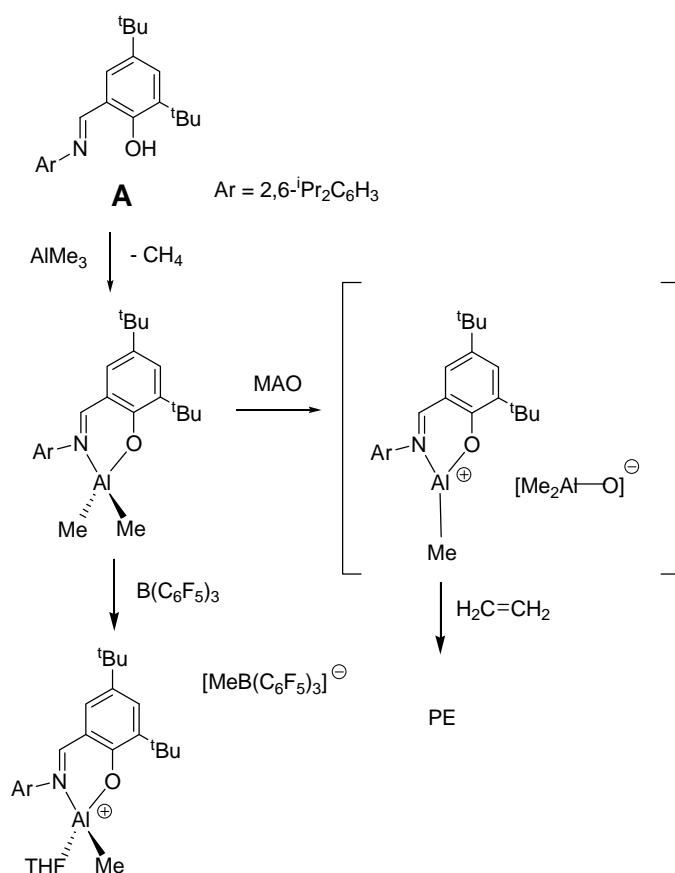
\*\*Reaction performed in absence of any copper(II) precatalyst, or ligand.

Complex **4** was poor because it produced very little polymer. Entries 1 and 2 of Table 2.5 revealed that at elevated and room temperatures the reaction was inactive. A baseline comparison was provided with Complex **1**. Grubbs and colleagues pointed out that nickel analogues of the bis(salicylaldiminato)copper(II) complexes were inactive.<sup>8</sup> MAO was unable to remove the SAL ligand and alkylate copper. MAO can remove monodentate anionic ligands. MAO could have removed the chloride ligand from complex **4**. The activating agent could have alkylated complex **4**. However, copper(II)-alkyl bonds are unstable. Copper(II)-carbon bonds decompose by homolytic cleavage or C-H activation. Polymer chains cannot grow on copper(II). An initial attempt to

polymerize ethylene with a crystal sample of complex **4** was unsuccessful. Purified samples were in short supply. Subsequent polymerization trials used unpurified samples of the complex. Complex **5** in entry 5 of Table 2.5 was run under the same conditions as complex **1**. Trace amounts of PE were recovered. MAO could have removed the chloride ligand from complex **5**. The activating agent could have alkylated complex **5**. However, copper(II)-alkyl bonds are unstable. Copper(II)-carbon bonds decompose by homolytic cleavage or C-H activation. Polymer chains cannot grow on copper(II). Complex **5** was not subjected to purification prior to polymerization trials. Extensive efforts to crystallize complex **5** were unsuccessful. Copper(II) complexes are inactive because copper-carbon bonds are unstable. Arylation and arylation experiments were unsuccessful. Pure copper(II)-alkyls and -aryls were not isolated. The alkylation and arylation experiments formed amorphous masses. Amorphous masses decomposed into brown colored oils and a variety of salts with different colors. Chain growth was unlikely by the coordination/insertion mechanism. Chain termination by  $\beta$ -hydrogen elimination was not ruled out by the arylation experiments. Entry 4 from Table 2.5 suggested that an aluminum catalyst may produce PE. Jordan proposed that aluminum catalyst have strong aluminum-carbon bonds resistant to  $\beta$ -hydrogen elimination.<sup>21</sup>

Compound **A** was combined with MAO to verify ligand transfer to TMA. Significantly more polyethylene (PE) product was formed (see entry 4 of Table 2.5). Aluminum complexes were resistant to chain termination. The complexes appeared to work by the coordination/insertion mechanism. TMA was not able to polymerize ethylene without compound **A**. There was insufficient pressure to polymerize ethylene by carboalumination. Trimethylaluminum will polymerize ethylene at 100 bars of pressure by the Aufbau reaction. Compound **A** is transferred to trimethylaluminum *in situ*.

There are various ways to access aluminum PE catalysts. Ligand transfer from complexes **4** and **5** are hypothetical arguments. Examples from the literature assisted in formulating the arguments. Neutral dialkyl aluminum complexes employing the salicylaldiminato ligand framework are activated by  $B(C_6F_5)_3$ . (left hand path of Scheme 2.3).<sup>22,23</sup>



**Scheme 2.2.** Synthesis and Activation of Aluminum Single Site Ethylene Polymerization Catalysts.

First, TMA was used to deprotonate the salicylaldiminato ligand. Methane was a side product and the neutral dialkylaluminum became the precatalyst. The resulting single

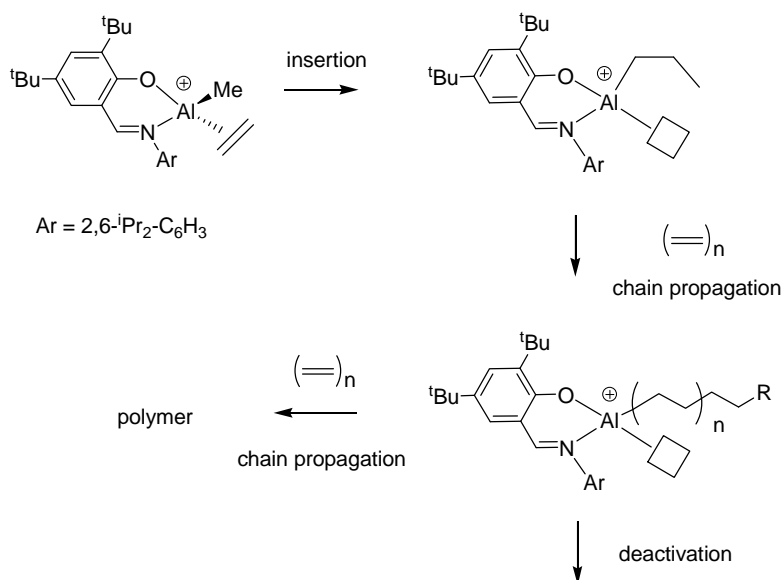
$\text{Ar} = 2,6\text{-}i\text{Pr}_2\text{C}_6\text{H}_3$

Copper(II)-alkyls are proposed to be formed *in situ* (Equation 2.8).



However, the intermediates were not isolated upon quenching the reaction. Copper disproportionation species should be in equilibrium with copper(I) chloride. Dark products were washed from the white polymer. The dark solids were copper(0). So, the cationic monoalkylaluminum intermediate could be formed by activation with MAO. The sterically bulky SAL ligand should protect the catalysts' open coordination site.

Ethylene polymerization by the coordination/insertion mechanism proceeds with olefin coordination to the open coordination site (Scheme 2.5).



**Scheme 2.4.** Proposed Mechanism for Ethylene Polymerization.

Insertion opened up a new coordination site as the alkyl chain proceeded to grow. Chain propagation proceeded until the process was deactivated by quenching or chain transfer.

## 2.3 CONCLUSION

Several important contributions were made in this project. Two publication quality crystal structures were solved. The copper(II) precatalysts were also characterized by elemental analysis, FT-IR, and magnetic susceptibility. Polymer chain growth was unlikely for copper(II) complexes. Alkylation and arylation experiments were unsuccessful. Copper-carbon bonds probably decompose by homolytic cleavage or C-H activation.  $\beta$ -hydrogen elimination was not ruled out as a cause behind chain termination. Copper(II) complexes demonstrate very low ethylene polymerization activity. Temperature and ligand environment for complexes **4** and **5** have negligible impact catalytic activity. No correlation exists between temperature and polyethylene yield. The bis(salicylaldiminato)copper(II) complex is inactive because MAO cannot abstract the bidentate SAL ligand. MAO cannot alkylate complex **1**. Polymer chain growth is impossible because ethylene cannot insert into the copper-carbon bond. Free SAL ligand and TMA polymerize ethylene. TMA was present in the MAO activator. Overall conclusions *suggested* that ethylene polymerization did not occur by a migratory insertion mechanism at the copper center. The salicylaldiminato ligands transferred to trimethylaluminum (TMA). Aluminum(III) displaced copper(II). A strong Lewis acid should displace a soft base from the SAL ligand. Aluminum-alkyls likely polymerized ethylene. Copper(II) decomposition products could not be isolated. However, small traces of dark copper(0) were observed after the polymerization reactions.

## 2.4 EXPERIMENTAL SECTION

### 2.4.1 General Considerations

All reactions were carried out using standard Schlenk techniques or in a glovebox. Glassware was flame and oven dried prior to use. THF, hexane, and toluene were dried using a Braun purification system. Sodium hydride was a 60% dispersion in mineral oil and was purchased from Sigma Aldrich. Copper(II) chloride 99.99% purity was purchased from Sigma Aldrich. Ethylene gas 99.9% purity was Polymer 3.0 grade and was purchased from Praxair. Reagents were not purified or dried prior to use. Substituted salicylaldehyde compounds **A**, **B** and **C**, were synthesized by slight modifications of the literature procedures.<sup>7</sup> Likewise, modified literature procedures were also used for making 2-hydroxy-biphenyl-3-carbaldehyde.<sup>24</sup> NMR spectra were recorded by a 500 MHz Bruker DRK NMR spectrometer with a 5 mm BBI probe. <sup>1</sup>H chemical shifts were referenced to the residual protons of the deuterated solvents (CDCl<sub>3</sub> at  $\delta$  7.26 and C<sub>6</sub>D<sub>6</sub> at  $\delta$  7.16). Elemental analyses were performed on a Perkin-Elmer 2400 CHN elemental analyzer. Potassium bromide FT-IR were performed on a Bruker Tensor 27 DTGS CsI. Magnetic susceptibility measurements were performed on a Johnson Matthey MSB Mark 1.

### 2.4.2 X-ray Structural Analysis for Complexes **4** and **6**

Crystallographic data was collected at -100°C on a Nonius Kappa CCD diffractometer, using the COLLECT program.<sup>25</sup> Cell refinement and data reductions used the programs DENZO and SCALEPACK.<sup>26</sup> SIR97<sup>27</sup> was used to solve the structure and SHELXL97<sup>28</sup> was used to refine the structure. ORTEP-3<sup>29</sup> for Windows

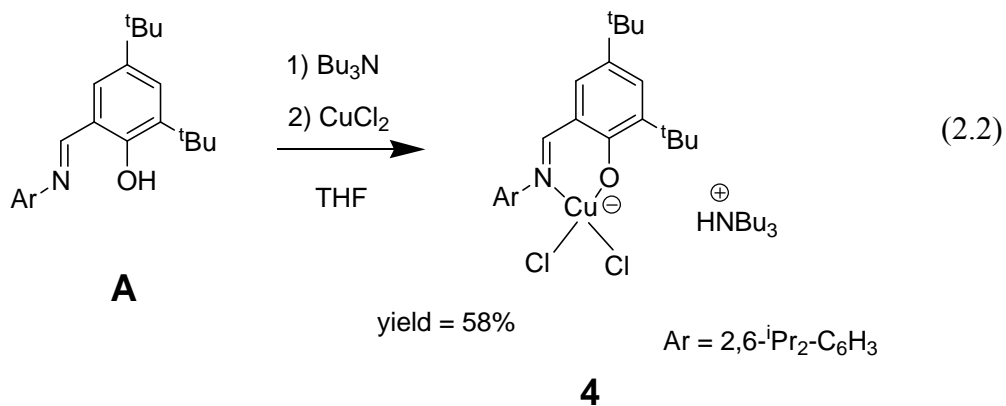
was used for molecular graphics for complex **4**, while XTAL3.7<sup>30</sup> was used for complex **6**, and PLATON<sup>31</sup> was used to prepare material for publication. Published diamagnetic corrections for chloride, and the tributylammonium counterion were used to determine effective magnetic moment.<sup>32,33</sup>

### 2.4.3 Ligand Synthesis

Synthetic details for compounds **A** and **B** are located in the first chapter (see Section 1.4.3, page 36).

### 2.4.4 Salicylaldiminato Copper(II) Complexes Synthesis

#### 2.4.4.1 (Tri-*n*-butylammonium) dichloro(2,6-diisopropylphenyl-3,5-di-*tert*-butylsalicylaldiminato)copper(II) (Complex **4**).

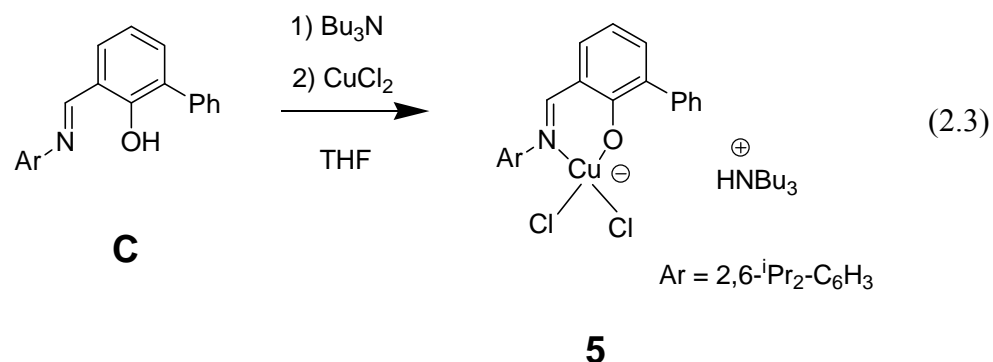


An oven dried Schlenk flask was charged with compound **A** (1.00 g, 2.54 mmol) and copper(II) chloride (0.34 g, 2.54 mmol). Dry reagents were quantitatively transferred with dry tetrahydrofuran (100 ml). The Schlenk flask was transferred from the glove box to the Schlenk line. The reaction mixture was stirred under nitrogen.



Tributylamine (1.21 ml, 5.08 mmol) was added via syringe. The solution was stirred for 12h. Solvent was removed *in vacuo*. A deep brown product was recovered. Yield 1.05 g, (58.1%). Anal. Calcd. For  $C_{39}H_{66}N_2O_1Cl_2Cu$ : C, 65.66%; H, 9.32%; N, 3.93%. Found: C, 64.96%; H, 8.99%; N, 3.74%. Decomp. 185.0 °C; IR (KBr,  $cm^{-1}$ ): 1612 (s) (C=N) (Appendix A16).  $\mu_{eff} = 1.87$  BM. Deep green crystals were grown in toluene at -25 degrees. The X-ray quality crystals were grown in the glove box freezer.

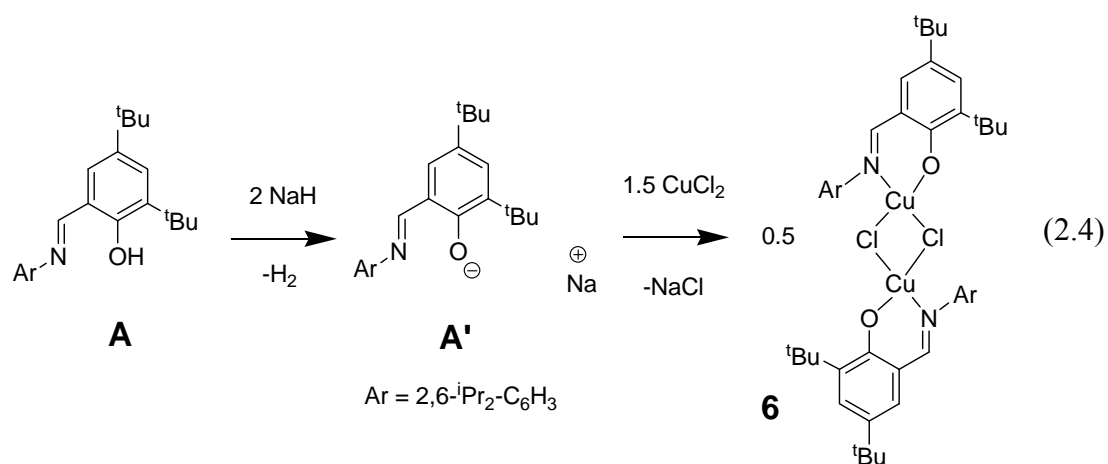
2.4.4.2 (Tri-n-butylammonium) dichloro(2,6-diisopropylphenyl-5-phenyl-salicylaldiminato)copper(II)  
(Complex **5**).



An oven dried Schlenk flask was charged with compound **C** (1.07 g, 3.01 mmol) and copper(II) chloride (0.41 g, 3.01 mmol). Dry reagents were quantitatively transferred with dry tetrahydrofuran (100 ml). The Schlenk flask was transferred from the glove box to the Schlenk line. The reaction mixture was stirred under nitrogen. Tributylamine (1.44 ml, 6.03 mmol) was added by syringe. The solution was stirred for 12h. Solvent was removed *in vacuo*. A light brown product was recovered. Yield 0.41 g, (43.6%). Anal. Calcd. For C<sub>37</sub>H<sub>54</sub>N<sub>2</sub>O<sub>1</sub>Cl<sub>2</sub>Cu: C, 65.61%; H, 8.04%; N, 4.14%. Found: C, 64.15%; H, 8.56%; N, 4.04%. Decomp.: 162.0 °C; (KBr, cm<sup>-1</sup>): 1605 (s) (C=N) (Appendix A17).  $\mu_{\text{eff}} = 1.84$  BM.

## 2.4.5 Chloride Bridged Salicylaldiminato Copper(II) Dimer Complex Synthesis

### 2.4.5.1 ( $\mu$ -Chloro)(2,6-diisopropylphenyl-3,5-di-*tert*-butylsalicylaldiminato)copper(II) (Complex **6**).



Complex **6** was initially made in a one-pot reaction. The reaction was performed in the glove box. The X-ray quality crystals were grown from the one-pot reaction. The sodium salt of the ligand was isolated in a separate reaction. Complex **A'** was synthesized in the glove box. Yield, elemental analysis, IR, and UV-Vis spectroscopic evidence of complex **6** were retrieved from two a step reaction.

#### 2.4.5.1.1 Procedure 1: One-Pot Reaction

An oven dried Shlenk flask was charged in the glove box with compound **A** (0.20 g, 0.51 mmol) and sodium hydride (0.02 g, 1.00 mmol). Dry reagents were quantitatively transferred into the flask with dry tetrahydrofuran (20 ml). The reaction mixture was stirred for 2h. Copper(II) chloride (0.10 g, 0.76 mmol) was added to the above solution. The contents of the Shlenk flask were stirred in the glove box for 12h. Solvent was not removed from the one-pot reaction. Green crystals were obtained from

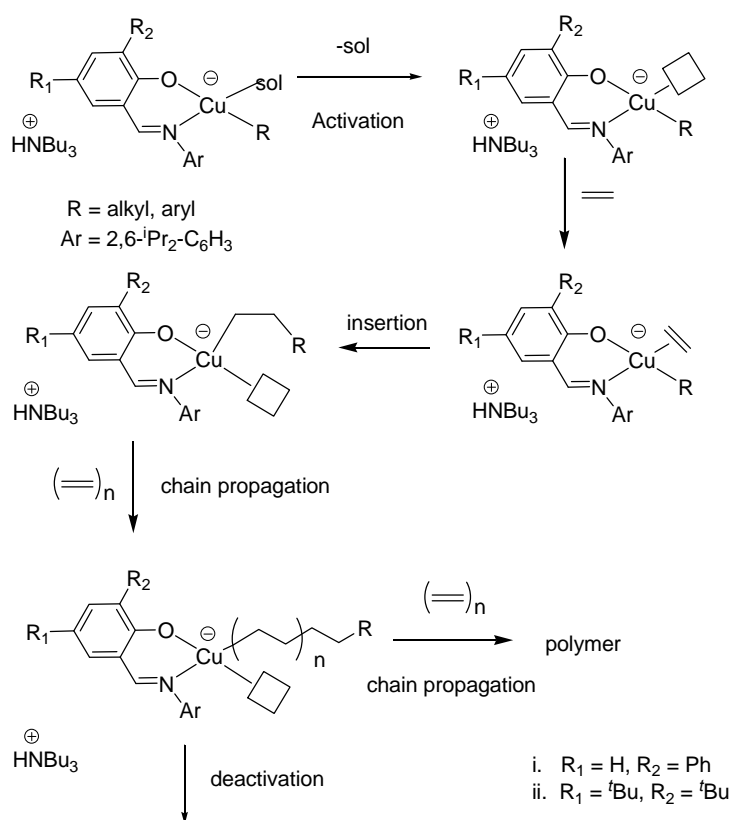
1:1 hexane and toluene. X-ray quality green crystals were grown in the glove box. The crystals were grown at ambient temperature.

#### 2.2.5.1.2 Procedure 2: Isolate Sodium Salt and Synthesize Chloride Bridged Dimer

An oven dried Schlenk flask was charged with compound **A** (0.30 g, 0.76 mmol) and sodium hydride (0.02 g, 0.76 mmol). Dry reagents were quantitatively transferred into the flask with dry tetrahydrofuran (20 ml). The solution was stirred for 6h. Compound **A'** was dried *in vacuo*. Copper(II) chloride (0.10 g, 0.76 mmol) was added to compound **A'**. Dry reagents were quantitatively transferred into the flask with dry tetrahydrofuran (20 ml). The Schlenk flask was transferred from the glove box to the Schlenk line. The reaction mixture was stirred under nitrogen for 12h. Solvent was removed *in vacuo*. A light brown product was recovered. Yield 0.14 g, (34.8%). Decomp. 170.0 °C; IR (KBr, cm<sup>-1</sup>): 1612 (s) (C=N) (Appendix A18).  $\mu_{\text{eff}} = 2.23$  BM.

## 2.4.6 General Procedure for Olefin Polymerization Reaction

### 2.4.6.1 Polyethylene Synthesis



**Scheme 2.4.** Proposed Mechanism for Copper(II) Precatalysts.

Precatalyst and solvent were added to the Fisher-Porter pressure vessel in the glove box. Complex **A** (0.01 g, 0.01 mmol) was dissolved with dry toluene (10 ml). The vessel was sealed to the polymerization rig. The polymerization rig and charged pressure vessel was transferred to the Schlenk line. Monomer gas feed line and vacuum hose were connected to the polymerization rig. Nitrogen was evacuated from the Fischer-Porter pressure vessel. The vessel was charged with ethylene gas (~ 10 psi).

The reaction mixture stirred vigorously. Methylaluminoxane (1.90 ml, 2.81 mmol) was added via syringe. The pressure vessel was Immersed in a hot oil bath (70 °C). Ethylene pressure was increased (80 psi). The reaction mixture was stirred for the duration of the reaction (12h). Ethylene gas was turned off. Pressure was released from the vessel. The reaction was quenched with 1:1 methanol to 1M hydrochloric acid mixture. Solid polymer was washed with methanol. Ethylene polymer was dried *in vacuo* and weighed. Anal. Calcd: C, 85.63%; H, 14.37%; N, 0.00%. Found: C, 85.6%; H, 14.4%; N, 0.00%.

## 2.5 REFERENCES AND NOTES

1. Britovsek, G. J. P.; Gibson, V. C.; Wass, D. F. The search for new-generation olefin polymerization catalysts: Life beyond metallocenes. *Angew. Chem. Int. Ed.* **1999**, 38 (4), 428-447.
2. Hlatky, G. G. Heterogeneous single-site catalysts for olefin polymerization. *Chem. Rev.* **2000**, 100 (4), 1347-1376.
3. Gibson, V. C.; Spitzmesser, S. K. Advances in non-metallocene olefin polymerization catalysis. *Chem. Rev.* **2003**, 103 (1), 283-316.
4. Gates, D. P.; Svejda, S. A.; Onate, E.; Killian, C. M.; Johnson, L. K.; White, P. S.; Brookhart, M. Synthesis of branched polyethylene using ( $\alpha$ -diimine)nickel(II) catalysts: Influence of temperature, ethylene pressure, and ligand structure on polymer properties. *Macromolecules* **2000**, 33 (7), 2320-2334.
5. Daugulis, O.; Brookhart, M. Polymerization of ethylene with cationic palladium and nickel catalysts containing bulky nonenolizable imine-phosphine ligands. *Organometallics* **2002**, 21 (26), 5926-5934.
6. Leatherman, M. D.; Svejda, S. A.; Johnson, L. K.; Brookhart, M. Mechanistic studies of nickel(II) alkyl agostic cations and alkyl ethylene complexes: Investigations of chain propagation and isomerization in ( $\alpha$ -diimine)Ni(II)-Catalyzed Ethylene Polymerization. *J. Am. Chem. Soc.* **2003**, 125 (10), 3068-3081.

7. Wang, C.; Friedrich, S.; Younkin, T. R.; Li, R. T.; Grubbs, R. H.; Bansleben, D. A.; Day, M. W. Neutral nickel(II)-based catalysts for ethylene polymerization. *Organometallics* **1998**, *17* (15), 3149-3151.
8. Younkin, T. R.; Connor, E. F.; Henderson, J. I.; Friedrich, S. K.; Grubbs, R. H.; Bansleben, D. A. Neutral, single-component nickel (II) polyolefin catalysts that tolerate heteroatoms. *Science* **2000**, *287* (5452), 460-462.
9. Ittel, S. D.; Johnson, L. K.; Brookhart, M. Late-metal catalysts for ethylene homo- and copolymerization. *Chem. Rev.* **2000**, *100* (4), 1169-1204.
10. Johnson, L. K.; Killian, C. M.; Brookhart, M. New Pd(II)- and Ni(II)-based catalysts for polymerization of ethylene and  $\alpha$ -olefins. *J. Am. Chem. Soc.* **1995**, *117* (23), 6414-6415.
11. Johnson, L. K.; Mecking, W.; Brookhart, M. Copolymerization of ethylene and propylene with functionalized vinyl monomers by palladium(II) catalysts. *J. Am. Chem. Soc.* **1996**, *118* (1), 267-268.
12. Bart, S. C.; Hawrelak, E. J.; Schmisser, A. K.; Lobkovsky, E.; Chirik, P. J. Synthesis, reactivity, and solid state structures of four-coordinate iron(II) and manganese(II) alkyl complexes. *Organometallics* **2004**, *23* (2), 237-246.
13. Britovsek, G. J. P.; Bruce, M.; Gibson, V. C.; Kimberley, B. S.; Maddox, P. J.; Mastroianni, S.; McTavish, S. J.; Redshaw, C.; Solan, G. A.; Stromberg, S.; White, A. J. P.; Williams, D. J. Iron and cobalt ethylene polymerization catalysts bearing 2,6-bis(imino)pyridyl ligands: Synthesis, structures, and polymerization studies. *J. Am. Chem. Soc.* **1999**, *121* (38), 8728-8740.

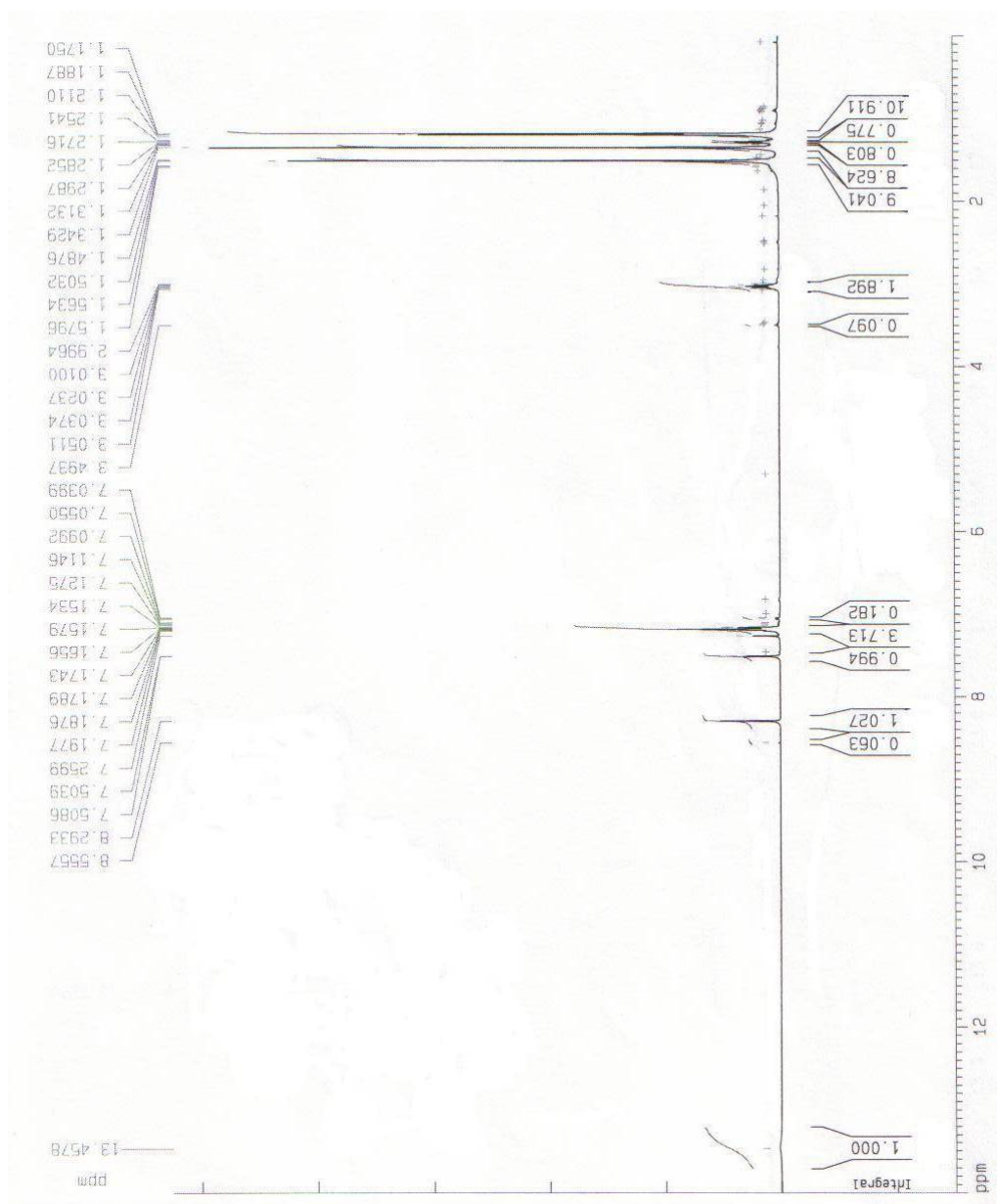


14. Small, B. L.; Brookhart, M.; Bennett, A. M. A. Highly active iron and cobalt catalysts for the polymerization of ethylene. *J. Am. Chem. Soc.* **1998**, *120* (16), 4049-4050.
15. Britovsek, G. J. P.; Gibson, V. C.; McTavish, S. J.; Solan, G. A.; White, A. J. P.; Williams, D. J.; Kimberley, B. S.; Maddox, P. J. Novel olefin polymerization catalysts based on iron and cobalt. *Chem. Commun.* **1998**, (No. 7), 849-850.
16. Gibson, V. C.; Tomov, A.; Wass, D. F.; White, A. J. P.; Williams, D. J. Ethylene polymerisation by a copper catalyst bearing  $\alpha$ -diimine ligands. *J. Chem. Soc., Dalton Trans.* **2002**, No. 11, 2261-2262.
17. Stibrany, R. T.; Schulz, D. N.; Kacker, S.; Patil, A. O.; Baugh, L. S.; Rucker, S. P.; Zushma, S.; Berluche, E.; Sissano, J. A. Polymerization and copolymerization of olefins and acrylates by bis(benzimidazole) copper catalysts. *Macromolecules* **2003**, *36* (23), 8584-8586.
18. Chen, E. Y.-X.; Marks, T. J. Cocatalysts for metal-catalyzed olefin polymerization: Activators, activation processes, and structure-activity relationships. *Chem. Rev.* **2000**, *100* (4), 1391-1434.
19. Zurek, E.; Ziegler, T. Theoretical studies of the structure and function of MAO (methylaluminoxane). *Prog. Polym. Sci.* **2004**, *29* (2), 107-148.
20. Foley, S. R. University of Saskatchewan, Saskatoon, SK. Personal communication, 2006

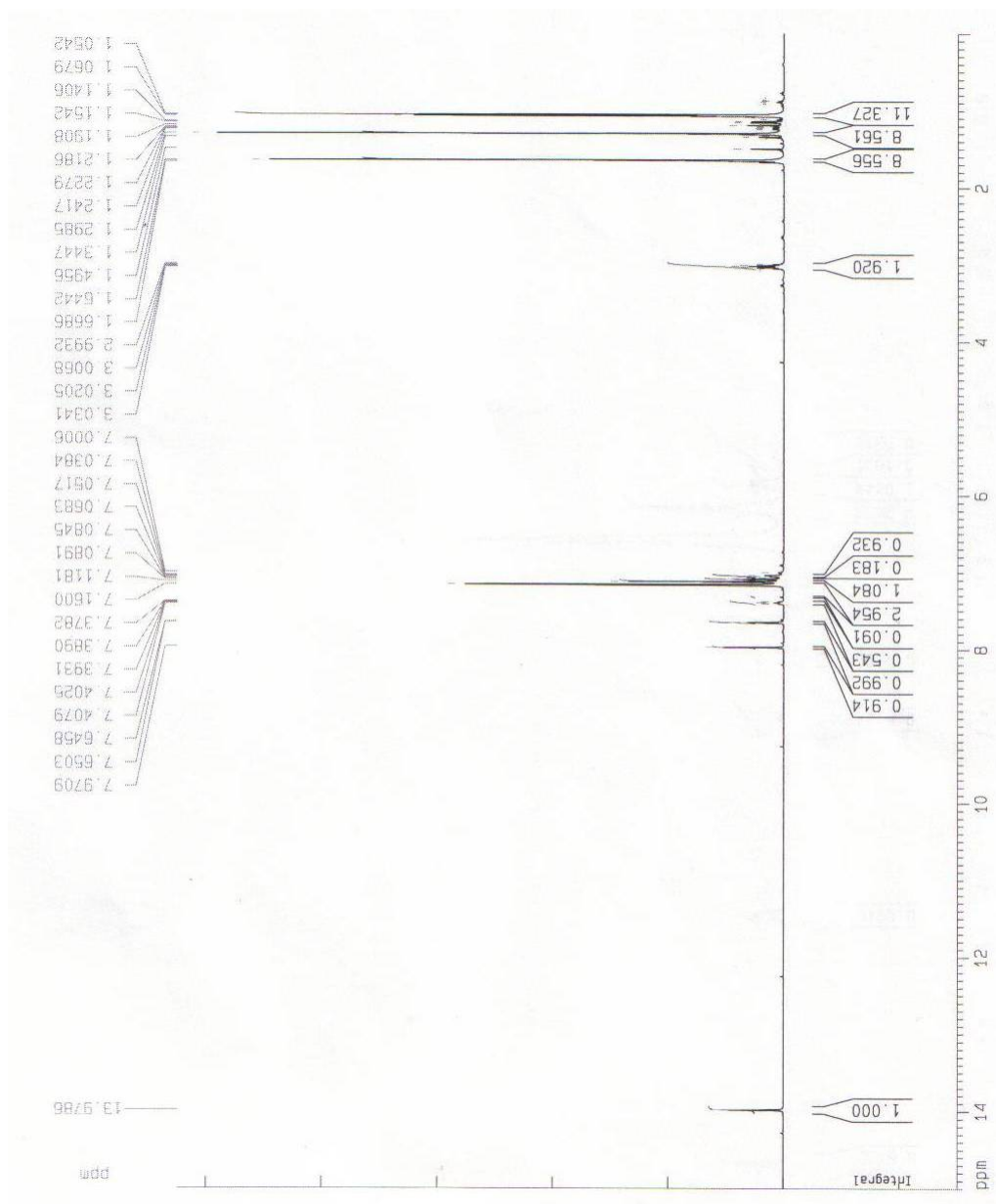
21. Coles, M. P.; Jordan, R. F. Cationic aluminum alkyl complexes incorporating amidinate ligands. Transition-metal-free ethylene polymerization catalysts. *J. Am. Chem. Soc.* **1997**, *119* (34), 8125-8126.
22. Cameron, P. A.; Gibson, V. C.; Redshaw, C.; Segal, J. A.; Solan, G. A.; White, A. J. P.; Williams, D. J. Synthesis and characterisation of neutral dialkylaluminium complexes stabilised by salicylaldiminato ligands, and their conversion to monoalkylaluminium cations. *J. Chem. Soc., Dalton Trans.* **2001**, (No. 9), 1472-1476.
23. Pappalardo, D.; Tedesco, C.; Pellecchia, C. New neutral and cationic dialkylaluminium complexes bearing imino-amide or imino-phenoxide ligands: Synthesis, characterization and reactivity with olefins. *Eur. J. Inorg. Chem.* **2002**, (No. 3), 621-628.
24. Casiraghi, G.; Casnati, G.; Puglia, G.; Sartori, G.; Terenghi, G. Selective reactions between phenols and formaldehyde. A novel route to salicylaldehydes. *J. Chem. Soc., Perkin Trans. I* **1980**, 1862-1865.
25. Nonius *COLLECT*; Nonius BV: Delft, The Netherlands, 1998.
26. Otwinowski, Z.; Minor, W. Methods in enzymology. In *Macromolecular crystallography*; Carter, C. W.; Sweet, R. M., Eds.; Academic Press: London, 1997; Vol. 276 Part A, pp 307-326.
27. Altomare, A.; Burla, M. C.; Camalli, M.; Cascarano, G. L.; Giacovazzo, C.; Guagliardi, A.; Moliterni, A. G. G.; Polidori, G.; Spagna, R. SIR97: a new tool for crystal structure determination and refinement. *J. Appl. Cryst.* **1999**, *32* (Part 1), 115-119.

28. Sheldrick, G. M. *SHELXL97*; University of Göttingen: Göttingen, Germany, 1997.
29. Farrugia, L. J. ORTEP-3 for Windows - a version of ORTEP-III with a graphical user interface (GUI). *J. Appl. Cryst.* **1997**, *30* (Part 5, No. 1), 565.
30. Hall, S. R.; du Boulay, D. J.; Olthof-Hazekamp, R., Eds.; *Xtal3.7 System*; University of Western Australia: 2000.
31. Spek, A. L. *PLATON*; University of Utrecht: Utrecht, The Netherlands, 2001.
32. Girolami, G. S.; Rauchfuss, T. B.; Angelici, R. J. The paramagnetic complex  $\text{Mn}(\text{acac})_3$ . In *Synthesis and technique in inorganic chemistry: A laboratory manual*; 3rd ed.; Stiefel, J., Ed.; University Science Books: Sausalito, CA, 1999; pp 117-130.
33. Pass, G.; Sutcliffe, H. Magnetic measurements. In *Practical inorganic chemistry*; 2nd ed.; John Wiley & Sons: New York, 1974; pp 206-215.

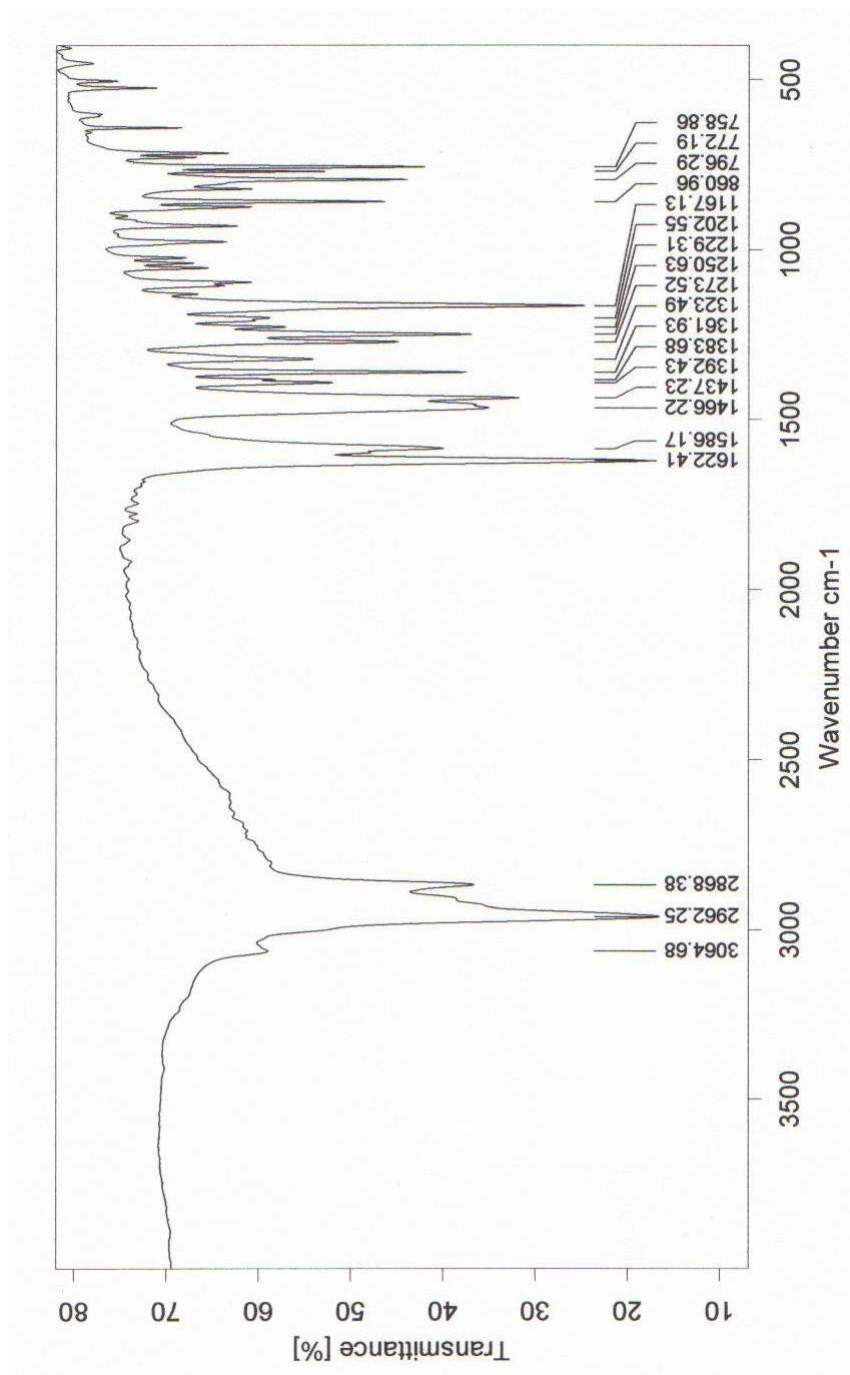
## APPENDICES



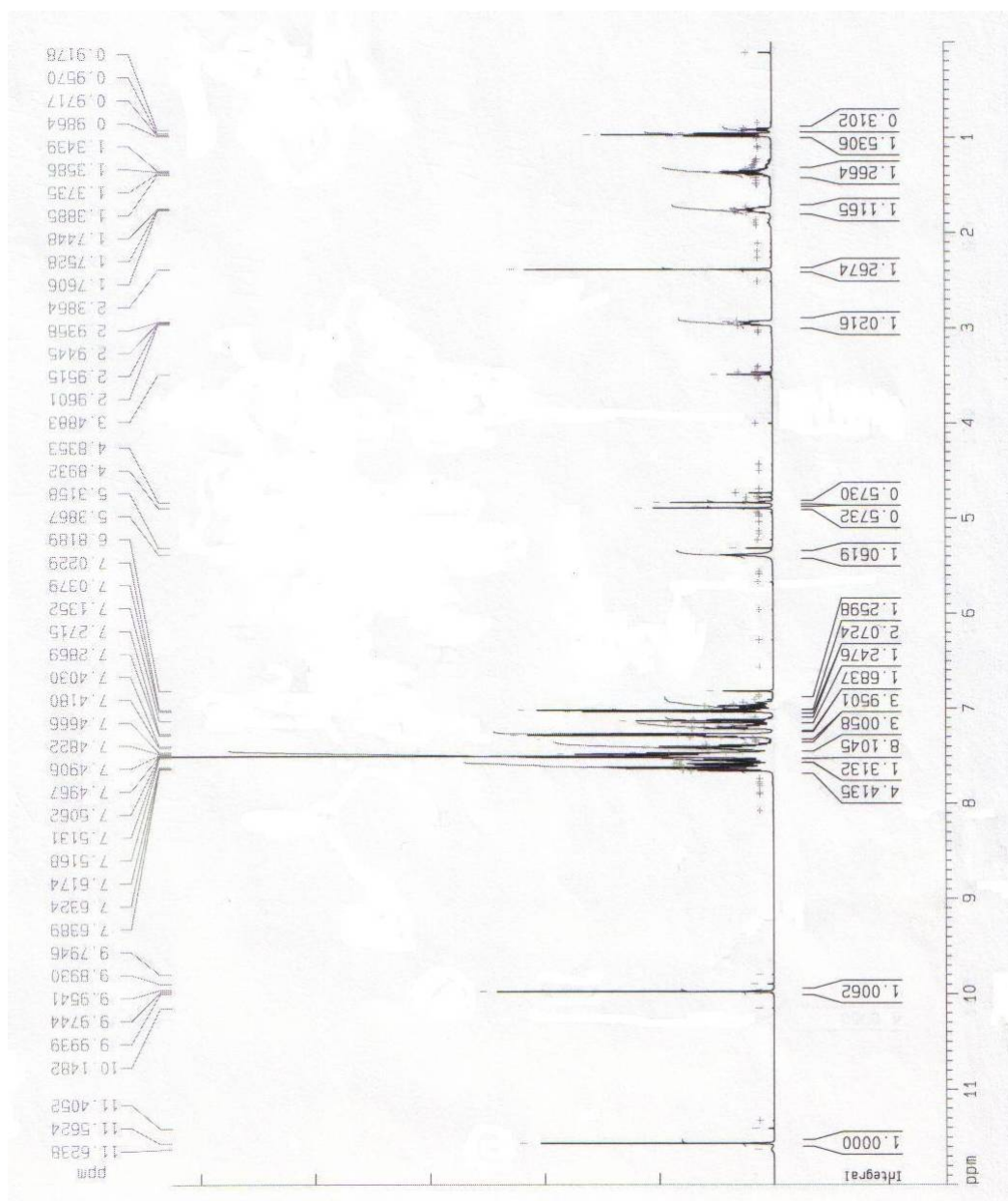
A1 Proton NMR Spectra of 2,6-Diisopropylphenyl-3,5-di-*tert*-butylsalicylaldimine, (Compound A) in CDCl<sub>3</sub>.



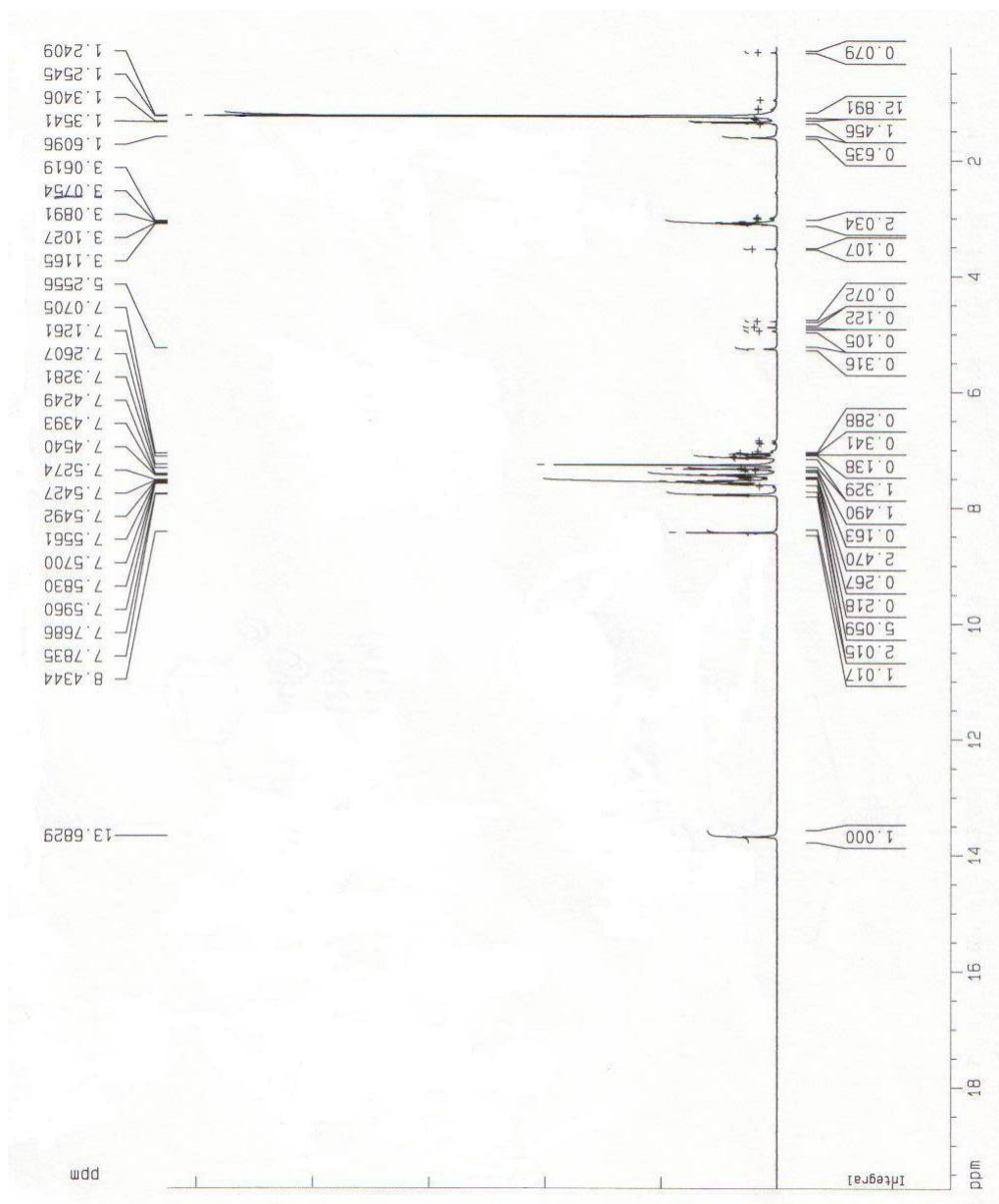
A2 Proton NMR Spectra of 2,6-Diisopropylphenyl-3,5-di-*tert*-butylsalicylaldehyde, (Compound A) in  $C_6D_6$ .



A3 FT-IR Spectra of 2,6-Diisopropylphenyl-3,5-di-*tert*-butylsalicylaldehyde (Compound A).

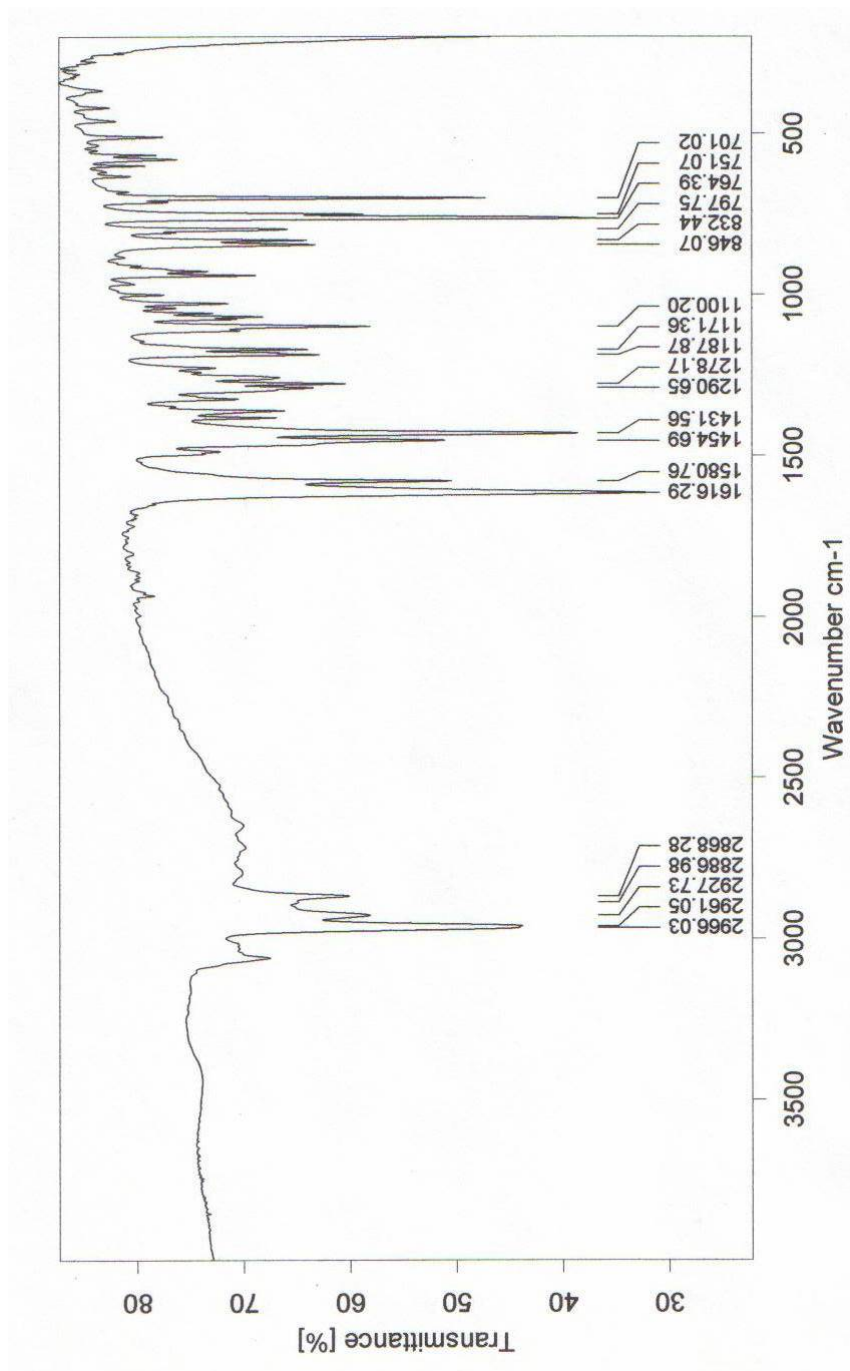


A4 Proton NMR Spectra of 2-Hydroxy-biphenyl-3-carbaldehyde in CDCl<sub>3</sub>.

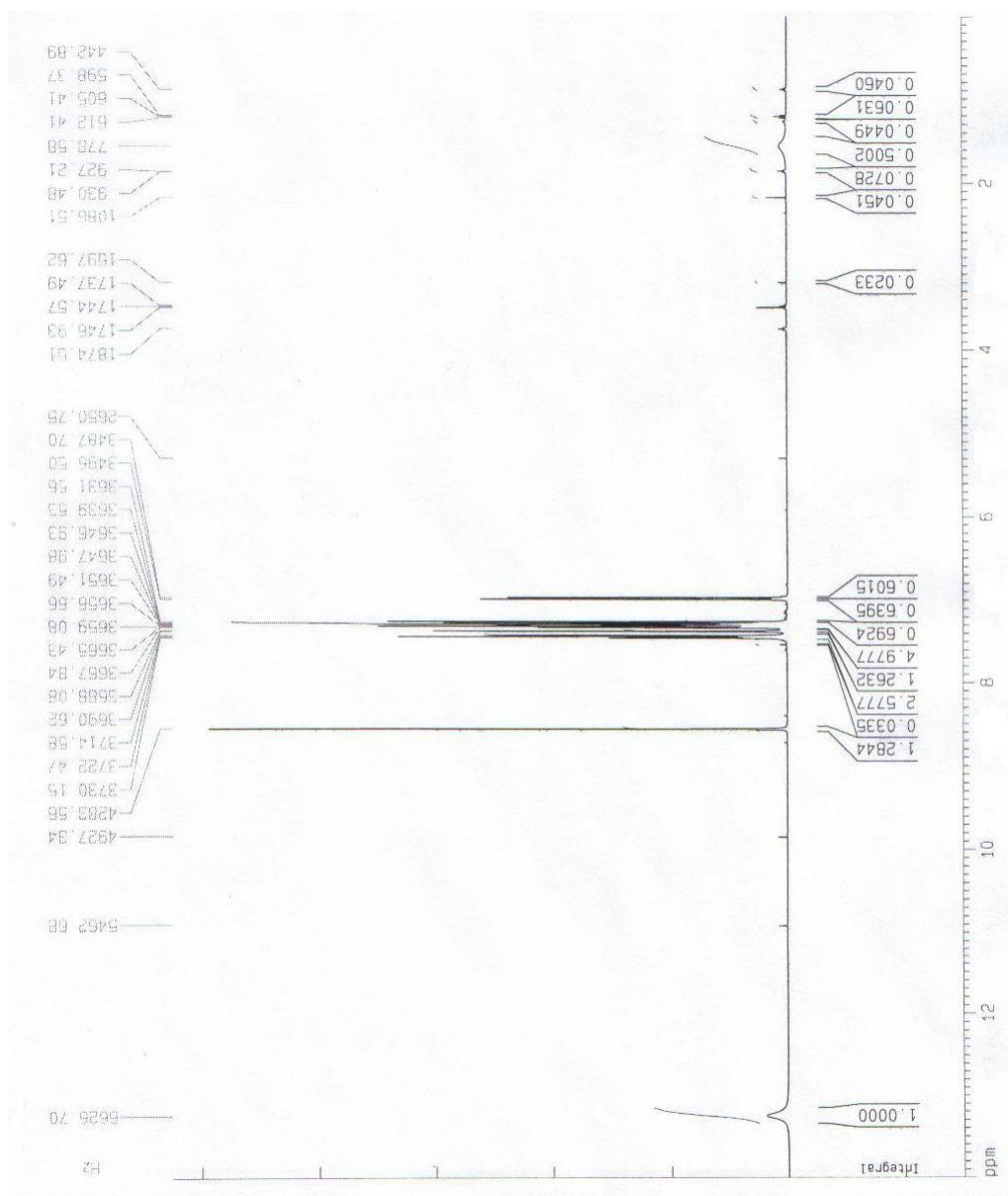


A5 Proton NMR Spectra of 2,6-Diisopropylphenyl-5-phenyl-salicylaldimine, (Compound **B**) in CDCl<sub>3</sub>.

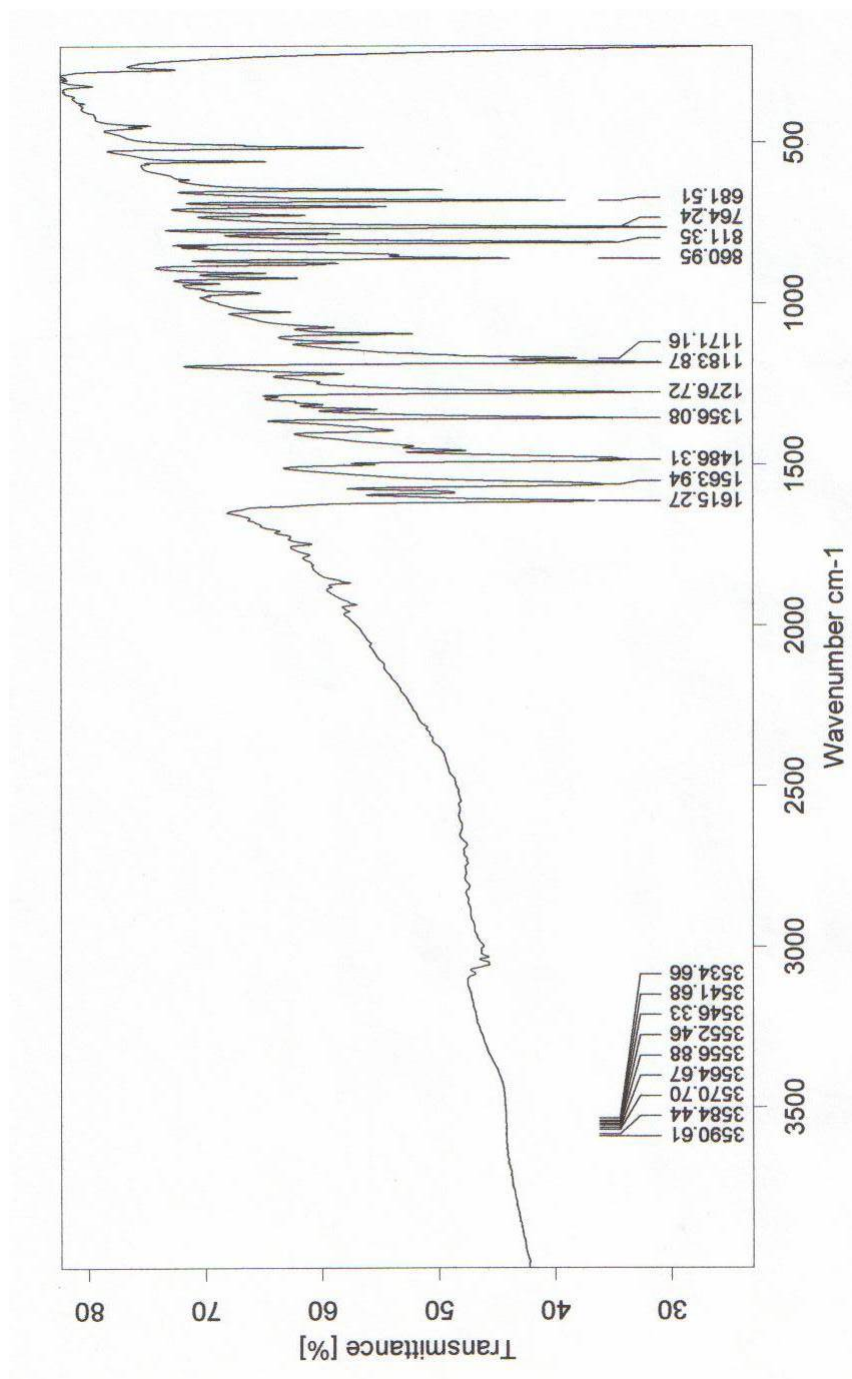




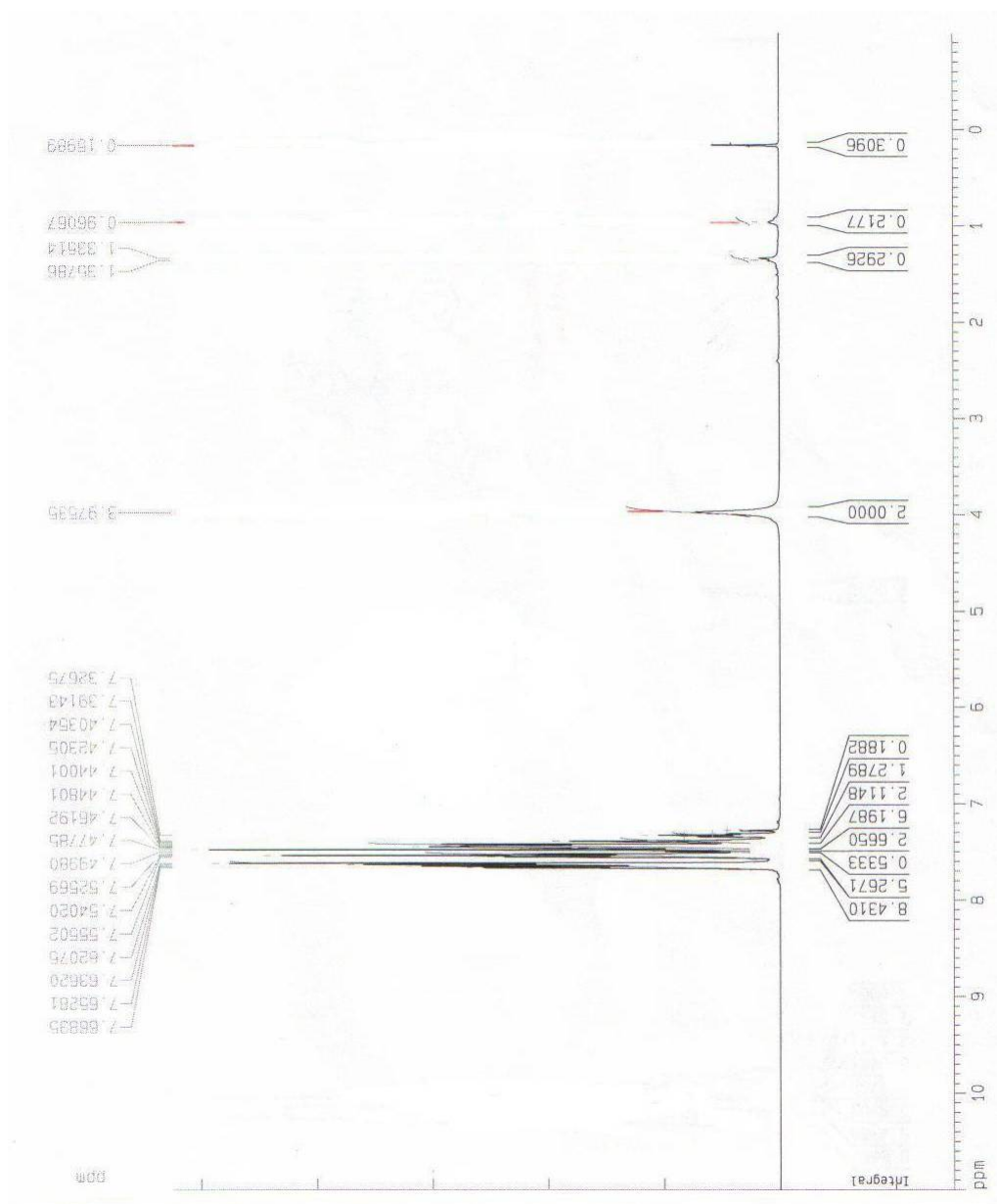
A6 FT-IR Spectra of 2,6-Diisopropylphenyl-5-phenyl-salicylaldehyde (Compound **B**).



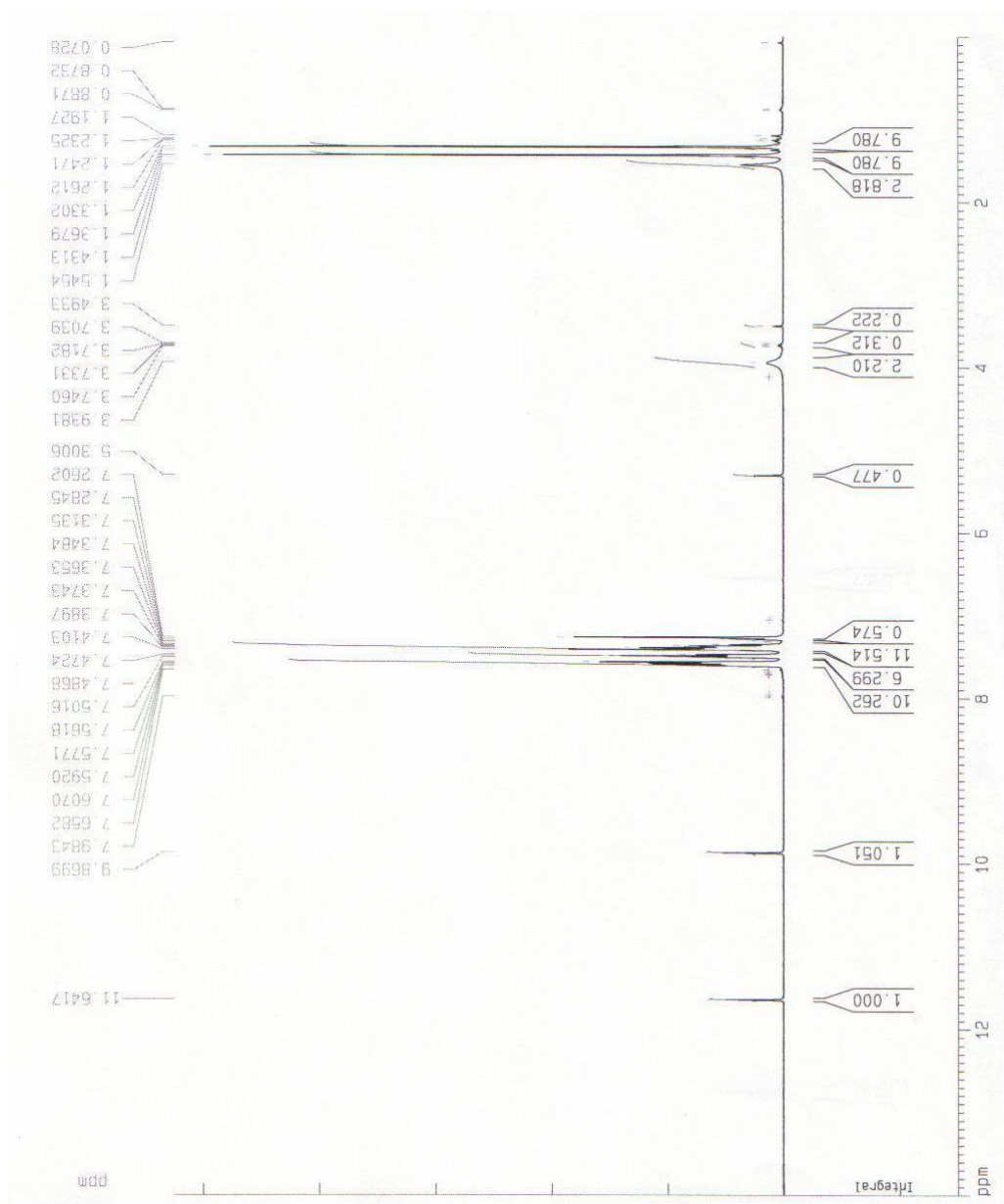
A7 Proton NMR Spectra of Phenyl-3-chloro-salicylalimine (Compound C) in CDCl<sub>3</sub>.



A8 FT-IR Spectra of Phenyl-3-chloro-salicylaldehyde (Compound C).



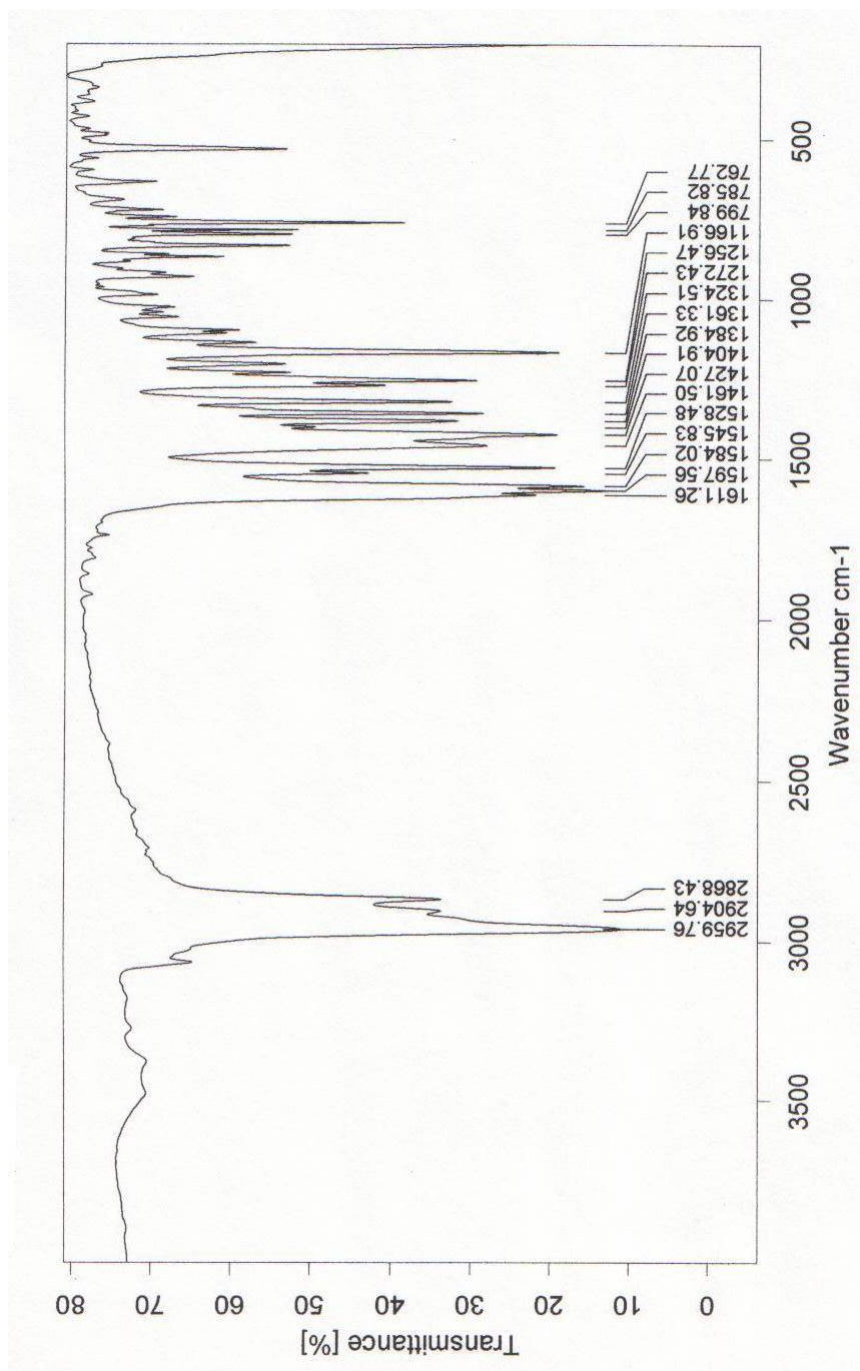
A9 Proton NMR Spectra of 2,4,6-Triphenylaniline in CDCl<sub>3</sub>.



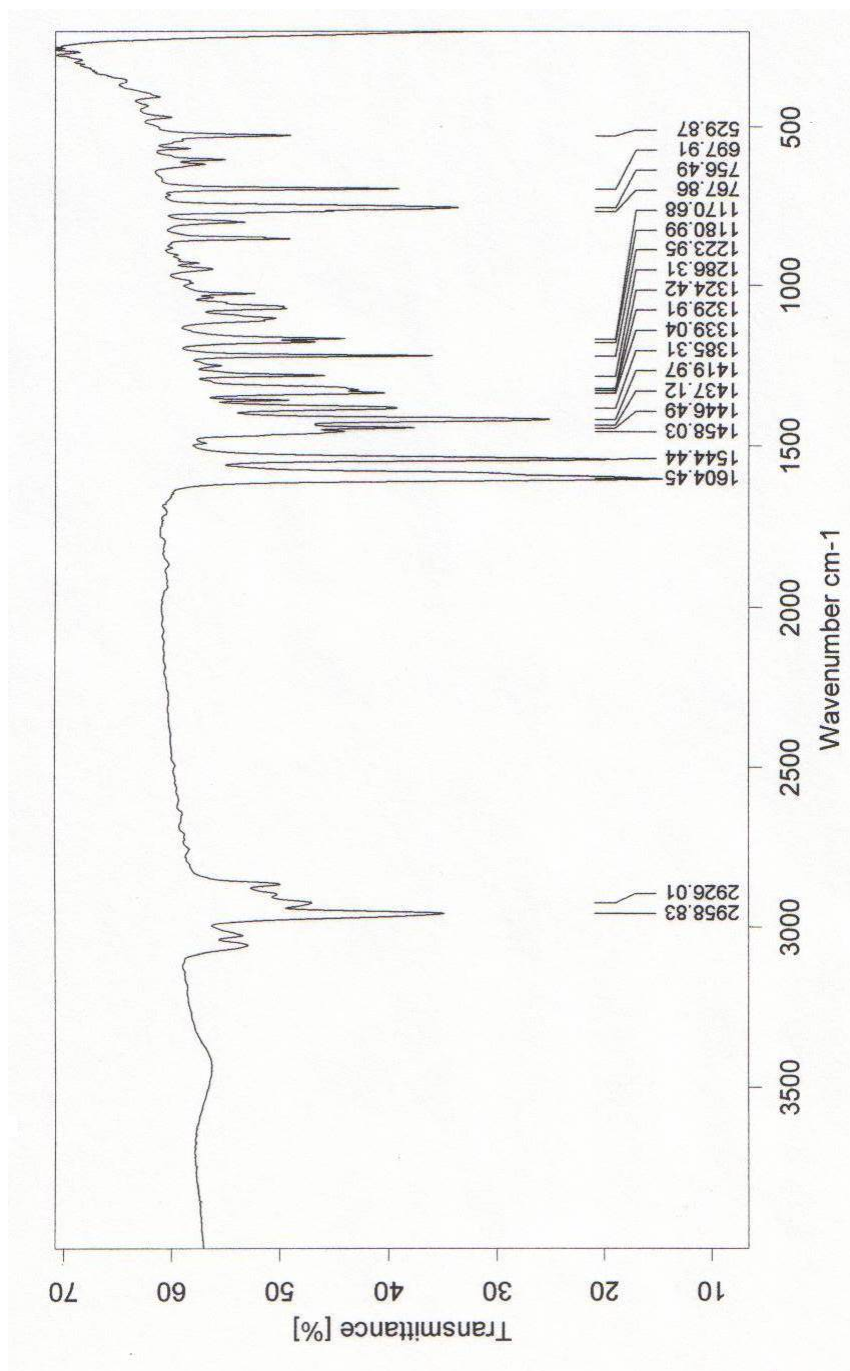
A10 Proton NMR Spectra of Incomplete Reaction to Synthesize 2,4,6-Triphenyl-5-phenyl-salicylaldehyde (Compound **D**) in CDCl<sub>3</sub>.





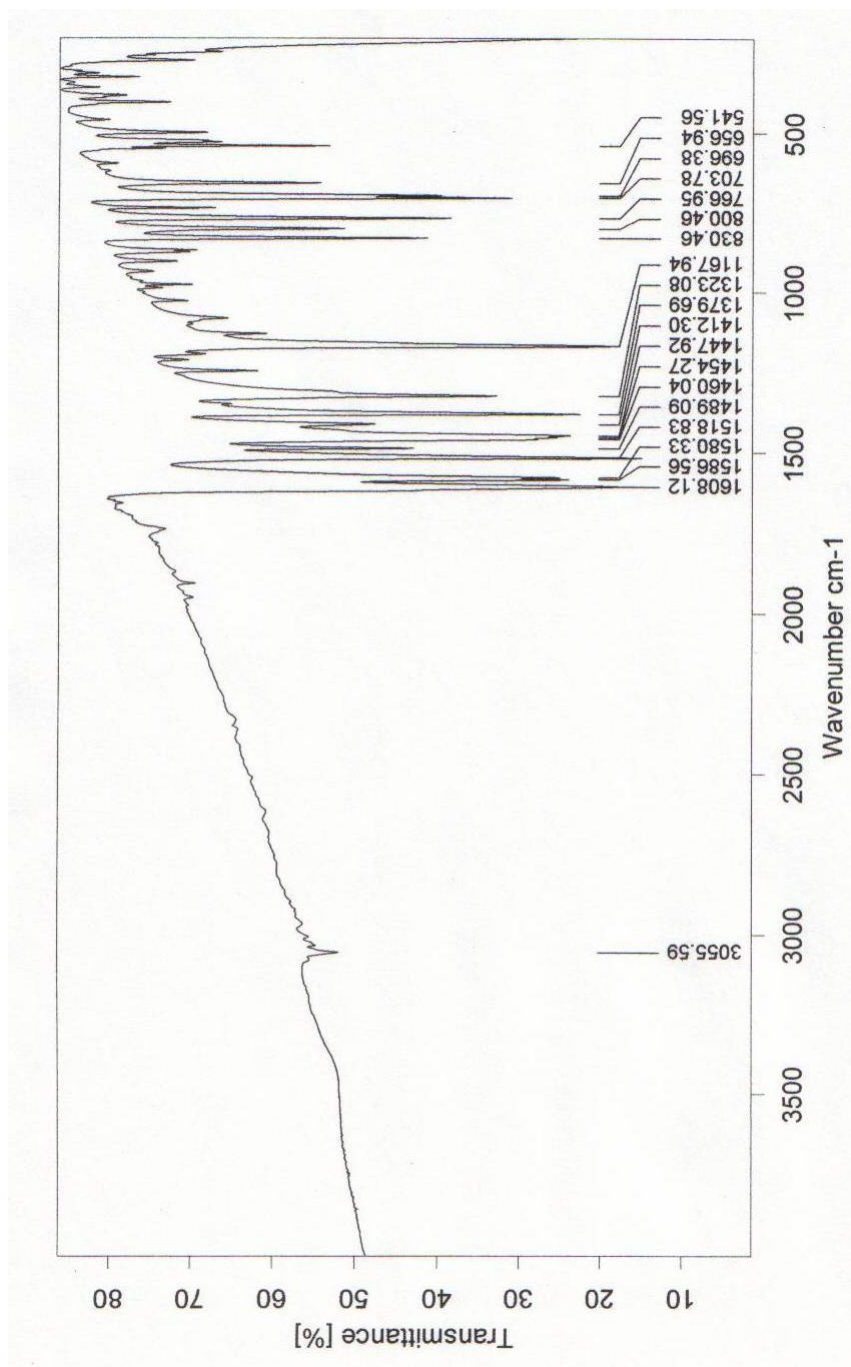


A12 FT-IR Spectra of Bis(2,6-diisopropylphenyl-3,5-di-*tert*-butylsalicylaldiminato)copper(II) (Complex **1**).

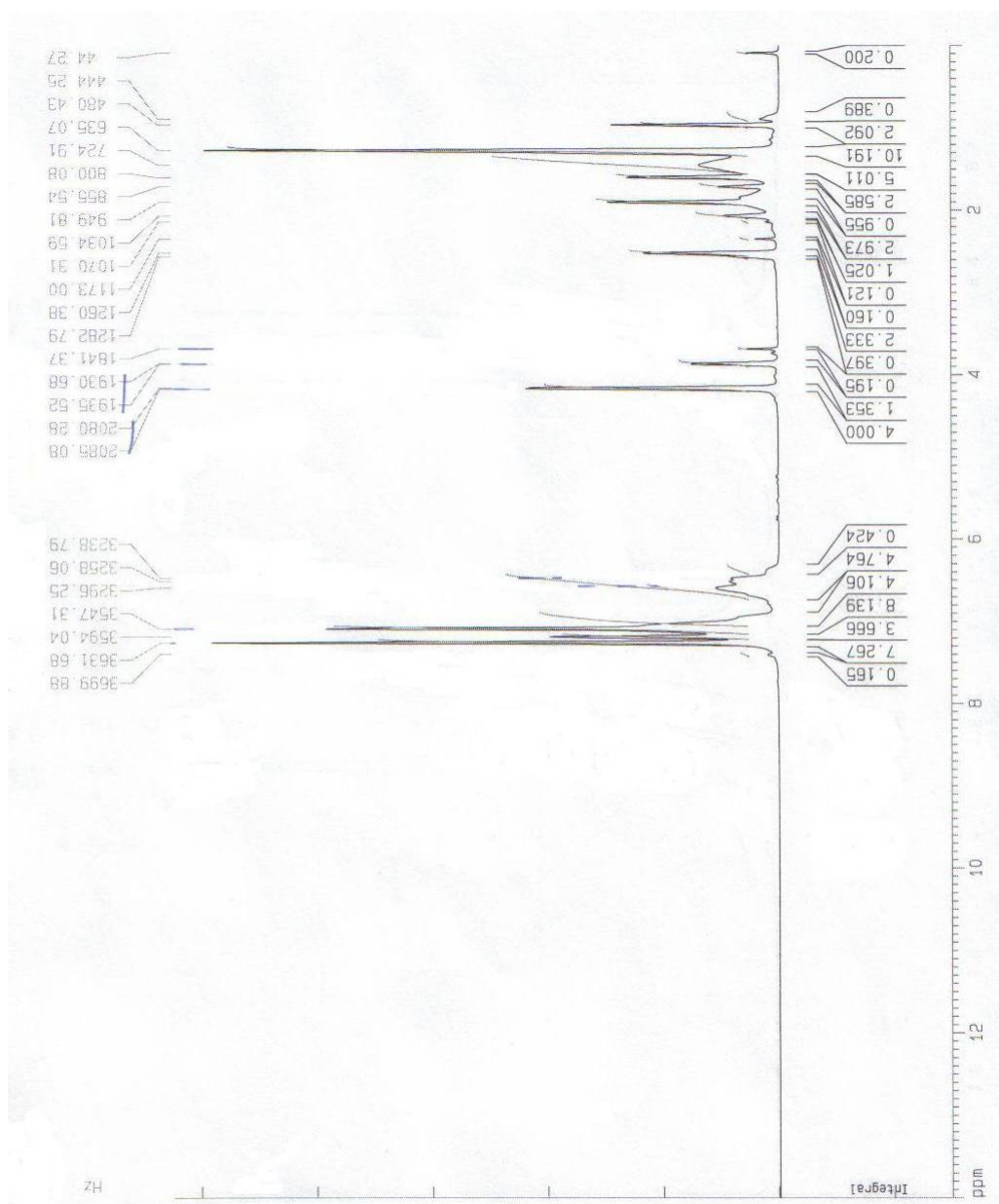


A13 FT-IR Spectra of Bis(2,6-diisopropylphenyl-5-phenyl-salicylaldiminato)copper(II) (Complex **2**).

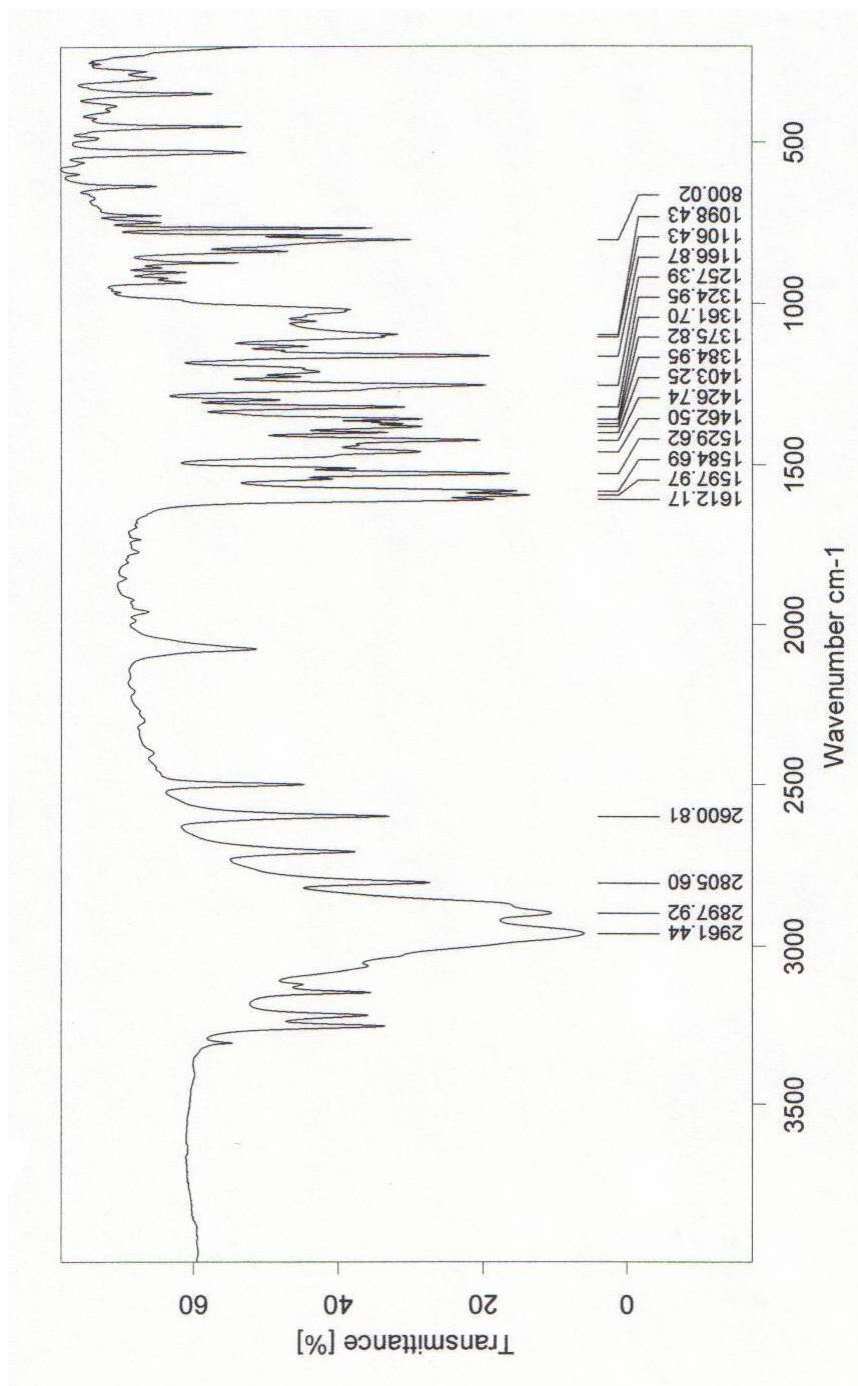




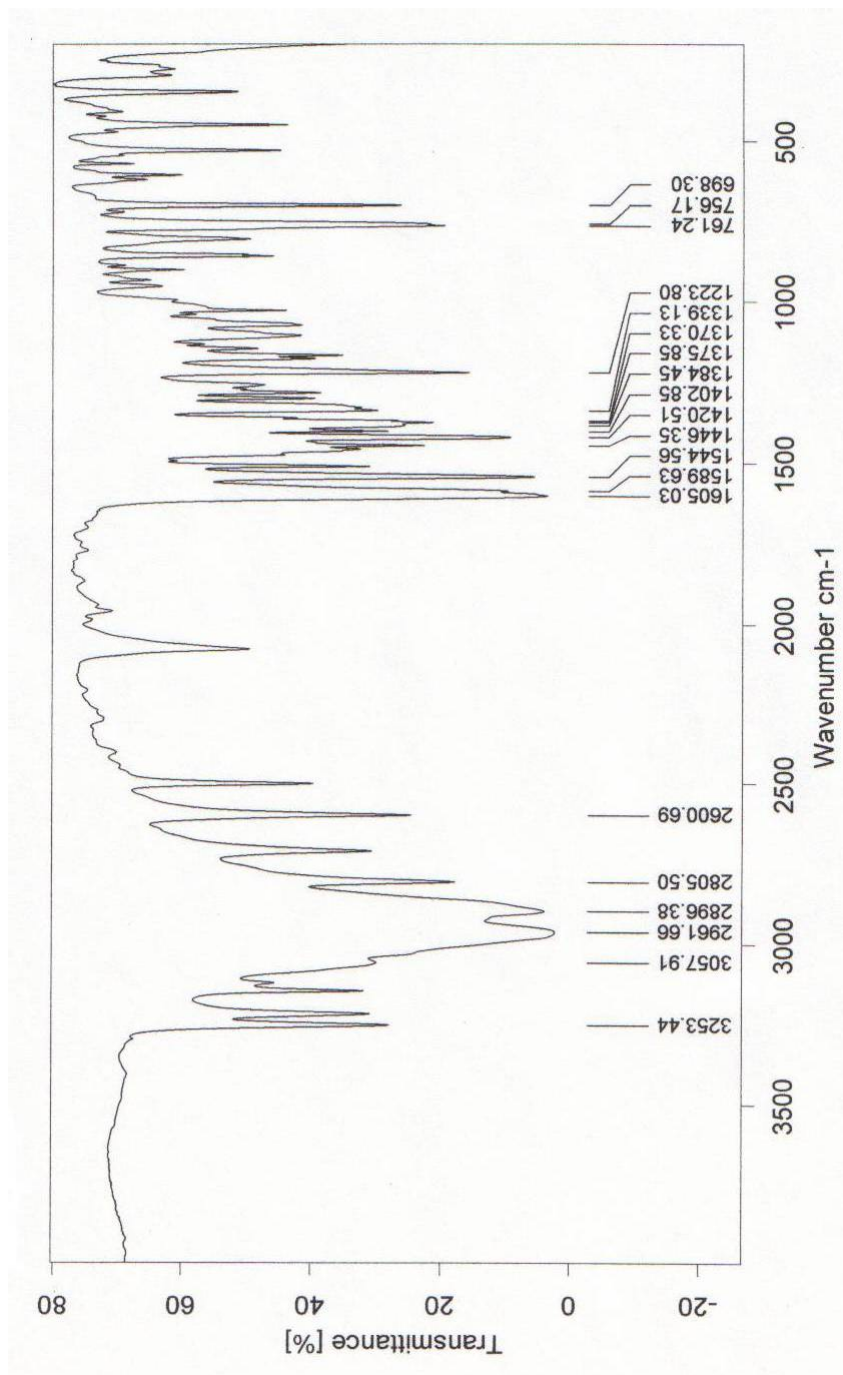
A14 FT-IR Spectra of Bis(phenyl-3-chloro-salicylaldiminato)copper(II) (Complex **3**).



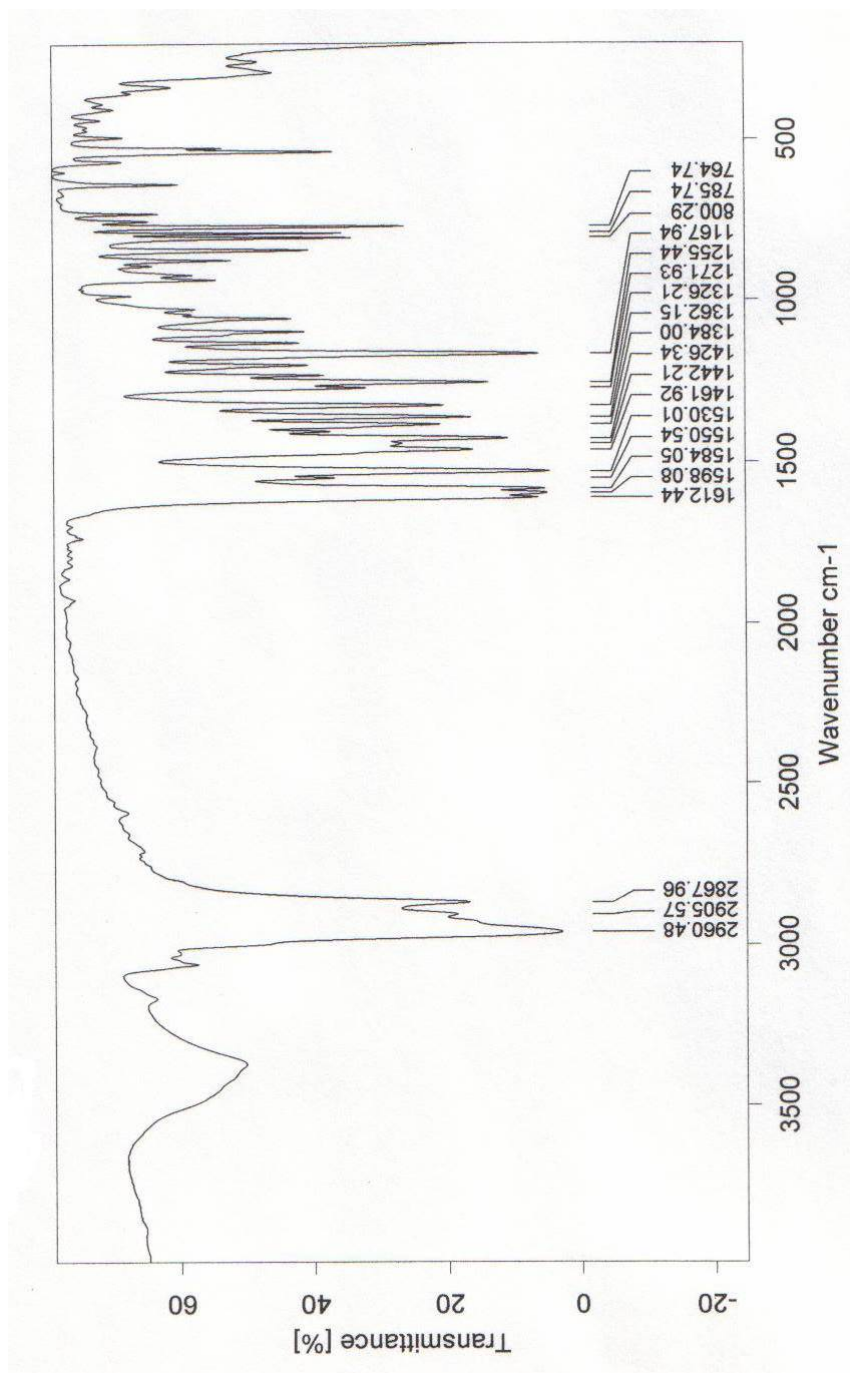
A15 Proton NMR Spectra of Cyclopropanation by Bis(phenyl-3-chloro-salicylaldiminato)copper(II) (Complex **3**) in CDCl<sub>3</sub> Corresponding to Entry 7 in Table 1.5.



A16 FT-IR Spectra of (Tri-n-butylammonium) dichloro(2,6-diisopropylphenyl-3,5-di-*tert*-Butylsalicylaldiminato)copper(II) (Complex **4**).



A17 FT-IR Spectra of (Tri-n-butylammonium) dichloro(2,6-diisopropylphenyl-5-phenyl-salicylaldiminato)copper(II) (Complex 5).



A18 FT-IR Spectra of ( $\mu$ -Chloro)(2,6-diisopropylphenyl-3,5-di-*tert*-butylsalicylaldiminato)copper(II) (Complex **6**).